Use of Water Isotope Tracers to Characterize the Hydrology of Prairie Wetlands in Alberta

by

Nicole Meyers

A thesis

presented to the University of Waterloo

in fulfilment of the

thesis requirement for the degree of

Master of Science

in

Biology

Waterloo, Ontario, Canada, 2018

Author's Declaration

I hereby declare that I am the sole author of this thesis. This is a true copy of the thesis, including any required final revisions, as accepted by my examiners.

I understand that my thesis may be made electronically available to the public.

Abstract

Our understanding of prairie wetland hydrology comes primarily from a handful of long-term research stations, but generalizing from a few intensively monitored areas to the entire prairie pothole region requires assumptions of meteorological conditions and landscape characteristics that may not be justified. To test whether generalization about the primary source of water, the influence of evaporation, and the sensitivity of water budgets to surrounding land use can be extended across the prairie pothole region, we require synoptic sampling across a more spatially extensive dataset. Temporal synchrony in hydrologic metrics across a large study region would support extrapolation, by suggesting that the same or highly correlated drivers are influencing hydrologic metrics over large areas. The aim of this study is to assess the relative importance of snowmelt and rainfall sources of precipitation and the relative evaporative influence in prairie pothole wetlands of varying permanence class. The study area includes 96 wetlands in the Parkland and Grassland Natural Regions in Alberta and contrasts influence of a normal climate year (2014) with a relatively dry year (2015) on wetland hydrological conditions. Water samples were collected at routine intervals during May-August, and analyzed for stable isotope ratios of oxygen ($\delta^{18}O$) and hydrogen ($\delta^{2}H$). An isotope-mass balance approach was used to generate hydrologic metrics (isotopic composition of source water, evaporation to inflow ratio) to assess the relative roles of snowmelt, rainfall and evaporation in the wetland water budgets. A measure of synchrony was used to test the generality of seasonal patterns of change in hydrological variables among wetlands across the large study region. Findings support prairie wetland hypotheses from intensively monitored research stations. Firstly, all study wetlands, regardless of Natural Region or permanence class,

receive the majority of their input water from snowmelt during spring, and summer rainfall does little to replenish these systems. Differences between hydrologic metrics in 2014 and 2015 were evident, but were not apparent between Grassland and Parkland regions in a normal climate year, indicating that meteorological conditions are a dominant driver of prairie wetland hydrology. However, differences between regions were evident in the relatively dry year, indicating that climate change may result in greater disparity in hydrologic function between the two natural regions. Despite differences between regions that emerged in the dry year, synchrony was actually higher in a dry year (2015) as compared to a normal climate year (2014). Findings reveal that the conceptual understanding of PPR hydrology, garnered from research stations in Saskatchewan and the United States, is applicable to the Alberta PPR. Extremely high synchrony results in hydrologic metrics indicate that PPR hydrology is driven by broad-scale processes, such as climate, rather than site-level differences.

Acknowledgements

I would like to thank Alberta Innovates: Energy and Environment Solutions, and Husky Energy for providing funding for this research.

I would like to thank my supervisors, Dr. Rebecca Rooney and Dr. Brent Wolfe for their encouragement and support throughout my research. Rebecca, I have the utmost respect for you, for your dedication to your students and all of the hard work you put into your lab; this has been an amazing learning experience and I am grateful for the opportunity to work in your lab. Brent, your enthusiasm during this process always gave me a boost of confidence and renewed motivation to slog on with my thesis work. I would also like to thank my committee members, Dr. Roland Hall and Dr. Derek Robinson, who provided me with insights and suggestions over the course of my studies. Special thanks to Derek for all of the GIS work he provided for this project. This research would not have been possible without the long days of sampling put in by all of the field assistants, and I am grateful to all of them. I would also like to thank the members of the Rooney lab and the Wolfe lab for providing encouragement, and sharing in this experience with me. I would especially like to thank Stephanie Roy, who showed me that with a little perseverance and a lot of coffee (or tea!), it is possible to finally finish writing your thesis.

I would also like to thank my family, for their love and support throughout this process. To Diana, thank you for your advice and compassion – you helped to lift me up when I was feeling down. Special thanks to my mother, Rosemary, and my mother-in-law, Olga, for helping to babysit my daughter. Without your help, this thesis would never have been finished.

Finally, thank you to my amazing partner, Peter, who has been my source of strength, inspiration, and resolve throughout this journey. Your boundless optimism and easygoing nature have helped to get me through the tough times. I am unbelievably fortunate to have you by my side, and without your love and support, none of this would have been possible. I promise that we will play all of the board games you want, now that I finally have spare time.

Table of Contents

List of Figures

List of Tables

1. General Introduction

The Prairie Pothole Region (PPR) of Canada is sometimes called the duck factory of North America due to the high density of productive marshes that offer critical ecosystem services, including waterfowl breeding habitat (McLean et al., 2016). Although we know that the ecosystem services provided by prairie pothole wetlands are contingent on wetland hydrology (e.g., LaBaugh et al., 1998; Steen et al., 2014), our understanding of the hydrology of prairie pothole wetlands largely stems from a handful of long-term research stations comprising 30 to 100 ponds that are intensively instrumented. For example, at the northern edge of the PPR, the hydrologic research station in the St. Denis National Research Area near Saskatoon, Saskatchewan, has been operational since 1968. The decades of monitoring and modeling associated with these long term research stations has formed the foundation of our understanding of prairie wetland hydrology. Whether we can extrapolate from a handful of intensively monitored sites to the entire expanse of the PPR remains uncertain. A spatially extensive assessment of prairie pothole wetland hydrology is needed to test assumptions about the primary water sources and influence of evaporation on these important wetland ecosystems.

1.1 Wetlands in the Prairie Pothole Region

Wetlands in the PPR are an integral component of the environment as they provide excellent habitat for amphibians, fish, and waterfowl, and can serve to filter and store surface water runoff as well as to buffer flood events (Zedler and Kercher, 2005). Abundant nutrients in these wetland soils elevate primary production rates, and variable water levels favour the

growth of productive herbaceous macrophytes over bryophytes (Zoltai and Vitt, 1995). Niemuth et al. (2010) emphasize the importance of including hydrology in studies of wetland biota, because hydroperiod (i.e., the duration of ponded water) has a major influence on wetland flora and fauna. Wetland ecosystem services such as waterfowl habitat provision and carbon storage depend on wetland hydrologic function.

The PPR is located in south-central Canada and the north-central United States, extending over more than 750,000 km^2 across three Canadian provinces and five US states (Johnson et al., 2010). The PPR is characterized by an abundance of shallow wetlands, known as potholes, formed by the retreat of Pleistocene glaciers. As the glaciers retreated they left pockets of ice imbedded in till deposits, which melted, leaving behind numerous depressions where water now collects (Johnson et al., 2008). The underlying glacial till produces variable permeability across the landscape, although the high clay content results in a generally low rate of seepage (van der Kamp and Hayashi, 2008).

The northwestern portion of the PPR is located in Alberta and is contained within two distinct Natural Regions, the Grassland and the Parkland, which are characterized by a flat to gently rolling topography with predominantly short to mid-height grasses (Downing and Pettapiece, 2006). Although climate conditions in the Parkland support the development of aspen forests and willow shrubs, in the Grassland, tree growth is limited by warmer and drier conditions (Downing and Pettapiece, 2006). Agriculture is the main land-use in both of these regions, which include some of the most intensively grazed and cultivated areas of the province (Stewart and Kantrud, 1971; Downing and Pettapiece, 2006).

Agriculture has had a huge effect on wetlands in the NPPR: 70% of Canadian prairie wetlands are estimated to have been filled or drained since settlement, largely attributed to agricultural activity (DUC, 2008). Many researchers have studied the influence of agricultural activity on prairie wetland biota (Bethke and Nudds, 1995) and there is some evidence that changes in land use in wetland catchments can also directly influence their hydrology (van der Kamp et al., 2003). To combat this loss, the Alberta Wetland Policy (Government of Alberta, 2013) outlined a wetland mitigation strategy, which includes restoration as a key mandate. However, it is unknown whether restored wetland sites have the same hydrologic function as natural sites.

Within the PPR, marshes are the dominant wetland form (Zoltai and Vitt, 1995). Alberta recently developed a wetland classification system (Alberta Environment and Sustainable Resource Development, 2015), which differentiates wetland classes within the province using vegetation forms and water types. In this system, all marshes are graminoid in form but are categorized into different types based primarily on salinity and water permanence. Salinity can vary from freshwater to brackish (up to a specific conductance of 15,000 µS/cm), while water permanence can vary from a few weeks (temporary marsh) to several months (seasonal to semi-permanent marshes) based on the wetland classification system of Stewart and Kantrud (1971). Historically, it has been estimated that temporary and seasonal marshes were the most abundant type on the PPR landscape (60% and 35%, respectively), while semi-permanent marshes represented about 5% overall (Johnson and Higgins, 1997). Marsh type influences the biological communities within the wetland, placing constraints on the plant and wildlife assemblages that are able to occupy the wetland.

1.2 Hydrology

The water balance of PPR wetlands is mainly controlled by variation in snowpack depth and evapotranspiration (van der Kamp and Hayashi, 2008; Shook and Pomeroy, 2012). In winter, windblown snow accumulates in and around wetland depressions, having been redistributed from thinly vegetated areas (Fang and Pomeroy, 2009). Snowmelt accounts for 80% of annual surface runoff in the PPR and is dependent on not only the size of the snowpack and rate of melt, but also local site characteristics such as soil infiltration, the size of the contributing area, and land use factors (Gray and Landine, 1988; Niemuth et al., 2010; Shook et al., 2015). In spring, due to the reduced infiltration capacity of frozen soils, snowmelt runoff from upland areas into wetlands can be high. However, infiltration rates are greatly increased in the summer, which reduces runoff from rainfall events (Granger et al., 1984; Woo and Rowsell, 1993). Therefore, water input to PPR wetlands is largely controlled by winter precipitation. Water exits these wetlands through surface evaporation, transpiration from plants within the wetland, or through soil infiltration (Woo and Rowsell, 1993). However, infiltrated water typically moves in a lateral direction, and is often intercepted and used up by plants (Hayashi et al., 1998). Groundwater exchange with wetlands is variable, being limited to localized shallow flow, and dependent on local conditions such as the landscape position, as well as the hydraulic conductivity of the underlying till (Sloan, 1972; Winter and LaBaugh, 2003; van der Kamp and Hayashi, 2008).

Many wetlands in the PPR are hydrologically isolated from surface-water connections. However, some wetlands occur in a cluster called a wetland complex, and when given ample precipitation, these wetlands may become connected to adjacent waterbodies through the fill-

and-spill mechanism (Shaw et al., 2012). This is the process whereby wetlands in the upland position on the landscape become saturated with water (filled), and overflow (spill) downslope to recharge wetlands that are lower on the landscape.

PPR wetlands have a variable hydroperiod, dependent on the water volumes received, basin morphometry, and the rate of evaporation, and are thought to exist along a continuum of water permanence and function (Euliss et al., 2004). The wetland continuum concept model proposes that wetlands experience variability in hydroperiod due to hydrologic function (recharge or discharge to groundwater), and natural fluctuations in climate, leading to drought and deluge conditions (Euliss et al., 2004). The model is characterised by hydrologic gradients along two separate axes, representing groundwater and atmospheric water, respectively, and predicts which plant communities will establish. It is theorized that wetlands claiming a lower landscape position, and thus receiving overland runoff inputs from the fill-and-spill mechanism, will retain water longer into the season, while shallow basins higher in the landscape may desiccate by mid-summer due to water loss by evapotranspiration and infiltration (van der Kamp et al., 2016). Hayashi et al. (2016) even suggests that the "groundwater" axis in the wetland continuum concept is misnamed, and should instead be labelled "hydrological position", to reflect the fill-and-spill connections with neighbouring wetlands. In this way, the wetland continuum model characterizes the variation in wetland function and hydroperiod based on both spatial (landscape position) and temporal (meteorological condition) scales (Hayashi et al., 2016).

1.3 Climate

Climate in the PPR is primarily affected by three air masses: Continental Polar, Maritime Polar, and Maritime Tropical (Bryson and Hare, 1974). These air masses interact to produce a semi-arid environment with high summer temperatures and low humidity, which result in high rates of evapotranspiration (Millet et al., 2009). Precipitation in the PPR is extremely variable regionally as well as inter-annually, with net annual precipitation deficits of 40-60 cm/year, and snow constituting approximately 30% of annual precipitation (Laird et al., 1996; Akinremi et al., 1999).

Climate change threatens to reduce the number of wetlands on the landscape by increasing temperatures and decreasing runoff from snowmelt and rainfall, inducing shorter hydroperiods with earlier and faster drawdown, and creating less resilient wetland ecosystems overall (Johnson et al., 2010; Steen et al., 2014). Climate models for the northern PPR predict small shifts (5%-10%) in precipitation, and a rise in temperature by 4^{o}C by 2100 (Solomon, 2007). In contrast, models applied by Zhang et al. (2011) substantiate a warming trend, but were less confident in predictions of precipitation patterns, which carry substantial weight in hydrological models. Regardless, an increase in the variability of the hydrological cycle is predicted, in addition to a later onset of winter and an earlier spring, which could cause an increase in the frequency of drought and deluge conditions (Ojima et al., 2002). In fact, Kienzle et al. (2017) evaluated temperature trends in Alberta between 1950-2010 and found that the number of heat waves has approximately doubled, while winter temperatures have increased significantly, lengthening the ice-free season by between one to five weeks.

1.4 Prior Research

In Canada, the St. Denis National Wildlife Area is a wetland ecosystem monitoring site, established in 1968 and located approximately 40km east of Saskatoon. The research focus at St. Denis includes wetland hydrology, soil science, and wildlife such as waterfowl. Relevant findings suggest that land-use is an important factor in both snow distribution and snowmelt infiltration into soils (van der Kamp et al., 2003). In this study, undisturbed grasses were more likely than cultivated fields to capture windblown snow, leading to a higher volume of available snowmelt in the catchment. However, meltwater was less likely to infiltrate into the compacted soil of cultivated fields, generating more runoff into wetlands (van der Kamp et al., 2003; Bodhinayake and Si, 2004). Additionally, studies at St. Denis emphasize the importance of catchment size, as smaller catchments typically have less groundwater influence, and landscape position, where wetlands higher on the landscape will dry out faster (van der Kamp and Hayashi, 2008; Hayashi et al., 2016). Much of the research here has focused on wetland complexes, which would receive a far greater effect from mechanisms like fill-and-spill than wetlands that are isolated on the landscape. Another notable research station in Canada, located in eastern Saskatchewan, is the Smith Creek Research Basin, which carries out many hydrological studies concerning climate change, wetland drainage, and land-use (e.g., Fang et al., 2010; Dumanski et al., 2015).

In the United States, Cottonwood Lake (North Dakota) and Orchid Meadows (South Dakota) are the primary research stations focussing on PPR wetlands, which have both had a large focus on the effects of climate change during recent years. Important findings from Orchid Meadows point out that climate change poses the most risk to seasonal and semi-

permanent wetlands, as well as wetlands in the western and central PPR, due to projected changes in air temperature (Johnson et al., 2016). There are risks in assuming we can extrapolate from this handful of intensively monitored research stations. These long-term research stations have given us our cornerstone of understanding the hydrology of prairie pothole wetlands, but there has been relatively little study in the northwestern portion of the PPR, where the climate, soils, and land use could all differ, potentially altering wetland hydrologic processes.

1.5 Water Isotope Tracer Method

Due to the vast size of the PPR region, as well as the large number of wetlands, it is difficult to characterize hydrologic variability across the entire landscape, and it is not practical to instrument and measure all wetlands. As discussed above, most of our current understanding has been derived from a few key study sites. However, knowledge is lacking on the hydrological conditions of wetlands in some portions of the PPR, including Alberta. Therefore, a method is needed to capture the hydrological conditions across a wide landscape, in order to determine if PPR wetlands in Alberta follow the same basic tendencies as wetlands studied in the eastern and southern portions of the region.

The water isotope tracer method is a useful technique for gathering hydrological information, without the need for installing any equipment in the field. Water samples can be collected quickly and easily from wetland sites, and once analyzed for stable isotope ratios, can be used in a mass-balance model to provide information about water source and water balance (e.g., Yi et al., 2008; Gibson et al., 2016). Applying this isotope-mass-balance approach will help

to determine whether our understanding of water source and evaporative influence, derived from a few heavily studied areas of the PPR, can be extrapolated and generalized to the Alberta portion of the PPR.

A water molecule contains one oxygen and two hydrogen atoms, with three naturally occurring isotopes. The common isotopic form is $H^1H^1O^{16}$, while the two less common forms ($H^1H^1O^{18}$, $H^1H^2O^{16}$) have a higher mass. Isotope compositions are represented using δ notation (δ^2H, $\delta^{18}O$), which denotes the permil (‰) value of the sample relative to a known standard, most commonly being the Vienna Standard Mean Ocean Water. Stable isotopes can be used effectively in hydrologic studies because the isotope composition of water changes in a well-known and predictable manner as water passes through the hydrologic cycle, due to mass-dependent fractionation (Craig and Gordon, 1965; Clark and Fritz, 1997; Edwards et al., 2004). The hydrologic cycle describes the exchange of water between the earth and the atmosphere, via processes such as precipitation and evaporation. Fractionation is a process whereby the ratio of heavy to light isotopes in water is altered, and occurs during phase-changes due to differences in molecular mass (Gat, 1980). During evaporation, the lighter isotopic forms will preferentially evaporate, leaving the wetland water enriched in the heavier isotopes (Clark and Fritz, 1997). Due to fractionation processes in precipitation, snow has an isotopic signature that is more depleted in heavy isotopes than rain (Gedzelman and Arnold, 1994). The rate at which isotopic partitioning occurs is fixed, and allows for the determination of evaporative effects, as well as water source, for a wetland water sample at a specific point in time.

For the purposes of this study, two linear relationships are defined between hydrogen and oxygen isotope compositions of water: the Global Meteoric Water Line (GMWL) and the

Wetland-specific Evaporation Line (WEL) (Figure 1-1). The GMWL is a fixed line ($\delta^2H = 8\delta^{18}O + 10$), determined by Craig (1961), and represents the globally averaged proportional relationship between δ^2H and $\delta^{18}O$ in precipitation. The WEL, determined using meteorological conditions and isotopic data local to the wetland(s) being studied, represents the evolution that water in a wetland, fed by the mean annual isotope composition of precipitation, will take as it evaporates to the point of desiccation (Clark and Fritz, 1997). Thus, the WEL is bound by the isotopic composition of mean annual precipitation (δ_P), located on the GMWL, and the isotopic composition of wetland water at the theoretical maximum potential isotopic enrichment condition (δ^*). A mass balance model also allows for calculation of the isotopic composition of a wetland under terminal basin steady-state conditions (δ_{SSL}), enabling a quick visualization (in δ^2H-$\delta^{18}O$ space) of whether a wetland is experiencing non-steady state evaporative effects (plotting beyond δ_{SSL}), or if it is receiving more inflow than is lost by evaporation. Typically, wetlands with isotopic values positioned below the WEL have a strong influence from snowmelt, whereas wetlands with isotopic values positioned above the WEL are more strongly influenced by rainfall. Water-balance metrics can be quantitatively assessed by using the coupled-isotope tracer method (Yi et al., 2008) to calculate the isotopic composition of input water (δ_I), and evaporation to inflow (E/I) ratio (Figure 1-2). These two metrics are used to assess the relative influence of snowmelt and rainfall to each basin (δ_I) as well as the effect of evaporation on wetland water balance (E/I) (e.g., Tondu et al., 2013; Turner et al., 2014).

The isotope tracer method has been used successfully in studies spanning lakes across the United States (Brooks et al., 2014), in northern climates of Canada (Bouchard et al., 2013; Tondu et al., 2013; Turner et al., 2014; Gibson et al., 2016), and also in the eastern portion of

the PPR in Canada (Pham et al., 2009). Because the isotope tracer method is well tested, it is a great tool to use for sampling many wetlands over a large spatial distance, which will allow us to gain knowledge about many sites, with minimal cost and sampling effort.

1.6 Research Objectives

The objective of this research is to attain a broader understanding of the hydrologic drivers of prairie pothole wetlands, by comparing numerous sites in a normal climate year (2014) to a drier climate year (2015) across a large spatial extent of Alberta, spanning the Grassland and Parkland regions. An isotopic mass-balance model will be used to quantitatively compare hydrologic metrics across the study region. The relative importance of snowmelt and rainfall to wetland water source will be assessed by calculating the isotopic composition of wetland-specific input water (δ_I). Additionally, the influence of evaporation on wetland water balances will be evaluated using evaporation to inflow (E/I) ratios. The level of synchrony will be tested among all wetlands, which will help to determine if it is prudent to generalize prairie wetland hydrology over a large spatial extent. Lastly, water source and evaporative influence will be used to assess whether patterns evident in natural wetlands are mirrored in restored ones. If so, it implies that their hydrologic function is comparable to natural wetlands and thus restoration is successful. If not, it suggests that there is some way in which restored wetlands are not functioning like natural wetlands.

1.7 Figures

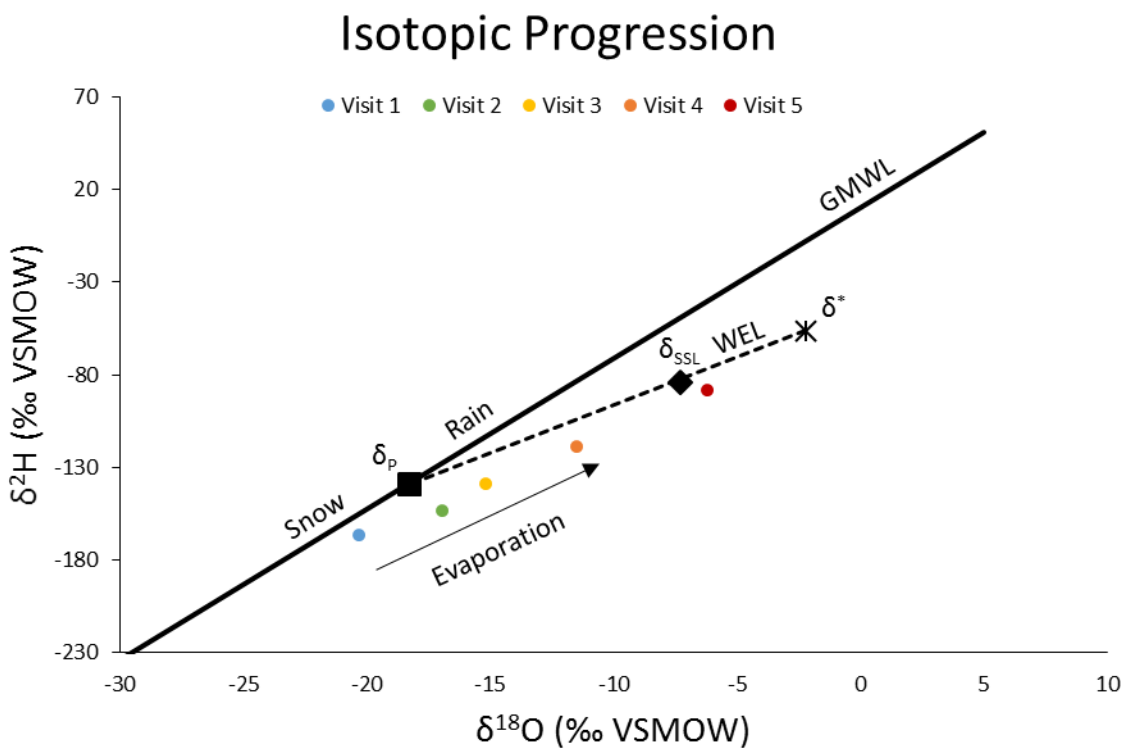

Figure 1-1. Wetland-specific evaporation line (WEL) and surface water isotope compositions from site visits 1-5 for the Parkland wetland 05CD 90, sampled in 2014. The WEL is bound by the isotope composition of mean annual precipitation (δ_P) and the limiting non-steady-state isotope composition (δ^*). Generally, wetland isotope compositions which fall below the WEL are sourced mainly by snowfall, while isotope compositions which fall above the WEL are sourced mainly by rainfall. The former is the case for the example shown. From site visits 1 through 5, surface water isotope compositions become more enriched with heavy isotopes, due to evaporation, as seen by the progression towards δ^*.

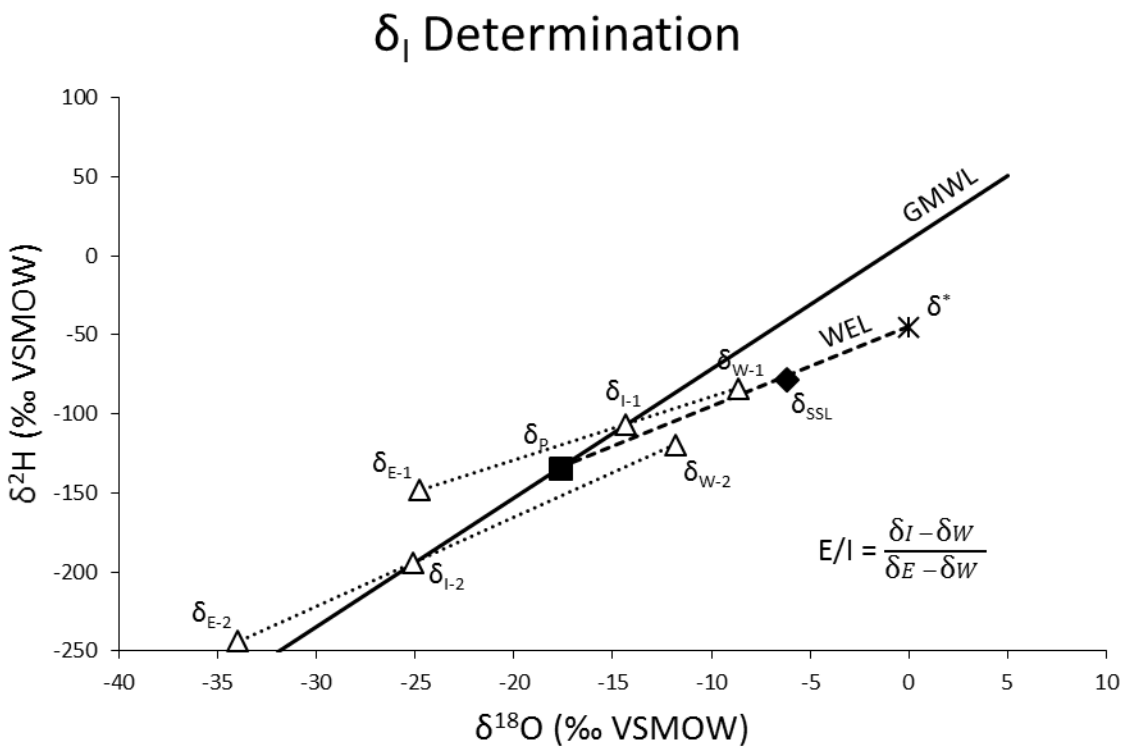

Figure 1-2. Wetland-specific evaporation line (WEL) and surface water isotope compositions, δ_{W-1} and δ_{W-2} (i.e., measured values) for two samples from the Grassland wetland 05CH 115 in 2014. This schematic shows that the intersection of the line passing through the wetland-defined δ^* and each water isotope composition with the Global Meteoric Water Line (GMWL) can be used to estimate the δ_I value for each sampling point in time. The isotope composition of evaporated vapour (δ_E) is located along the same line, and is used to also determine the evaporation to inflow (E/I) ratio.

2. Assessing drivers of prairie pothole wetland hydrology in Alberta using water isotope tracers

2.1 Introduction

The Prairie Pothole Region (PPR) of North America spans approximately 750,000 km^2 of central Canada and the United States and contains between 5-8 million small, depressional wetlands called prairie potholes (Johnson et al., 2010). Ecosystem services provided by wetlands in the PPR are reliant on hydrologic function (e.g., LaBaugh et al., 1998; Steen et al., 2014). Decades of research have helped develop a detailed conceptual model of prairie wetland hydrology (reviewed in Hayashi et al., 2016), but this understanding is strongly grounded in work from a few intensively monitored research stations, such as the St. Denis National Research Area and the Smith Creek watershed in Saskatchewan. Significantly, less study has been made of prairie wetland hydrology at the northwestern edge of the PPR, in Alberta.

In our current understanding of prairie wetland water budgets, winter precipitation plays an important role in the formation and persistence of wetlands in the PPR (Hayashi et al., 2016). Although snow only constitutes 30% of annual precipitation, it is estimated that 80% of annual surface runoff is derived from snowmelt (Gray and Landine, 1988; Akinremi et al., 1999). The amount of snowmelt runoff generated in any given year is dependent on a combination of climate factors such as snow accumulation and rate of melt, and local site characteristics such as soil infiltration and the size of the contributing area (Shook et al., 2015) as well as land use factors (Niemuth et al., 2010). During the winter months, blowing snow is redistributed across

the landscape, but tends to accumulate in PPR wetlands due to their depressional topography as well as the type and height of vegetation found there (Fang and Pomeroy, 2009). In early spring, the accumulated snowpack melts, generating runoff over frozen soils, which typically have low infiltration rates (Granger et al., 1984). In summer, soil infiltration rates in the PPR reduce runoff, and evaporation exceeds input from rainfall, creating a water deficit (Woo and Rowsell, 1993). In the northern part of the PPR, net precipitation deficits are estimated at around 40-60 cm/year (Laird et al., 1996). Although summer precipitation is understood to be less influential as a water source, relative to snowmelt, large rainfall events can occur during summer, which may cause basin-scale runoff and increased flow to wetlands (Shook and Pomeroy, 2012) and may connect otherwise isolated wetlands through a fill-and-spill mechanism (Shaw et al., 2012). Consequently, prairie wetlands tend to fill in spring and draw down gradually throughout the summer, with a rate depending on evapotranspiration rates, which are in turn dependent on relative humidity and vegetation (van der Kamp and Hayashi, 2008; Shook and Pomeroy, 2012).

Many prairie wetlands regularly dry up entirely, and so they are often categorized based on the duration of ponded water (i.e., the wetland hydroperiod). For example, Alberta recently developed a wetland classification system, which differentiates wetland permanence classes within the province (Alberta Environment and Sustainable Resource Development, 2015). Under this system, water permanence can vary from a few weeks (temporary marsh) to several months (seasonal to semi-permanent marshes), presumably dependent on the rates of water loss through evapotranspiration. Another category of wetland, known as restored or constructed wetlands, exist on the PPR landscape. These wetlands have been designed to

compensate for the loss of natural wetlands, in both area and function, as mandated by the Alberta Wetland Policy (Government of Alberta, 2013). It is not known whether the hydrologic function of restored wetlands is analogous to that of natural wetlands in the PPR. However, several authors have examined restored wetlands and concluded that they do not provide the same functions and values as natural wetlands (e.g., Moreno-Mateos, 2012; Jessop et al., 2015).

The wetland continuum concept model, developed by Euliss et al. (2004), suggests that wetlands within the PPR exist in a dynamic state, where biological communities may differ each year based on the current hydrologic relations with groundwater and atmospheric water, from the extremes of drought to deluge. This is partly attributed to the extreme variability in precipitation characteristic of the PPR. Precipitation is naturally variable regionally as well as inter-annually, which greatly affects the wetland water budget, resulting in a range of annual hydrological conditions (Bragg, 1995; Euliss et al., 2004). Extrapolating from our understanding of prairie wetland hydrology developed in intensively monitored research centres, the hydrologic functions of wetlands in the PPR are driven largely by variation in snowpack depth and evapotranspiration, two climatic variables which control the wetland's water budget (van der Kamp and Hayashi, 2008). Thus, we expect that wetland hydrologic functions will be particularly sensitive to climate variables.

Consequently, climate change presents a major threat to continued provision of wetland ecosystem services (e.g. Steen et al., 2014; McLean et al. 2016; Rashford et al. 2016). Downscaled climate models for the northern PPR project that temperature will increase by 4^{o}C, while precipitation will experience small shifts of approximately 5% to 10% by 2100 (Solomon,

2007). However, model confidence is reduced when predicting patterns in precipitation, compared to temperature (Zhang et al., 2011). Climate models project that the snow season will come later in the fall and end earlier in the spring, with an increasingly variable hydrological cycle causing incidents of drought and deluge to become more frequent (Ojima et al., 2002). These predictions have already been substantiated in Alberta, where the snow season has decreased between one to five weeks, and the number of heat waves has almost doubled, since 1950 (Kienzle et al., 2017). The leading concerns of climate warming in the PPR include earlier snowpack melting, decreasing wetland water depths and volumes, shorter hydroperiods, faster drawdown, and reduced snowmelt and rainfall, creating less resilient wetland ecosystems (Johnson et al., 2010; Johnson et al. 2016). Indeed, recent simulation work suggested that wetlands at the northwestern margin of the PPR may be the most sensitive to climate change (Werner et al., 2013), likely because of the natural aridity gradient, which increases from east to west (Johnson et al. 2016).

These projections, however, are based on a conceptual understanding of the determinants of prairie wetland hydrology developed from intensive, long term monitoring in a limited number of locations. It is not clear whether the hydrologic drivers identified as most important in places like the St. Denis research station in the northeast of the PPR or the Cottonwood hydrologic research centre in the middle of the PPR will be equally important for wetlands across the Parkland and Grassland Natural Regions of Alberta, at the northwestern margin of the PPR. This limits our ability to predict how climate change might influence wetlands in Alberta, where models predict they may be most sensitive (Werner et al., 2013).

The water isotope tracer method has been used successfully to determine hydrological characteristics such as water source, and to describe variability in lake water balances, evaporative effects, and the influence of catchment conditions over a broad spatial extent (e.g. Gibson and Edwards, 2002; Brooks et al., 2014; Turner et al., 2014). Of particular relevance, Pham et al. (2009) used the isotope tracer method to explore synchronous seasonal hydrological changes within closed-basin lakes in the prairie region of Saskatchewan. Synchrony is an important phenomenon observed at scales from the cellular level to the dynamics of populations spaced thousands of kilometers apart. For example, studies have used a measure of synchrony to detect insect outbreaks (Williams and Liebhold, 2000) as well as to track predator-prey cycles (Stenseth et al., 2004). Synchrony is an aspatial technique that measures the correlation among time series data, which can be used to test the universality of seasonal patterns of change in hydrological variables among wetlands across a geographic region. This technique has been used to test for temporal coherence of hydrological and biological metrics in lakes spanning short (seasonal) and long (decadal) time periods (e.g., Rusak et al., 1999; Patoine and Leavitt, 2006; Pham et al., 2009). High synchrony in our study region would indicate that wetlands in the PPR of Alberta respond to the same or highly correlated drivers that operate at regional scales.

The aim of this research is to test whether 1) the primary source of water to prairie wetlands across the study region is consistently winter precipitation, with rainfall contributing little to the wetland water budget; 2) the evaporative influence is greater in Grassland wetlands than in Parkland wetlands, where the deficit between precipitation and potential evapotranspiration is less; and 3) wetlands will exhibit synchronous evaporative isotopic

enrichment across the entire study region, despite differences between Natural Regions, suggesting that the hydrology of prairie wetlands is driven by broad trends in meteorological conditions rather than local landscape differences. The dominant water source to each wetland (rain or snowmelt) will be determined by comparing the wetland-specific input water isotopic compositions to that of mean annual precipitation. The relative influence of evaporation in the different Natural Regions will be quantified by calculating evaporation to inflow ratios for each wetland using isotopic mass-balance equations and comparing wetlands in the Parkland to wetlands in the Grassland. Additionally, the importance of seasonal and year-to-year variation in meteorological conditions in determining wetland hydrologic functions will be explored by comparing data collected across the ice-free season in two consecutive years. In particular, the water isotope tracer method will be used to describe the hydrology of selected prairie wetlands in Alberta, contrasting a normal climate year (2014) with a dry year (2015) to test the hypothesis that synchrony in evaporation among wetlands will be higher in a dry year (2015) compared to a normal climate year (2014). If this is the case, it would be expected that climate change will lead to even greater synchrony among wetlands, as climate projections suggest that the moisture deficit will increase in the future. Lastly, the hydrologic function of restored wetlands will be compared to that of natural wetlands. In particular, I will test the predictions that 1) the hydrology of restored wetlands behaves more synchronously than natural wetlands, and that 2) restored wetlands experience less influence of evaporation, due to differences in basin morphology and greater wetland basin connectivity than natural wetlands. Overall, my thesis will test whether our understanding of the drivers of prairie wetland hydroperiod based on decades of work in a limited spatial range can be extrapolated to the whole PPR of Alberta.

2.2 Methods

2.2.1 Site Selection

Sites were randomly selected, with the assistance of members within the broader project team, to accurately represent the frequency distribution of marshes less than one hectare in size on a sub-watershed basis (Figure 2-1), using a geographic information system (GIS). In addition, selected sites spanned a range of disturbance levels along a gradient of increasing agricultural land use categorized by percent area within a 500 m buffer surrounding the wetland. All of the selected sites were closed basins contained within one of six pre-selected sub-watersheds within the Parkland and Grassland Natural Regions of Alberta. Three of the sub-watersheds were located within the Parkland region, while the remaining three were located within the Grassland region. The sub-watersheds were chosen such that they did not cross any state or provincial borders, and were entirely confined within one Natural Region (Parkland or Grassland). In 2014, eight wetlands were sampled within each of the six sub-watersheds of the study region, for a total of 48 wetlands. In 2015, four wetlands within each sub-watershed were resampled, and four new wetlands within each sub-watershed were sampled to improve spatial resolution, for a total of 48 wetlands. An additional 24 restored wetlands were sampled in the Parkland region in 2015 (Appendix A). These were all restored by ditch-plugging by Ducks Unlimited Canada on land purchased by them and resold with conservation easements in place. Restoration projects were all undertaken by Ducks Unlimited staff between 2004 and 2013, and where projects included multiple wetlands or wetland complexes, only one wetland basin per project was sampled.

2.2.2 Climate Data

For the 2014 and 2015 sampling seasons, climate data were obtained from the Alberta AgroClimatic Information Service (ACIS). The ACIS weather station closest to each site was determined using GPS coordinates, and daily values for air temperature, precipitation, relative humidity, and evapotranspiration were downloaded for the months when sampling took place, as well as the 6 months prior to sampling, to determine antecedent conditions. For isotope mass-balance equations, temperature and relative humidity for each wetland were flux-weighted using daily potential evapotranspiration for the period May 1-Aug 31 for 2014 and 2015. The flux-weighting approach weights temperature and relative humidity values so that mass-balance calculations are more representative of the ice-free season, when rates of evaporation are highest (Gibson and Edwards, 2002).

In 2014, mean ice-free season temperature (measured from May 1-Aug 31 at ACIS meteorological stations) was comparable to the long–term average ice-free season temperature. However, in 2015 the mean ice-free season temperature exceeded the long-term average by approximately 0.5 °C (Figure 2-2a; Appendix B). The mean Grassland ice-free season temperature (May 1-Aug 31) was approximately 1 °C higher than in the Parkland for both years. In 2013-2014, the winter-time mean temperature (measured from Nov 1-Apr 31 at ACIS meteorological stations) was approximately 2 °C lower than the long-term winter average temperature, but in 2014-2015, the winter-time average temperature was approximately 2 °C higher than the long–term winter average temperature (Figure 2-2a; Appendix B). Winter-time average temperatures in the Grassland and Parkland Natural Regions were similar in both years. However, an important difference between study years was that in 2015, the mean

temperature reached above zero in March for both Natural Regions, one month earlier than occurred in 2014. This indicates that the spring freshet likely occurred about one month earlier in 2015 than in 2014 in both Natural Regions. Further, the snow pack was lower than normal in a large portion of the study area in mid-March 2015, while the soil moisture content was higher than normal at the end of March 2015 (Appendix C and D), likely indicating that the snow pack melted and saturated the soil earlier in 2015 than in 2014.

Average relative humidity was 7% higher in the 2014 ice-free season (i.e., from May 1-Aug 31) than during the 2015 ice-free season. Comparing the regions, average ice-free season relative humidity was 5% lower in the Grassland than the Parkland in both years (Figure 2-2b; Appendix B).

Total ice-free season precipitation (i.e., from May 1-Aug 31) in 2014 was similar to the long-term average, but was below the long-term average in 2015 (Figure 2-2c; Appendix B). Notably, the Grassland Natural Region received 15 mm less precipitation than the Parkland during the 2014 ice-free season, but 42 mm less precipitation than the Parkland during the 2015 ice-free season, indicating that although the difference in mean ice-free season temperature between regions was consistent across years, the difference in total precipitation between the two regions was greater in 2015. Total winter-time precipitation (i.e., from Nov 1-Apr 30) was relatively low in both 2013-2014 and 2014-2015, compared with the long-term average winter-time precipitation (Figure 2-2c; Appendix B). Comparing winter-time precipitation between the two Natural Regions, the Grassland received 42 mm less precipitation than the Parkland in 2013-2014, but only 25 mm less in 2014-2015.

2.2.3 Field Methods

In Situ

In 2014 and 2015, water depth was measured at each wetland on all site visits (i.e., at approximately three-week intervals from May to September) from staff gauges. Staff gauges were installed at the estimated deepest point of each wetland basin to facilitate measurements of water depth.

Collection of Water Samples for Analysis of Isotope Composition

In 2014 and 2015, water samples were collected from each wetland for the purpose of oxygen and hydrogen stable isotope analysis. Water samples were collected from the middle of the water column, in the deepest portion of the basin, in 30 mL high-density polyethylene bottles which were rinsed three times with wetland water and then filled to ensure no head space. Water samples were taken from each site every 2-3 weeks, May through August, resulting in a total of 5 sampling visits each year. Because these wetlands draw-down progressively during the summer, the number of sites from which water samples could be acquired was greatest on the first site visit and reduced as wetlands went dry. Precipitation samples were also collected from sites that had snow within the wetland boundary, or from sites where the volume of rainfall was sufficient to sample during a site visit. Rainfall samples were collected in 30 mL bottles, with no head space. Snow samples were melted completely and melt water was transferred to the sample bottle, while the rain samples were collected in a clean, dry container before being transferred to sample bottles.

2.2.4 Laboratory Methods

Water Isotope Analysis

Water samples were analyzed for water isotope ratios ($^{2}H/^{1}H$, $^{18}O/^{16}O$) at the University of Waterloo Environmental Isotope Laboratory (UW-EIL) by means of a Los Gatos Research Liquid Water Isotope Analyser. Results are reported in δ notation ($\delta^{2}H$, $\delta^{18}O$), which represents the permil (‰) value of the sample relative to the Vienna Standard Mean Ocean Water (VSMOW),

$$\delta^{2}\mathrm{H} \text{ or } \delta^{18}\mathrm{O} = \frac{R_{\mathrm{Sample}}}{R_{\mathrm{VSMOW}}} - 1$$

where R is the ratio of $^{2}H/^{1}H$ or $^{18}O/^{16}O$ in the sample and the VSMOW standard. All $\delta^{2}H$ and $\delta^{18}O$ values have been normalized to -428‰ and -55.5‰, respectively, using Standard Light Antarctic Precipitation (Coplen, 1996). Analytical uncertainties based on duplicate samples are ±0.8‰ for $\delta^{2}H$ and ±0.2‰ for $\delta^{18}O$.

2.2.5 Isotope Modelling

Isotopic Framework

Water isotope results for $\delta^{2}H$ and $\delta^{18}O$ were assessed using a conventional $\delta^{18}O$-$\delta^{2}H$ plot, which includes two reference lines known as the Global Meteoric Water Line (GMWL) and, for the purposes of this study, the Wetland-specific Evaporation Line (WEL). The GMWL is defined as $\delta^{2}H = 8\delta^{18}O+10$ and represents the proportional relationship between $\delta^{2}H$ and $\delta^{18}O$ in precipitation (Craig, 1961). The WEL represents the expected isotopic composition of surface water, fed by the mean annual isotope composition of precipitation, as it experiences varying degrees of evaporation. The WEL can be predicted based on the linear resistance model of

Craig and Gordon (1965) and using local atmospheric conditions (Edwards et al., 2004). Due to the expansive area covered in my study, a single, generalized WEL would not be equally representative of all wetland sites, as the WEL is sensitive to local conditions such as temperature and relative humidity. Thus, a novel approach was taken, where local climate information was used to derive a WEL specific to each individual wetland, improving the model's prediction accuracy over a large spatial extent. These WELs were used in my isotopic mass balance calculations, but to facilitate visual interpretation of my figures, I present only the regionally-averaged WEL rather than a unique WEL for each wetland. In general, a WEL is bound by two distinct end points, δ_P and δ^*. δ_P represents the isotope composition of mean annual precipitation. δ^* represents the limiting non-steady-state isotope composition, which is the maximum potential isotopic enrichment value of water in a basin, as it approaches absolute desiccation. Another key point along the WEL is δ_{SSL}, which falls between δ_P and δ^*, and represents the isotope composition of water in a closed basin at steady-state conditions, where water input is equal to that of water output (evaporation). In general, wetlands with isotopic values positioned below the WEL receive a strong influence from snowmelt, whereas wetlands with isotopic values positioned above the WEL are more strongly influenced by rainfall.

To determine the position of the WEL for each wetland, δ_P values for all site locations were obtained from www.waterisotopes.org, which uses a global dataset to calculate location-specific estimates of modern mean annual δ^2H and $\delta^{18}O$ in precipitation (Bowen and Wilkinson, 2002; Bowen and Revenaugh, 2003; Bowen et al., 2005). δ^* values for each wetland were calculated using the equation derived by Gonfiantini (1986),

$$\delta^* = (h\delta_{As}+\varepsilon_K+\varepsilon^*/\alpha^*)/(h-\varepsilon_K-\varepsilon^*/\alpha^*)$$

where h is the relative humidity, δ_{As} is the isotope composition of ambient atmospheric moisture in the summer season (Gibson and Edwards, 2002),

$$\delta_{As} = (\delta_{Ps} - \varepsilon^*)/\alpha^*$$

where δ_{Ps} is the isotopic composition of summer precipitation, obtained from www.waterisotopes.org, ε_K is the kinetic isotopic enrichment factor,

$$\text{for } \delta^{18}O \quad \varepsilon_K = 0.0142(1 - h)$$

$$\text{for } \delta^{2}H \quad \varepsilon_K = 0.0125(1 - h)$$

ε^* is the equilibrium separation factor,

$$\varepsilon^* = \alpha^* - 1$$

and α^* is the equilibrium liquid-vapour fractionation (Horita and Wesolowski, 1994),

$$\text{for } \delta^{18}O \quad 1000 \ln \alpha^* = 7.685 + 6.7123(10^3/T) - 1.6664(10^6/T^2) + 0.35041(10^9/T^3)$$

$$\text{for } \delta^{2}H \quad 1000 \ln \alpha^* = 1158.8(T^3/10^9) - 1620.1(T^2/10^6) + 794.84(T/10^3) - 161.04 + 2.9992(10^9/T^3)$$

where T represents the temperature in Kelvin. To calculate δ_{SSL} for each wetland, the following equation was used:

$$\delta_{SSL} = \alpha^*\delta_I(1\text{-}h+\varepsilon_K)+\alpha^*h\delta_{As}+\alpha^*\varepsilon_K+\varepsilon^*$$

where δ_I is the isotope composition of input water, and is assumed to equal δ_P (Gonfiantini, 1986). WELs were derived using a line through δ_P and δ^*.

Isotope Mass-Balance Calculations

Using the coupled isotope tracer method (Yi et al., 2008), δ_I and evaporation to inflow (E/I) ratios were calculated for all wetland site visits in 2014 and 2015. δ_I values were determined from the intersection of the line passing through each sampled water isotope composition and the wetland-defined δ^* with the GMWL, and were used to determine the relative importance of snowmelt and rainfall to each basin for each sampling point in time. Source water is snowmelt dominated when $\delta_I \leq \delta_P$, whereas source water is rainfall dominated when $\delta_I > \delta_P$ (e.g., Turner et al., 2014). E/I ratios for each sampling point were determined using the following equation (Edwards et al., 2004):

$$\mathrm{E/I} = (\delta_I - \delta_L)/(\delta_E - \delta_L)$$

where δ_E represents the isotope composition of evaporated vapour, and was determined by the following equation (Craig and Gordon, 1965; Gonfiantini, 1986):

$$\delta_E = [(\delta_L - \varepsilon^*)/ \alpha^* - h\delta_{AS} - \varepsilon_K]/ (1 - h + \varepsilon_K)$$

An E/I ratio equal to 1.0 indicates that evaporation is equal to input. An E/I ratio greater than 1.0 indicates that a basin is experiencing net evaporative effects (negative water balance), whereas an E/I ratio less than 1.0 signifies that a basin is receiving more water than it is losing (positive water balance).

2.2.6 Statistical Analyses

Synchrony

To test whether wetlands exhibited synchronous evaporative isotopic enrichment synchrony values were calculated for $\delta^{18}O$, $\delta^{2}H$, and E/I. This was achieved by first determining

the Pearson correlation coefficients among repeated measures of $\delta^{18}O$, $\delta^{2}H$, or E/I at each pair-wise combination of wetlands, and then averaging across all possible wetland pairs to produce a synchrony value for each response variable (as described in Patoine and Leavitt, 2006). A coefficient value of 1.0 indicates that changes in the response variable among wetlands are perfectly synchronous, whereas a coefficient value of 0.0 indicates that changes are completely independent. Confidence intervals (90%) were generated by bootstrapping with 70% resampling without replacement, to assess the statistical significance of differences in synchrony between 2014 and 2015, Grassland and Parkland, and natural and restored Parkland sites. Synchrony values with non-overlapping confidence intervals are considered statistically significantly different. All analyses were performed using SYSTAT (Systat Software, San Jose, CA).

Mann-Whitney U

Mann-Whitney *U* tests ($\alpha = 0.05$) were performed in SYSTAT (Systat Software, San Jose, CA) to determine whether $\delta^{18}O$, $\delta^{2}H$, δ_I, E/I, and water depth differed among wetlands compared between 2014 and 2015, Grassland and Parkland, and natural and restored Parkland sites. E/I values for wetlands undergoing extreme evaporation, and well beyond steady state conditions (E/I >> 1), were standardized to 1.5 for this analysis because the isotope-mass balance model does not accurately capture these conditions. A similar approach was adopted by MacDonald et al. (2017).

2.3 Results

2.3.1 Physical Measures

Water depth decreased at all wetlands as the ice-free season progressed, although some refilling was apparent after intense rainfall in late July-early August during both years. Mean water depths decreased from site visits 1-5 for all wetland groups, with the lowest mean depths occurring in the Grassland in 2015, and the highest mean depths occurring in the restored sites in the Parkland, which were only sampled in 2015 (Figure 2-3). Mann-Whitney *U* tests revealed that water depth was significantly lower in 2015 compared with 2014 on each site visit. In 2014, the Parkland and Grassland wetlands had equivalent water depth, but in 2015, water depths were significantly lower in the Grassland later in the ice-free season (Table 2-1). Contrasting the natural and restored wetlands that were sampled in the Parkland in 2015, natural wetlands had significantly lower water depths than restored wetlands on all site visits (Table 2-1).

2.3.2 Water Isotope Compositions and Water Balance Metrics

Water isotope compositions among all wetlands sampled in each year spanned a broad range (Figure 2-4; Table 2-2; Appendix E), indicating a wide range in hydrological conditions. Water isotope compositions of the subset of 24 wetlands that were sampled in both years were significantly higher in 2015 than 2014 for visits 1-4 (Table 2-1). With this in mind, comparisons between Grassland and Parkland sites were made within-year, rather than averaged across years. The isotope composition of water samples from the Grassland and Parkland spanned a similar range within-year, though Grassland sites were consistently higher than Parkland sites (Table 2-2; Appendix E), and were significantly higher for visits 1-4 in 2015 (Table 2-1). When

comparing water isotope compositions of restored and natural sites in the Parkland (2015), the range of values were highly similar (Table 2-2; Appendix E), and were not found to be significantly different, except for $\delta^{18}O$ on visit 5 (Table 2-1). The measured isotope compositions of precipitation were not used in any analyses as there were an insufficient number of samples, and many did not fall on the GMWL, indicating that they likely experienced evaporation during the collection process. Nonetheless, these data are presented in Appendix F.

The majority of surface water isotope compositions plotted below the regionally-averaged WEL throughout the study, though they started at the lowest values in May and approached the regionally-averaged WEL as the ice-free season progressed (Figure 2-4). The individual WEL slope values are displayed in Appendix G. Results indicate that the study wetlands received the majority of their input water from snowmelt during the spring and then experienced a varying degree of evaporative isotopic enrichment throughout the summer months. This seasonal trend was evident in both 2014 and 2015 (Figure 2-4a). However, wetlands in 2015 displayed a more rapid and extreme enrichment attributable to warmer and drier meteorological conditions. For the last site visit, some water isotope compositions did not follow the expected trajectory, plotting closer to the GMWL, likely due to the substantial rainfall in July (Figure 2-2c). This rainfall may have had a strong influence on the isotope composition of the wetlands because they had so little water remaining in them late in the ice-free season that even a small volume of rainwater could provoke a change in isotope composition. Seasonal isotopic patterns were similar in the Grassland and the Parkland (Figure 2-4b,c), although wetlands in the Grassland displayed more evaporative enrichment overall in

2015 (Figure 2-4b). When comparing water isotope compositions in natural to restored wetlands, both types of wetland appear to primarily receive snowmelt and to experience progressive drying throughout the summer. However, more natural wetlands desiccated than restored wetlands, with several natural wetlands being completely dry by the third site visit (Figure 2-4c).

Based on model estimates of the isotope composition of input water (δ_I), all wetlands received the majority of their water from spring snowmelt, with low δ_I values during the first site visits. However, a seasonal trend of increasing δ_I values across site visits was evident, indicating that the relative influence of rainfall increased as the summer progressed (Figure 2-5; Appendix E). The relative influence of rainfall increased gradually from visits 1 through 4, and then sharply increased for visit 5 (Figure 2-5), potentially because smaller water volumes remaining by the end of the ice-free season would be more sensitive to rainwater inputs. Contrasting measurements collected in 2014 and 2015 by repeated sampling of the same wetlands (n = 24), mean δ_I values were lower in 2014 (Figure 2-5a; Appendix E), indicating a higher influence of snowmelt in 2014 than in 2015. However, the values converged as the ice-free season progressed, with significant differences between years in visits 1 and 2, whereas visits 3-5 were similar (Figure 2-5a, Table 2-1). The means of δ_I values were similar in the Grassland and Parkland in both 2014 and 2015 (Figure 2-5b,c), although Parkland sites displayed significantly more influence of snowmelt during the first visit in 2014, and visits 1-4 in 2015 (Table 2-1). Comparing δ_I values in natural and restored wetlands, although values at the start of the 2015 ice-free season were similar, they diverged in visits 4 and 5 (Figure 2-5d), such

that by the fifth visit, restored sites showed significantly more influence from snowmelt than natural wetlands (Table 2-1).

Evaporation to inflow (E/I) ratios varied considerably among wetlands, with low values common during the first site visit, and high values becoming common later in the ice-free season (Figure 2-6). Generally, patterns with respect to seasonal progression of values between sample years, Natural Regions, and wetland origin (natural vs restored) follow those observed in δ_I values. Comparing E/I ratios for the 24 wetlands sampled in both years, values in 2015 were generally higher than in 2014 (Figure 2-6a), significantly so for visits 1, 3, and 4 (Table 2-1). In 2014, wetland E/I ratios were similar in the Grassland compared to the Parkland (Figure 2-6b). In contrast, 2015 E/I ratios were significantly higher in the Grassland than in the Parkland at the start of the ice-free season (i.e., visits 1 and 2; Figure 2-6c; Table 2-1). Note that caution must be exercised in comparing values from the fifth site visit in 2015, as only a single Grassland wetland contained sufficient water to sample on that date. Comparing natural and restored sites, E/I ratios in natural wetlands were initially similar to those in restored wetlands, but diverged as the season progressed, with E/I ratios in restored sites significantly exceeding those of natural sites by visit 5 (Figure 2-6d; Table 2-1).

2.3.3 Synchrony

Water isotope compositions were highly synchronous in both 2014 and 2015 for the subset of 24 sites sampled in both years, whereas significantly higher synchrony was observed for E/I ratios in 2015 (dry climate) compared to 2014 (normal climate; Figure 2-7a, Appendix I). In 2014, Grassland and Parkland synchrony values were similar for water isotope composition values and E/I ratios. However, synchrony was notably lower for E/I ratios than for the raw

water isotope composition values (Figure 2-7b). In 2015, Grassland sites were significantly more synchronous than Parkland sites in terms of their $\delta^{18}O$, $\delta^{2}H$, and E/I values (Figure 2-7c, Appendix I). Restored Parkland sites were significantly more synchronous than natural Parkland sites in terms of E/I values, but not for $\delta^{18}O$ or $\delta^{2}H$, which were very high for both natural and restored wetlands (Figure 2-7c).

2.4 Discussion

Our understanding of PPR wetland hydrology comes primarily from a few key study sites, which have found that water is supplied to wetlands via snowmelt in spring, and that evapotranspiration is the primary mode of water output from these systems (e.g., van der Kamp and Hayashi, 2009; Hayashi et al. 2016). Yet the universality of this understanding is untested and the shortcomings of extrapolation from a few intensively monitored sites to the expanse of the PPR has long been recognized (e.g., Conly and Van der Kamp, 2001). The aim of this research was to determine whether this hydrologic pattern of snowmelt fill and evaporative loss throughout the ice-free season is generalizable across the spatially extensive northwestern portion of the PPR. The water isotope tracer method was used to describe the hydrology of selected prairie wetlands in Alberta, and to explore the importance of seasonal and year-to-year variation in meteorological conditions, contrasting a normal climate year (2014) with a dry year (2015).

Analysis of water isotope composition and δ_I values indicates that the water balance of prairie pothole wetlands is mainly controlled by the amount of winter precipitation, which is in agreement with results found elsewhere in the PPR (e.g., Akinremi et al., 1999; van der Kamp

and Hayashi, 2008; Shook et al., 2015). Not only did wetlands display a strong isotopic signature from snowmelt during the first site visit in May, but the majority of δ_I values remained below δ_P throughout the ice-free season, indicating that summer rainfall was not a significant source of water to these wetlands and only became relatively important late in the season in wetlands that had virtually dried out through evaporation.

Further, results indicate that in Albertan prairie pothole wetlands, meteorological conditions are a stronger driver of hydrology than local differences in catchment topography or land use, as stable isotopes, water source, and evaporative influence were generally consistent across the Grassland and Parkland regions and highly synchronous across the entire study region. In fact, the level of synchrony observed in raw isotope values was extremely high indicating near perfect agreement across the study region: a range of latitude exceeding three degrees. When comparing δ_I, and E/I ratios, the differences are more pronounced between years (2014 and 2015) than between regions (Grassland and Parkland). This indicates that the hydrology is affected similarly across a large area with differing landscape features, but when meteorological conditions differ (normal climate year vs dry year), the hydrology varies. Similar to what Pham et al. (2009) found in Saskatchewan lakes, prairie pothole wetlands in Alberta experienced higher synchrony in drier conditions. Comparisons of water isotope compositions and E/I ratios showed extremely high synchronous evaporative enrichment across the study region, with E/I values being significantly higher in the dry year of 2015 than in the normal climate year of 2014. In general, this spatially extensive study supports the broad application of a climate-driven wetland hydrology model within Alberta's PPR and suggests that regional

differences are relatively minor and local. This implies that site-level differences are somewhat insignificant in determining hydrologic seasonal patterns in these wetlands.

2.4.1 Comparing a Normal Year to a Dry Year

To gain a better understanding of the effects of varying meteorological conditions on wetland hydrology, 24 wetlands were sampled in a normal climate year (2014) and in a relatively dry year (2015), and differences in water isotope composition, δ_I values, E/I ratios, and water depth were assessed. Overall, May-Aug 2015 was warmer, received less rainfall, and was less humid than the same period in 2014. This created conditions favourable for intense evaporation of wetland waters, contributing to a shorter hydroperiod in 2015. Water isotope compositions were significantly more enriched in 2015 for the majority of site visits, and more measurements plotted beyond δ_{SSL}, indicating that wetland waters were more influenced by evaporation in 2015 than in 2014.

Further demonstrating that changes in evaporation were mainly producing the difference between years, δ_I values were significantly different for only the first two site visits indicating that differences in source water between 2014 and 2015 converged during the ice-free season, whereas E/I ratios were significantly different between 2014 and 2015 for the majority of visits. Water depths were also significantly lower in 2015, compared to 2014, for all site visits.

These results agree with the findings of other authors (e.g., Euliss et al., 2004; van der Kamp and Hayashi, 2009) who conclude that hydroperiod is sensitive to variability in precipitation. Although a large amount of rainfall occurred during July and August 2015, this

did not appear to recharge wetland waters. However, δ_I values showed a stronger influence of rainfall on the fifth and final site visit for both 2014 and 2015. This is likely a consequence of a small volume of water remaining in most basins, and so even a small contribution from rainfall was able to influence the water isotope composition. Rainfall entering the wetlands earlier in the ice-free season likely failed to produce a shift in isotope composition because it was diluted by a large volume of residual snowmelt water. Thus, care must be exercised in interpreting water source from water isotope measurements collected late in the ice-free season, as wetlands have already experienced substantial water-level drawdown.

2.4.2 Comparing Natural Regions

To test for differences in wetland hydrology between the Grassland and Parkland Natural Regions, water isotope compositions, δ_I values, E/I ratios, and water depths were compared, treating samples from 2014 and 2015 separately to isolate any influence of year-to-year variation. Interestingly, although the difference in average ice-free season temperature between the two Natural Regions was consistently about 1 degree Celsius in 2014 and 2015, the difference in ice-free season precipitation between the two regions was more extreme in 2015: 42 mm less rainfall in the Grassland in 2015 compared with only 15 mm less rainfall in the Grassland in 2014. No significant differences in water isotope composition, δ_I, or E/I ratios between regions were detected in 2014, except for δ_I values during the first visit, which were lower in the Parkland. This result can be explained by recent snowmelt input to the Parkland wetlands, as evidenced by a soil moisture deficit in the Parkland at the end of April 2014 (Appendix D), indicating that snowmelt had not yet saturated the soil and thus runoff from snow must have been entering the wetlands during the first sample date.

In contrast, numerous differences between the Grassland and Parkland were evident in 2015. Water isotope compositions were significantly higher in the Grassland compared to the Parkland, suggesting greater evaporation in the Grassland. Yet, because the temperature differential between regions was not greater in 2015, it is unlikely that the difference in isotopic signature is due to a greater evaporative influence in the Grassland in 2015. Indeed, E/I ratios were only significantly higher in the Grassland than the Parkland at the start of the ice-free season (visits 1 and 2), likely because the earlier date of snowmelt in 2015 meant that the water accumulated in wetlands had already experienced substantial evaporation by the first two sampling dates relative to 2014, when the spring freshet occurred about a month later.

Though the temperature difference between Parkland and Grassland was consistent between sample years, the difference in total precipitation was notably greater in 2015, which likely contributed more than temperature to the regional differences in isotope composition in the drier 2015. The influence of precipitation in 2015 was likely stronger because the water levels were significantly lower than in 2014. Thus, the same amount of rainfall would have less influence on wetland isotope composition or E/I ratios in 2014 because it would have been diluted in a greater volume of water already in the wetland. Supporting this interpretation, δ_I values were only significantly higher in the Grassland compared with the Parkland on visit 4, which took place just after the Grassland began to receive a substantial increase in rainfall.

It is important to note that many more of the study wetlands desiccated in 2015 than in 2014, especially in the Grassland region, where only a single wetland retained ponded water on the last date of sampling. This was reflected in 2015 water depth comparisons, where wetlands were significantly shallower in the Grassland region than the Parkland for site visits 3-5. In

general, during a normal climate year, there is little difference in wetland hydrology between the Grassland and Parkland Natural Regions. However, warmer and drier conditions may amplify small differences between regions, as it appears that evaporative effects may be felt more keenly in the Grassland, which is typically warmer and drier than the Parkland. This has important implications in terms of projected climate change, as deviations in hydrologic function between the two Natural Regions may become more extreme under future climate conditions.

2.4.3 Seasonal Variation

Seasonal variation in wetland hydrology was assessed by comparing trends in hydrologic metrics across five visits spaced approximately every three weeks apart during the ice-free season (May-August) in two consecutive years. In both 2014 and 2015, similar seasonal patterns were found. For the majority of wetlands sampled in both years, an increase in $\delta^{18}O$ and $\delta^{2}H$ values occurred across the five visits due to increased influence of evaporation and a decrease in water depth (Figures 2-4 and 2-6; Appendix E). δ_I values indicated that the water source was snowmelt for the majority of wetlands in both years, with an influence from rainfall detectable only toward the end of the ice-free season, once wetland ponded water volumes were naturally reduced by evaporative losses. This strong seasonal trend was especially evident when considering the synchrony results, where $\delta^{18}O$, $\delta^{2}H$, and E/I values were highly synchronous in both years, meaning that wetlands were progressing along a similar seasonal trajectory for those parameters. This supports conclusions drawn by Pham et al. (2009), who observed high synchrony in E/I and heavy isotopes in lakes in Saskatchewan. Although climate conditions varied between 2014 and 2015, the same seasonal trends emerged in hydrologic

metrics. However, the warmer, drier conditions in 2015 strengthened the synchrony among wetlands.

2.4.4 Implications

Considering that wetlands respond synchronously across such a large spatial gradient, across different wetland classes and Natural Regions, it stands to reason that climate change will influence the hydrology of these wetlands in a similar fashion. As conflicting climate projections emerge, there is uncertainty in how meteorological conditions may evolve in the future, especially with regards to the timing and amount of precipitation (e.g., Solomon, 2007; Zhang et al., 2011). However, my results emphasize that the amount of winter precipitation and subsequent snowpack development is critical to the formation and ponded-water permanence of prairie pothole wetlands. This supports our existing understanding of how meteorological conditions influence wetland hydroperiods (e.g., Johnson et al. 2016, Hayashi et al. 2016). A decrease in snowpack, caused by higher winter temperatures and lower winter precipitation, would result in less snowmelt runoff into wetland depressions during the spring freshet, which is universally the primary source of water to prairie pothole wetlands in Alberta. An increase in summer precipitation is not likely to compensate for this loss of snowmelt runoff, as summer rains, under the current precipitation regime, do not substantially replenish the water in these wetland basins. Rather, the influence of rainfall as a water source was only evident isotopically when ponded water volumes had greatly diminished following evaporative losses that accumulated throughout the ice-free season. Results also indicate that an increase in summer temperature and a decrease in humidity would cause wetlands to drawdown and

desiccate at a faster rate, in agreement with the model by Johnson et al. (2016) and the simulations by Werner et al. (2013).

If we begin to experience shorter winters as well as warmer, drier, and longer summers, wetland ponded water periods would shift (e.g., ponded water may be present in the wetland from March to June rather than the current ice-free season from May to August). This could have serious implications for the wildlife that depend on wetlands for foraging, breeding, and habitat requirements. Researchers have already noted the risks to waterfowl (e.g., Steen et al. 2014; McLean et al. 2016; Steen et al. 2016) and even to wetland productivity (e.g., Rashford et al., 2016). Moreover, these effects on wetland diversity and productivity may not be linearly related to climate variables (Johnson et al., 2016). However, several have argued that understanding the effects of climate change on PPR wetlands depends not only on reliable climate projections, but also on understanding the role of land use or other local factors that influence wetland hydrology (e.g., Anteau et al., 2016). Yet, the strong agreement in isotopic metric values and seasonal patterns between the Grassland and Parkland Natural Regions and the overwhelmingly strong synchrony observed in this thesis indicate that these local factors are far less influential than the meteorological determinants of relative humidity and the timing and volumes of precipitation. The fact that synchrony in E/I ratios was elevated in 2015 compared with 2014 actually suggests that, if anything, the projected changes in climate will only lessen the importance of local factors. Thus, the hydrology of prairie pothole wetlands will be undeniably affected by a changing climate, but the degree to which it will be influenced depends on changes in snowpack, the timing of the spring freshet, as well as changes to temperature and humidity during the ice-free season.

The stable isotope approach was used to evaluate the success of restoration via ditch plugging at reinstating natural hydrologic patterns and functions, as mandated by the Alberta Wetland Policy (Government of Alberta, 2013). If restored sites behave differently than natural ones, it suggests that they do not provide adequate compensation for the loss of natural wetlands and that hydrologic function in a landscape context may be impaired by policies enabling wetland mitigation banking. To test whether restored wetlands mirrored the hydrologic patterns evident in natural wetlands, water isotope metrics from these wetland types were compared in the Parkland during 2015. Though the water isotope metrics in restored wetlands were almost indistinguishable to those of natural wetlands at the start of the ice-free season, values diverged as the ice-free season progressed and by the fifth visit $\delta^{18}O$, δ_I, and E/I values were significantly different between natural and restored wetlands. This is attributed to the significant difference in water depth between natural and restored wetlands, with restored wetlands being significantly deeper. Both restored and natural wetlands were originally sourced by snowmelt, but as the ice-free season progressed and wetlands dried out, the deeper restored wetlands exhibited relatively less influence of rainfall than the shallower natural wetlands (affecting $\delta^{18}O$ and δ_I values). The difference in E/I ratios between natural and restored sites on the fifth visit can be explained by the lower number of natural sites with sufficient ponded water remaining to be sampled and the lower water depth of natural sites, making them more sensitive to rainfall inputs. In fact, two fully dried natural sites refilled with rain water immediately preceding the fifth sample visit in 2015. Therefore, although the hydrological conditions of natural and restored wetlands are similar at the outset of the ice-free season, differences in basin morphology ultimately lead restored wetlands to deviate from

characteristics of natural wetlands, in terms of water source and evaporative influence. This should have consequences for the productivity and waterfowl habitat value of restored wetlands relative to natural wetlands, as wetland productivity depends on regular cycles of wet and dry periods (Euliss et al. 2004), and increases in ponded water permanence can lead to greater fish presence in PPR wetlands, which reduces their value to waterfowl (McClean et al., 2016). For restored wetlands to mirror the hydrologic patterns characteristic of natural wetlands, restoration practitioners will likely need to reconsider their design criteria and endeavour to incorporate some shallower water systems that are more prone to seasonal draw down cycles. Yet, in light of climate change projections and the vulnerability of shallow wetlands to reduced snow-pack and increased evaporation, it is possible that the deeper basins characteristic of restored wetlands will actually make them more resistant to climate change effects. Future research into the potential consequences of constructing deeper wetlands as a measure to resist the effects of climate change is warranted to determine what the net consequences would be for waterfowl and wildlife.

In conclusion, the water isotope tracer method was a valuable tool in testing whether our conceptual understanding of prairie pothole wetland hydrology can be universally generalized to wetlands across Alberta's PPR, even though it was derived largely from the study of a few, isolated long-term monitoring stations in other states or provinces. The cost-effective and time saving approach enabled characterization of seasonal, inter-annual, and inter-regional differences in wetland water source and evaporative influence across a broad spatial extent. From this, I was able to draw conclusions about the success of wetland restoration and the risks

of climate change to wetland hydrology, and by extension to wetland productivity and waterfowl habitat value.

2.5 Figures

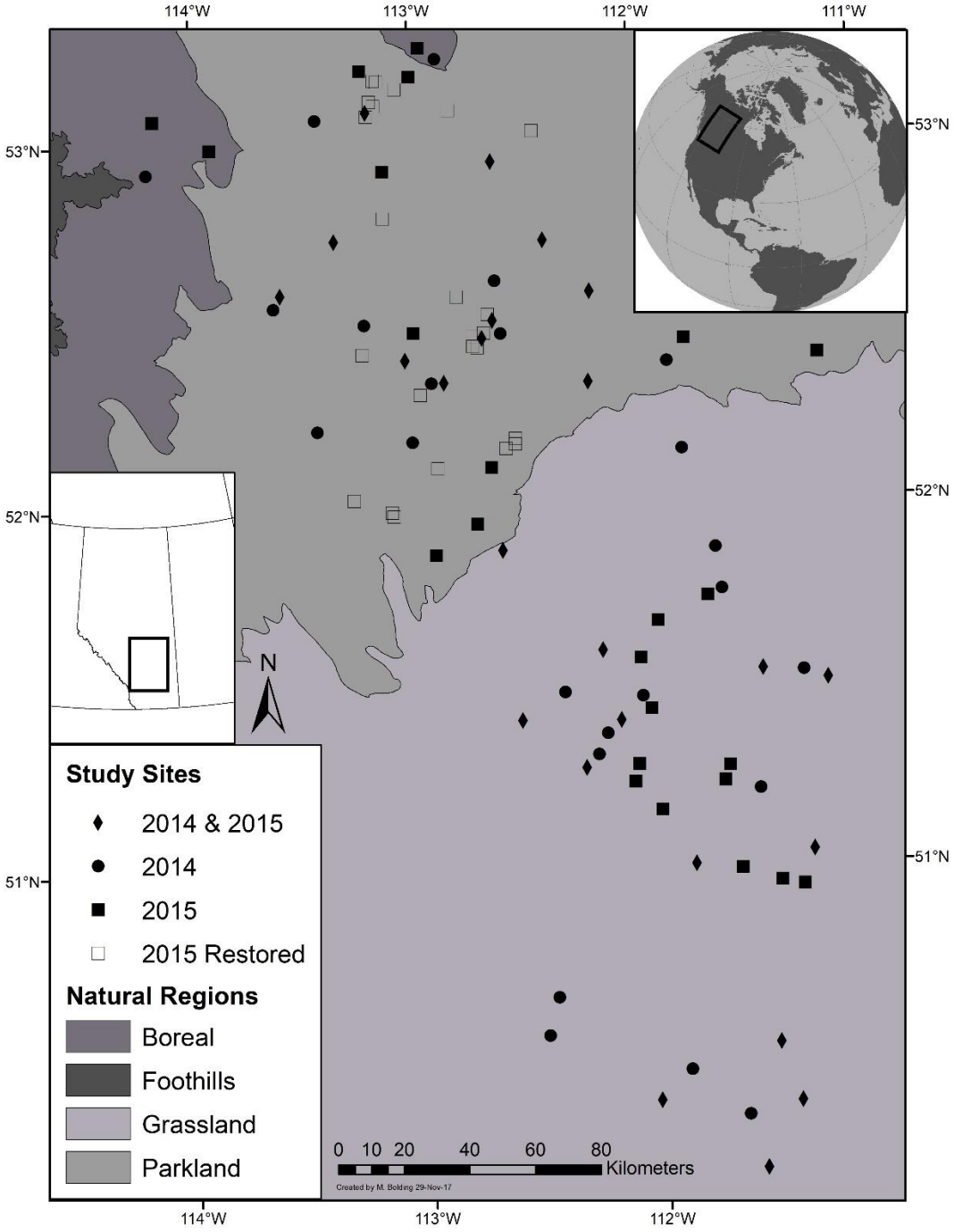

Figure 2-1. Study wetlands as located within the Parkland and Grassland Natural Regions of Alberta. Symbology reflects the year each wetland was sampled for water isotope composition.

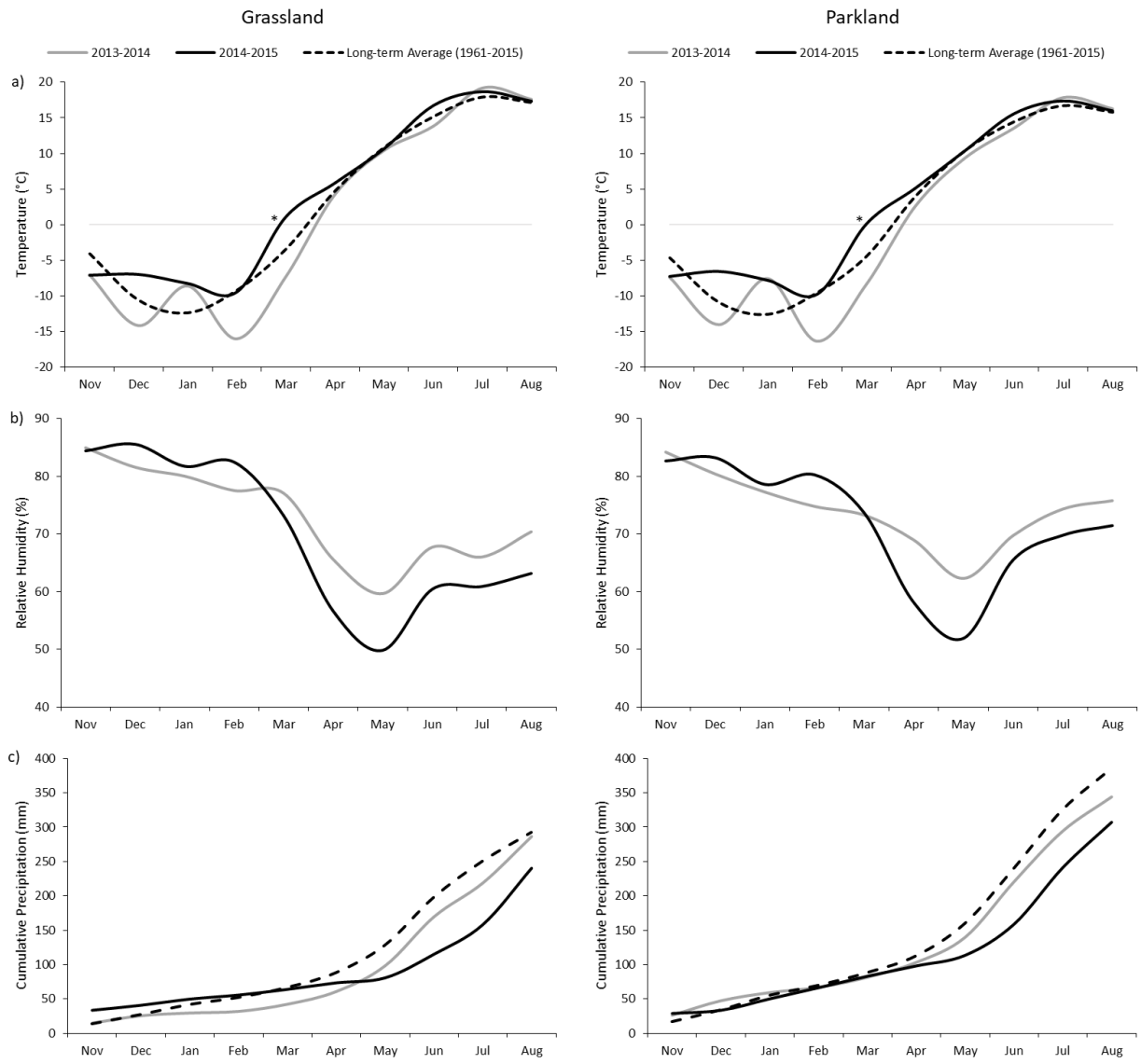

Figure 2-2. Average monthly temperature, relative humidity, and cumulative precipitation for the Alberta Grassland and Parkland study regions from November to August 2013-2014 and 2014-2015 (from Alberta AgroClimatic Information Service meteorological stations). Long-term average (1961-2015) temperature and cumulative precipitation also shown. Asterisk (*) highlights the earlier thaw in 2015, compared to 2014.

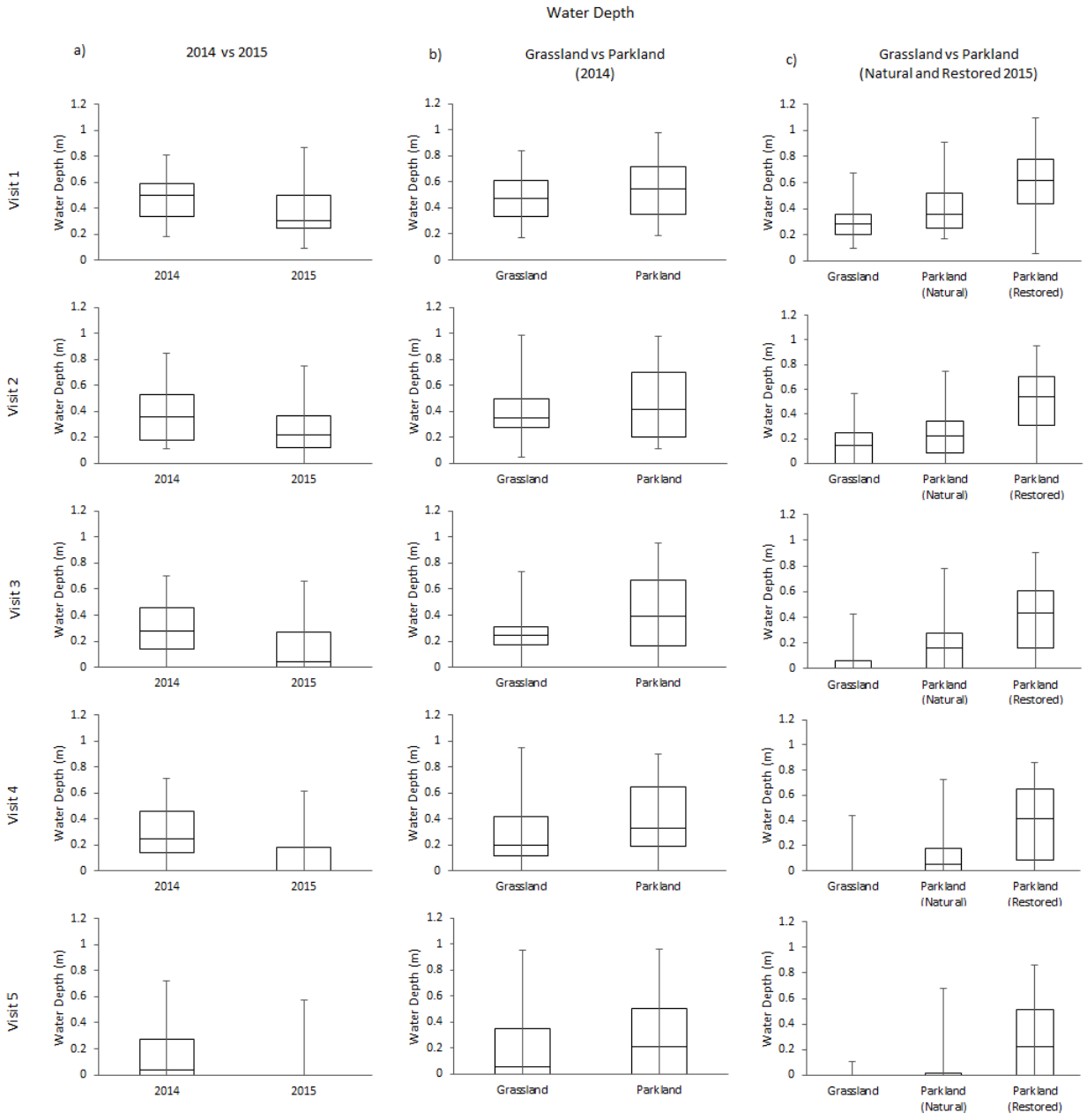

Figure 2-3. Water depths displayed in boxplots for each site visit of the 96 study wetlands, comparing 24 sites across two years (first column), 24 sites in the Grassland to 24 sites in the Parkland in two separate years (middle and last column), and 24 natural sites to 24 restored sites in the Parkland in 2015 (last column).

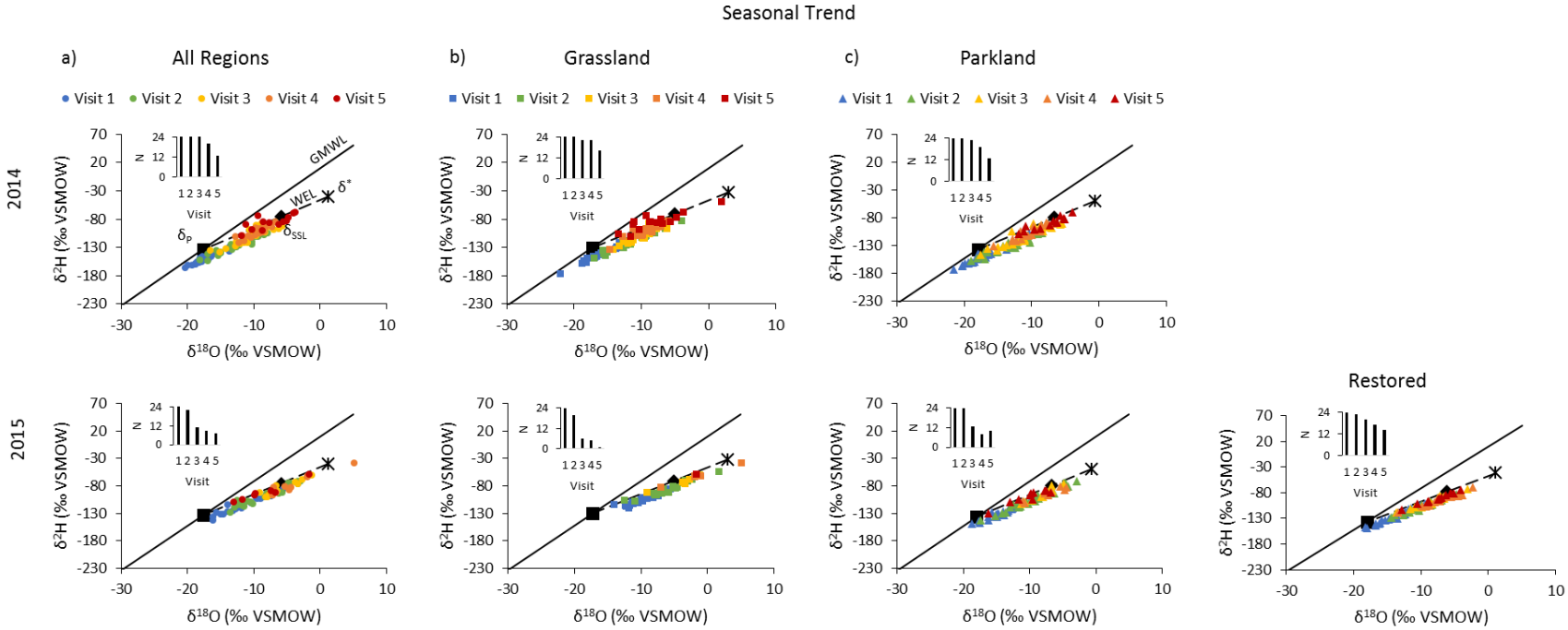

Figure 2-4. Water isotope compositions for the 96 study wetlands located in the Grassland and Parkland regions, sampled 1-5 times from May through August in 2014 and 2015. All Regions column displays the 24 wetlands sampled in both 2014 and 2015. Grassland and Parkland columns display the 24 wetlands sampled from each Natural Region in each year. Restored column displays the 24 restored wetlands sampled in 2015, in the Parkland region. Inset bar charts show the number of wetlands sampled during each visit (i.e., water samples could not be collected from dry basins). WELs displayed were calculated based on an average of δ_P, δ_{SSL}, and δ^* values from wetlands within each separate comparison. Values used to define regionally-averaged WELs are located in Appendix H.

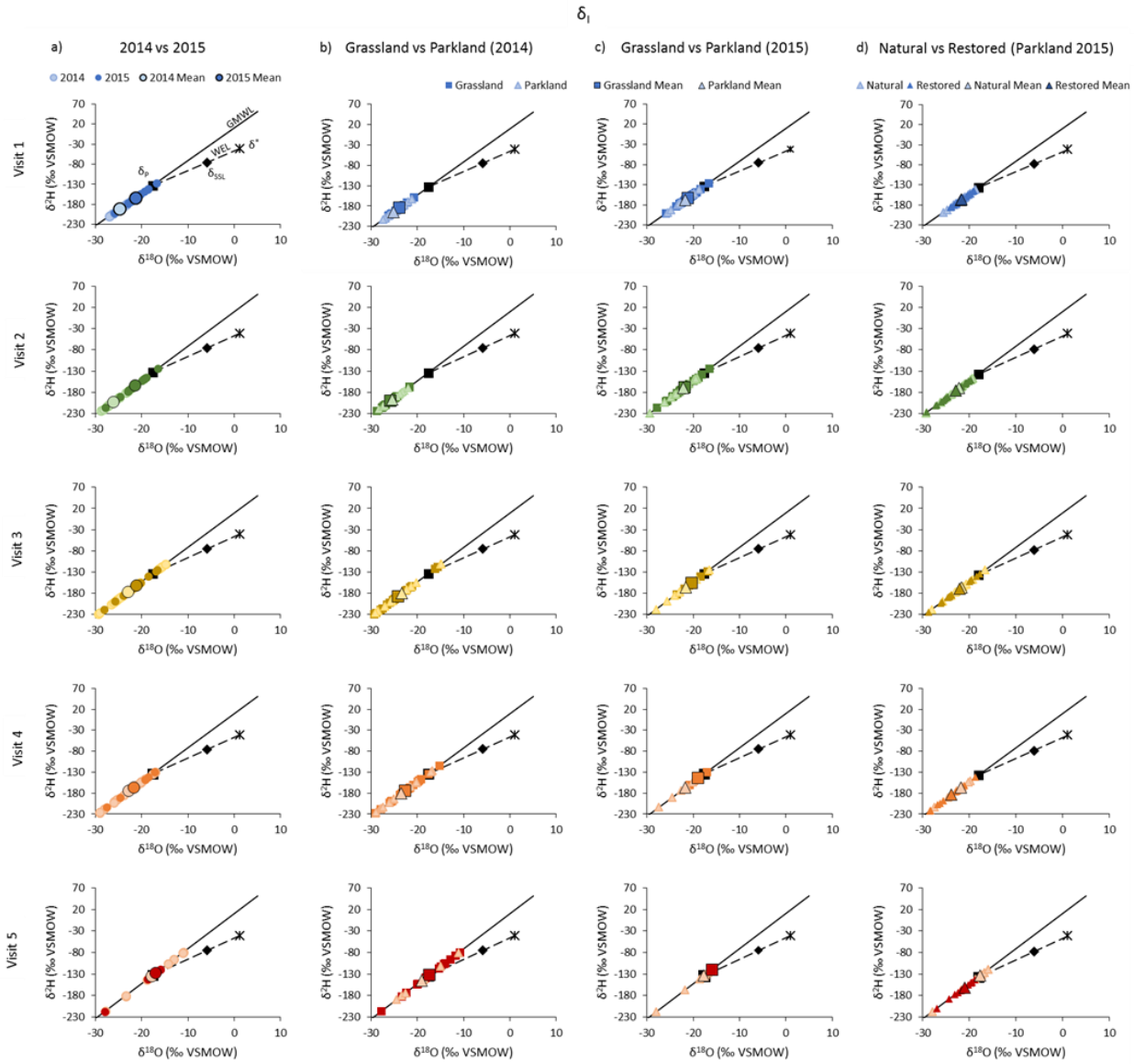

Figure 2-5. Isotope compositions of the input water (δ_I) for each site visit of the 96 study wetlands, comparing 24 sites across two years (first column), 24 sites in the Grassland to 24 sites in the Parkland in two separate years (middle columns), and 24 natural sites to 24 restored sites in the Parkland in 2015 (last column). WELs displayed were calculated based on an average of δ_P, δ_{SSL}, and δ^* values from wetlands within each separate comparison. Values used to define regionally-averaged WELs are located in Appendix H.

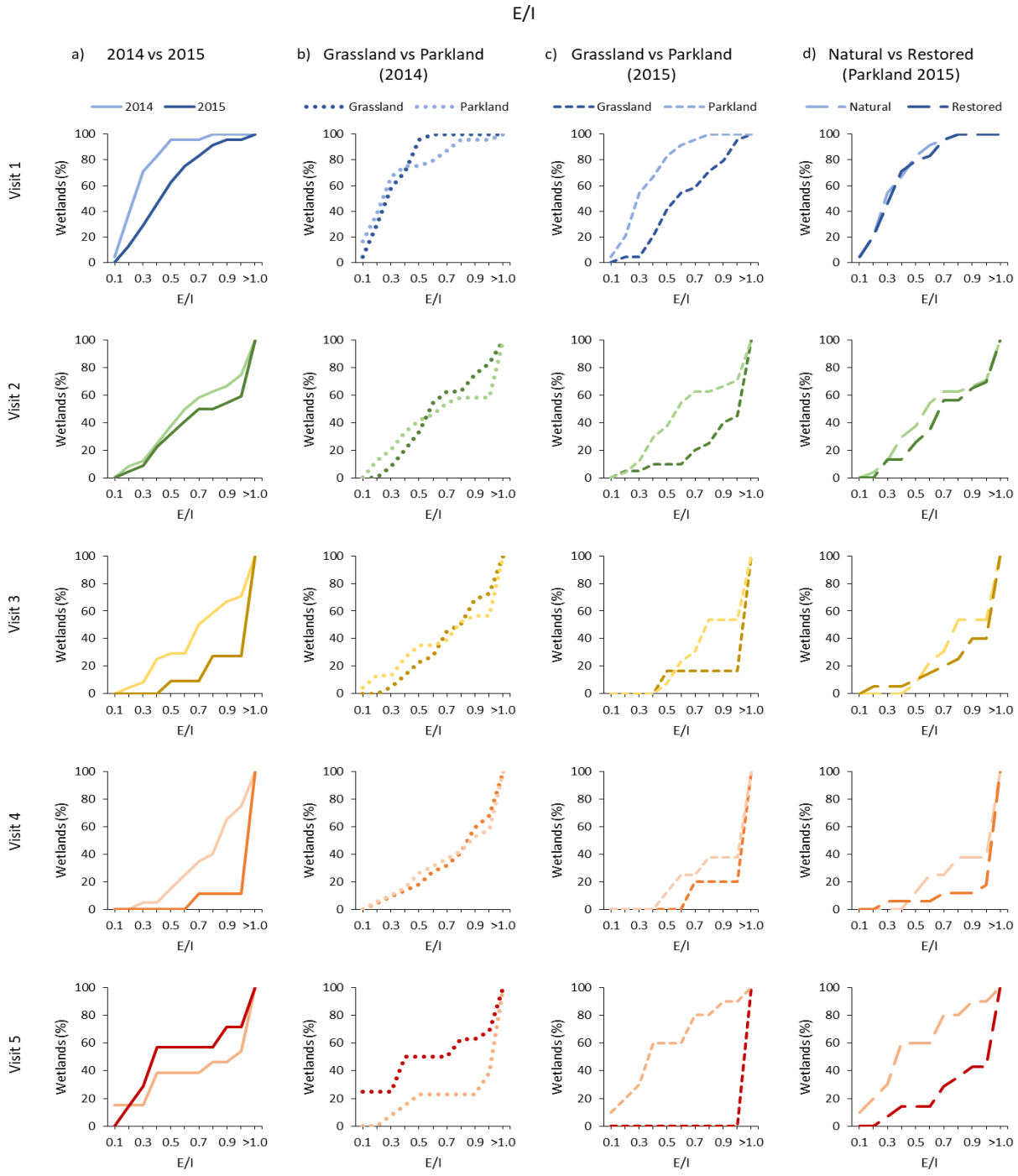

Figure 2-6. Cumulative proportions of evaporation to inflow ratios (E/I) for each site visit of the 96 study wetlands, comparing 24 sites across two years (first column), 24 sites in the Grassland to 24 sites in the Parkland in two separate years (middle columns), and 24 natural sites to 24 restored sites in the Parkland in 2015 (last column). Note that the number of samples declines with each visit because water samples could not be collected from dry basins (see Figure 2-4 inset for per visit sample size).

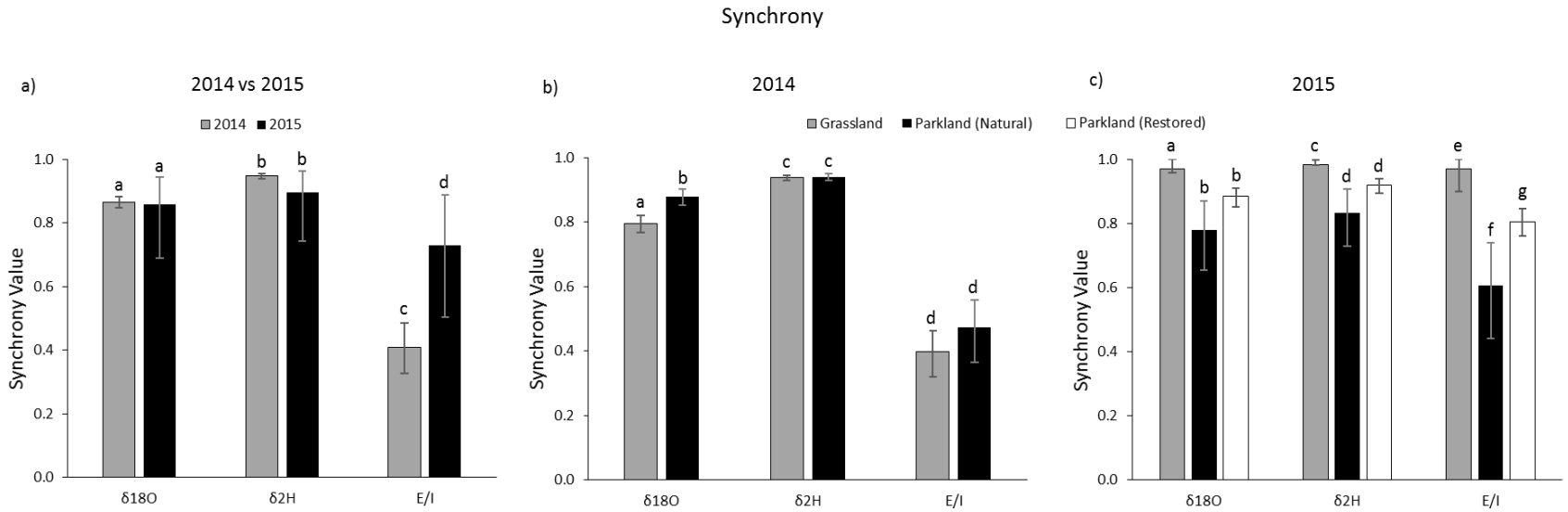

Figure 2-7. Synchrony values for $\delta^{18}O$, $\delta^{2}H$, and E/I ratios comparing a) 24 sites across two years, b) and c) 24 sites in the Grassland to 24 sites in the Parkland in two separate years, and c) 24 natural sites to 24 restored sites in the Parkland in 2015. 90% confidence intervals of the mean shown, where intervals sharing a letter are not significantly different.

2.6 Tables

Table 2-1. Mann-Whitney *U* test results comparing raw isotope values, δ_I values, E/I ratios, and water depth among wetlands in different years, regions, and natural/restored status. Asterisk (*) beside significant values.

Response Variable	Site Visit	2014 vs 2015				2014 Grassland vs Parkland			
		U-statistic	*p*-value		N (2014, 2015)	*U*-statistic	*p*-value		N (Grassland, Parkland)
$\delta^{18}O$	1	47.0	<0.00001	*	24, 24	341.0	0.27446		24, 24
	2	108.0	0.00060	*	24, 22	337.0	0.31232		24, 24
	3	25.0	0.00014	*	24, 11	298.0	0.30689		22, 23
	4	2.0	0.00003	*	20, 9	280.0	0.06342		22, 19
	5	57.0	0.36214		13, 7	91.0	0.56862		16, 13
$\delta^{2}H$	1	21.0	<0.00001	*	24, 24	353.0	0.18016		24, 24
	2	64.0	0.00001	*	24, 22	341.0	0.27446		24, 24
	3	28.0	0.00022	*	24, 11	278.0	0.57028		22, 23
	4	12.0	0.00024	*	20, 9	275.0	0.08443		22, 19
	5	63.0	0.16552		13, 7	129.0	0.27294		16, 13
δ_I	1	41.0	<0.00001	*	24, 24	398.0	0.02332	*	24, 24
	2	46.0	0.00005	*	24, 22	128.0	0.34385		24, 24
	3	75.0	0.28071		24, 11	155.0	0.69023		22, 23
	4	43.0	0.46336		20, 9	196.0	0.33758		22, 19
	5	32.0	0.76970		13, 7	66.0	0.10208		16, 13
E/I	1	145.0	0.00319	*	24, 24	302.0	0.77283		24, 24
	2	223.0	0.35884		24, 22	272.0	0.73833		24, 24
	3	68.0	0.01784	*	24, 11	251.0	0.96294		22, 23
	4	35.0	0.00658	*	20, 9	205.0	0.91461		22, 19
	5	53.0	0.53920		13, 7	62.0	0.05356		16, 13
Water Depth	1	338.5	0.04899	*	24, 24	183.0	0.40152		24, 24
	2	386.0	0.04325	*	24, 24	254.0	0.48317		24, 24
	3	410.5	0.01053	*	24, 24	213.0	0.12157		24, 24
	4	388.5	0.00496	*	24, 24	213.0	0.17880		24, 24
	5	345.0	0.04108	*	24, 24	269.5	0.69206		24, 24

Table 2-1 (continued)

Response Variable	Site Visit	2015 Grassland vs Parkland				2015 Parkland Natural vs Restored			
		U-statistic	*p*-value		N (Grassland, Parkland)	*U*-statistic	*p*-value		N (Natural, Restored)
$\delta^{18}O$	1	522.0	<0.00001	*	24, 24	279.0	0.85278		24, 24
	2	394.0	0.00028	*	20, 22	259.0	0.71751		22, 23
	3	69.0	0.00851	*	6, 13	123.0	0.79648		13, 20
	4	36.0	0.01917	*	5, 8	63.0	0.77084		8, 17
	5	10.0	0.11385		1, 10	29.0	0.01636	*	10, 14
$\delta^{2}H$	1	528.0	<0.00001	*	24, 24	278.0	0.83664		24, 24
	2	411.0	0.00006	*	20, 22	254.0	0.63965		22, 23
	3	72.0	0.00380	*	6, 13	119.0	0.68527		13, 20
	4	38.0	0.00842	*	5, 8	63.0	0.77084		8, 17
	5	10.0	0.11385		1, 10	41.0	0.08950		10, 14
δ_I	1	343.0	0.25676		24, 24	286.0	0.96711		24, 24
	2	202.0	0.94602		20, 22	260.0	0.48106		22, 23
	3	52.0	0.25421		6, 13	134.0	0.49616		13, 20
	4	22.0	0.03301	*	5, 8	44.0	0.26892		8, 17
	5	9.0	0.20590		1, 10	113.0	0.01181	*	10, 14
E/I	1	474.0	0.00013	*	24, 24	281.0	0.88523		24, 24
	2	340.5	0.01412	*	20, 22	243.5	0.48335		22, 23
	3	50.0	0.28285		6, 13	109.0	0.39802		13, 20
	4	24.0	0.47450		5, 8	54.0	0.27644		8, 17
	5	9.5	0.15379		1, 10	26.0	0.00814	*	10, 14
Water Depth	1	196.5	0.05912		24, 24	152.0	0.00504	*	24, 24
	2	221.5	0.16963		24, 24	126.5	0.00087	*	24, 24
	3	194.5	0.03554	*	24, 24	161.0	0.00801	*	24, 24
	4	190.0	0.01808	*	24, 24	148.0	0.00337	*	24, 24
	5	226.0	0.03731	*	24, 24	178.0	0.01130	*	24, 24

Table 2-2. Range and mean of stable isotope composition of wetland waters, spanning all site visits.

Comparison	Wetlands (n)	Range of $\delta^{18}O$ (‰)	Mean of $\delta^{18}O$ (‰)	Range of $\delta^{2}H$ (‰)	Mean of $\delta^{2}H$ (‰)
2014 vs 2015	2014 (24)	-20.3 to -3.8	-11.8	-166.4 to -68.0	-117.7
	2015 (24)	-16.2 to 5.1	-8.5	-141.9 to -38.1	-98.1
2014	Grassland (24)	-22.1 to 1.9	-11.2	-176.1 to -49.4	-113.0
	Parkland (24)	-21.6 to -4.0	-12.2	-172.5 to -69.8	-119.9
2015	Grassland (24)	-14.0 to 5.1	-6.7	-120.2 to -38.1	-89.2
	Natural Parkland (24)	-18.7 to -2.9	-10.6	-149.3 to -71.6	-109.3
	Restored Parkland (24)	-18.3 to -2.3	-9.6	-148.5 to -69.3	-104.7

3. General Conclusions

The aim of my thesis was to test whether our current understanding of prairie pothole wetland hydrology is supported by data collected across a large spatial extent, particularly with respect to water source and evaporative influence. To better understand the temporal and spatial drivers of wetland hydrology, I used isotope tracers to examine differences in water balance metrics (namely isotopic composition of input water (δ_I) and evaporation to inflow (E/I) ratios) between a normal climate year and a relatively dry year, as well as between the Grassland and Parkland Natural Regions, and finally between natural wetlands and restored ones. I hypothesized that evaporative influences would be stronger in a relatively dry year, though source water would be primarily from snowmelt in both the dry and more normal climate years. I further hypothesized that the Grassland would be more subject to evaporative influences than the Parkland, due to regional differences in climate. However, I also hypothesized that water balance metrics would exhibit high synchrony within and across regions, because the broad influence of climate would overshadow local influences on isotope tracers. Lastly, I hypothesized that restored wetland water balance metrics would differ from those in wetlands of natural origin, due primarily to their greater depth and hydrologic connectivity in comparison with natural wetlands in the Parkland. My findings are in agreement with many studies of PPR wetlands (e.g., Pham et al., 2009; Niemuth et al., 2010; Hayashi et al., 2016), in that the hydroperiod and water balance are highly influenced by precipitation inputs during the winter months, and subsequent snowmelt.

When using the water isotope tracer method to capture hydrological conditions of prairie pothole wetlands, wetland-specific measurements of temperature and relative humidity more accurately estimate framework values than regional averages. Although it may be appropriate to use average temperature and humidity values across some landscapes, it is not appropriate in this study, due to the large spatial extent, as well as the evaporative nature of prairie pothole wetlands. In an attempt to reduce model error and increase accuracy, framework parameters were unique to each wetland, using measurements from the nearest meteorological station to construct wetland-specific WELs. The use of wetland-specific WELs was a major innovation in my approach to apply a stable isotope tracer method to elucidate the hydrologic processes operating in NPPR wetlands in Alberta.

A key assumption of the isotope mass-balance model is that measurements represent steady-state conditions. As prairie pothole wetlands naturally evaporate over time, conditions are unlikely to be at steady-state for all measurements over the course of a season. Although PPR wetlands violate this assumption of the steady-state model, the mass-balance metrics yielded are still meaningful, as the model is robust, and has been used successfully in several other studies that have knowingly violated this assumption (e.g., Pham et al., 2009; Brooks et al., 2014; MacDonald et al., 2017). To address occasions where conditions in the wetland exceeded the capacity of the framework to calculate E/I ratios, I replaced the calculated value with a measure of 1.5 to represent that evaporation was dominant for that sample.

It would perhaps be more appropriate to employ a non-steady-state mass-balance model to this particular dataset, since the wetlands in this study were all operating under non-steady-state conditions. However, the accepted non-steady-state model requires a

measurement of basin volume, which was not possible to acquire for the sites in this study. Therefore, it would have been less economical and more time intensive to employ a non-steady-state model. Given the findings of this study, the steady-state model has proven to be an effective method to estimate hydrologic parameters such as δ_I and E/I ratios, and use these results comparatively across a large region as has been done elsewhere (e.g. Gibson and Edwards, 2002; Brooks et al., 2014; Turner et al., 2014). It was not possible to install MET stations and piezometers at every site; therefore, the influence of groundwater on the wetlands is unknown. However, groundwater is most likely snow-fed in this region (van der Kamp and Hayashi, 2008), and it would be impossible to distinguish snowmelt from groundwater based on isotopic signature of wetlands alone. It is possible that some wetlands may have been influenced by groundwater later in the season, but there was no definitive way to capture and assess that within the bounds of this study. It is possible that wetlands maintaining a steadily depleted input signature throughout the course of the season would be fed by groundwater, but this could only be postulated.

My research results indicate a need to review restoration practices for prairie pothole wetlands. Although restored wetlands appear to be hydrologically similar to natural wetlands in terms of water source and evaporative influence, restored wetlands were deeper and had a longer hydroperiod, on average, than the natural wetlands in this study. Therefore, the natural range in permanence class characteristic of wetlands in the region may not be accurately reflected in restored wetlands. Restored wetlands appear to be more permanent in nature, which is not representative of the distribution of natural wetland permanence classes across the landscape. Many wetland restoration designs aim to restore systems to their historic

condition, but if we are making PPR wetlands too deep, we are not achieving that objective. To achieve a functional equivalence, some wetlands should be restored as isolated, ephemeral systems, which are more influenced by evaporation, and less hydrologically connected. Although, it would not be recommended to eliminate the deeper systems entirely, as they may prove to be more resistant to the hydrologic impacts of climate change. Further research, in terms of the implications of different wetland designs for resistance to climate change effects and habitat value for diverse biota, is needed.

More research is needed to predict climate change effects in this region in order to properly manage PPR wetlands. Multiple models predict a decrease in winter precipitation which would greatly influence these systems. Since we know that PPR wetlands are primarily fed by snowmelt, a decrease in winter precipitation would dramatically reduce the amount of water available to wetlands in this region, presumably reducing hydroperiod as well as affecting the available moisture in the region in late summer (as many more wetlands would have evaporated by that time, leaving less water to evaporate off of the land and return to the atmosphere, possibly leading to an even drier climate regime). Continued water isotope monitoring would be valuable to track whether our ideas about climate change are really reflecting changes in the water balance of these systems. Other regions should consider adopting this isotopic tracer approach in order to validate conceptual understandings of hydrologic drivers of wetland function.

4. References

Akinremi, O.O., Mcginn, S.M., Cutforth, H.W., 1999. Precipitation trends on the Canadian prairies. J. Clim. 12, 2996–3003.

Alberta Environment and Sustainable Resource Development (ESRD). 2015. Alberta Wetland Classification System. Water Policy Branch, Policy and Planning Division, Edmonton, AB.

Anteau, M.J., Wiltermuth, M.T., van der Burg, M.P., Pearse, A.T., 2016. Climate trends of the North American prairie pothole region 1906-2000. Wetlands 36, 407–421. https://doi.org/10.1007/s13157-016-0766-3

Bethke, R. W., & Nudds, T. D., 1995. Effects of Climate Change and Land Use on Duck Abundance in Canadian Prairie-Parklands. *Ecological Applications*, *5*(3), 588–600. http://doi.org/10.2307/1941969

Bodhinayake, W., Si, B.C., 2004. Near-saturated surface soil hydraulic properties under different land uses in the St Denis National Wildlife Area, Saskatchewan, Canada. Hydrol. Process. 18, 2835–2850. https://doi.org/10.1002/hyp.1497

Bouchard, F., Turner, K.W., MacDonald, L.A., Deakin, C., White, H., Farquharson, N., Medeiros, A.S., Wolfe, B.B., Hall, R.I., Pienitz, R., Edwards, T.W.D., 2013. Vulnerability of shallow subarctic lakes to evaporate and desiccate when snowmelt runoff is low. Geophys. Res. Lett. 40, 6112–6117. https://doi.org/10.1002/2013GL058635

Bowen, G.J., Revenaugh, J., 2003. Interpolating the isotopic composition of modern meteoric precipitation. Water Resour. Res. 39, n/a-n/a. https://doi.org/10.1029/2003WR002086

Bowen, G.J., Wassenaar, L.I., Hobson, K.A., 2005. Global application of stable hydrogen and oxygen isotopes to wildlife forensics. Oecologia 143, 337–348. https://doi.org/10.1007/s00442-004-1813-y

Bowen, G.J., Wilkinson, B., 2002. Spatial distribution of δ18O in meteoric precipitation. Geology 30. https://doi.org/10.1130/0091-7613(2002)030<0315:SDOOIM>2.0.CO;2

Bragg T. B., 1995. The physical environment of Great Plains grasslands. In: Joern A, Keeler KH (eds) The changing prairie: North American grasslands. Oxford University Press, New York, pp 49–81.

Brooks, J.R., Gibson, J.J., Jean Birks, S., Weber, M.H., Rodecap, K.D., Stoddard, J.L., 2014. Stable isotope estimates of evaporation : inflow and water residence time for lakes across the United States as a tool for national lake water quality assessments. Limnol. Oceanogr. 59, 2150–2165. https://doi.org/10.4319/lo.2014.59.6.2150

Bryson RA, Hare FK (eds), 1974. World survey of climatology. Climates of North America, vol 11. Elsevier, New York, p 420

Clark, I.D., and Fritz, P. 1997. *Environmental Isotopes in Hydrogeology*. Boca Ranton, Florida, CRC Press. 328.

Conly, M., Van der Kamp, G., 2001. Monitoring the hydrology of Canadian prairie wetlands to detect the effects of climate change and land use changes. Environ. Monit. Assess. 67, 195–215. https://doi.org/10.1023/A:1006486607040

Coplen, T. B., 1996. New guidelines for reporting stable hydrogen, carbon, and oxygen isotope-ratio data. Geochimica et Cosmochimica Acta, 60(17), 3359-3360.

Craig, H., 1961. Isotopic variations in meteoric waters. *Science*, *133*(3465), 1702-1703.

Craig, H., and Gordon, L. J. 1965. Deuterium and oxygen 18 variations in the ocean and the marine atmosphere. In Tongiorgi, E. (ed.), Stable Isotopes in Oceanographic Studies and Paleotemperatures. Pisa, Italy: Laboratorio di Geologia Nucleare. 9–130.

Downing, D. J., & Pettapiece, W. W., 2006. Natural Regions and Subregions of Alberta, Natural Regions Committee. *Government of Alberta, Alberta*.

[DUC] Ducks Unlimited Canada, 2008. The impacts of wetland loss. Information Sheet, Ducks Unlimited Canada, 4pp.

Dumanski, S., Pomeroy, J.W., Westbrook, C.J., 2015. Hydrological regime changes in a Canadian Prairie basin. Hydrol. Process. 29, 3893–3904. https://doi.org/10.1002/hyp.10567

Edwards, T. W. D., Wolfe, B. B., Gibson, J. J., & Hammarlund, D., 2004. Use of water isotope tracers in high latitude hydrology and paleohydrology. In *Long-term environmental change in Arctic and Antarctic Lakes* (pp. 187-207). Springer Netherlands.

Euliss, N.H., LaBaugh, J.W., Fredrickson, L.H., Mushet, D.M., Laubhan, M.K., Swanson, G. a., Winter, T.C., Rosenberry, D.O., Nelson, R.D., 2004. The wetland continuum: A conceptual framework for interpreting biological studies. Wetlands 24, 448–458. https://doi.org/10.1672/0277-5212(2004)024[0448:TWCACF]2.0.CO;2

Fang, X., Pomeroy, J.W., 2009. Modelling blowing snow redistribution to prairie wetlands. Hydrol. Process. 23. https://doi.org/10.1002/hyp.7348

Fang, X., Pomeroy, J.W., Westbrook, C.J., Guo, X., Minke, A.G., Brown, T., 2010. Prediction of snowmelt derived streamflow in a wetland dominated prairie basin. Hydrol. Earth Syst. Sci. 14, 991–1006. https://doi.org/10.5194/hess-14-991-2010

Gat, J.R., 1980. The isotopes of hydrogen and oxygen in precipitation. In: P. Fritz and J.-Ch. Fontes (Eds), Handbook of Environmental Isotope Geochemistry, Vol. 1, The Terrestrial Environment., A. Elsevier, Amsterdam, pp. 21-48.

Gedzelman, S. D., and R. Arnold. 1994. Modeling the isotopic composition of precipitation. J. Geophys. Res. 99, 10455–10472.

Gibson, J.J., Birks, S.J., Yi, Y., 2016. Stable isotope mass balance of lakes: A contemporary perspective. Quat. Sci. Rev. 131. https://doi.org/10.1016/j.quascirev.2015.04.013

Gibson, J.J., Birks, S.J., Yi, Y., Moncur, M.C., McEachern, P.M., 2016. Stable isotope mass balance of fifty lakes in central Alberta: Assessing the role of water balance parameters in

determining trophic status and lake level. J. Hydrol. Reg. Stud. 6, 13–25. https://doi.org/10.1016/j.ejrh.2016.01.034

Gibson, J.J., Edwards, T.W.D., 2002. Regional water balance trends and evaporation-transpiration partitioning from a stable isotope survey of lakes in northern Canada. Global Biogeochem. Cycles 16, 10-1-10–14. https://doi.org/10.1029/2001GB001839

Gonfiantini, R., 1986. Environmental isotopes in lake studies. In Fritz, P., and Fontes, J. C. (eds.), Handbook of Environmental Isotope Geochemistry. New York: Elesvier. Vol. 2: 113–168.

Goverment of Alberta, 2013. Alberta Wetland Policy. Environment & Sustainable Resource Development, Water Policy Branch, Edmonton, AB.

Granger, R.J., Gray, D.M., Dyck, G.E., 1984. Snowmelt infiltration to frozen Prairie soils. Can. J. Earth Sci. 21, 669–677. https://doi.org/10.1139/e84-073

Gray, D.M., Landine, P.G., 1988. An energy-budget snowmelt model for the Canadian Prairies. Can. J. Earth Sci. 25.

Hayashi, M., van der Kamp, G., Rudolph, D.L., 1998. Water and solute transfer between a prairie wetland and adjacent uplands, 1. Water balance. J. Hydrol. 207 (1–2), 42–55.

Hayashi, M., van der Kamp, G., Rosenberry, D.O., 2016. Hydrology of Prairie Wetlands: Understanding the Integrated Surface-Water and Groundwater Processes. Wetlands 36. https://doi.org/10.1007/s13157-016-0797-9

Horita, J., Wesolowski, D.J., 1994. Liquid-vapor fractionation of oxygen and hydrogen isotopes of water from the freezing to the critical temperature. Geochim. Cosmochim. Acta 58. https://doi.org/10.1016/0016-7037(94)90096-5

Jessop, J., Spyreas, G., Pociask, G.E., Benson, T.J., Ward, M.P., Kent, A.D., Matthews, J.W., 2015. Tradeoffs among ecosystem services in restored wetlands. Biol. Conserv. 191, 341–348. https://doi.org/10.1016/j.biocon.2015.07.006

Johnson, R.R., and K.F. Higgins. 1997. Wetland Resources of Eastern South Dakota. Brookings, SD: South Dakota State University Press.

Johnson, R.R., Oslund, F.T., Hertel, D.R., 2008. The past, present, and future of prairie potholes in the United States. J. Soil Water Conserv. 63.

Johnson, W.C., Werner, B. & Guntenspergen, G.R., 2016. Non-linear responses of glaciated prairie wetlands to climate warming. Climatic Change. 134: 209. https://doi.org/10.1007/s10584-015-1534-8

Johnson, W.C., Werner, B., Guntenspergen, G.R., Voldseth, R.A., Millett, B., Naugle, D.E., Tulbure, M., Carroll, R.W.H., Tracy, J., Olawsky, C., 2010. Prairie Wetland Complexes as Landscape Functional Units in a Changing Climate. Bioscience 60, 128–140. https://doi.org/10.1525/bio.2010.60.2.7

LaBaugh J, Winter T, and Rosenberry D. 1998. Hydrologic Functions of Prairie Wetlands. *Gt Plains Res A J Nat Soc Sci*.

Laird, K. R., Fritz, S. C., Maasch, K. A., and Cumming, B. F., 1996. Greater drought intensity and frequency before AD1200 in the Northern Great Plains, USA. *Nature* 384: 552–554.

Macdonald, L.A., Wolfe, B.B., Turner, K.W., Anderson, L., Arp, C.D., Birks, S.J., Bouchard, F., Edwards, T.W.D., Farquharson, N., Hall, R.I., Mcdonald, I., Narancic, B., Ouimet, C., Pienitz, R., Tondu, J., White, H., 2017. A synthesis of thermokarst lake water balance in high-latitude regions of North America from isotope tracers 1 149, 118–149.

McLean KI, Mushet DM, Stockwell CA, 2016. From "Duck Factory" to "Fish Factory": Climate Induced Changes in Vertebrate Communities of Prairie Pothole Wetlands and Small Lakes. Wetlands 36:1–15. doi: 10.1007/s13157-016-0766-3

Moreno-Mateos, D., Power, M.E., Comín, F.A., Yockteng, R., 2012. Structural and functional loss in restored wetland ecosystems. PLoS Biol. 10. https://doi.org/10.1371/journal.pbio.1001247

Niemuth, N.D., Wangler, B., Reynolds, R.E., 2010. Spatial and Temporal Variation in Wet Area of Wetlands in the Prairie Pothole Region of North Dakota and South Dakota. Wetlands 30, 1053–1064. https://doi.org/10.1007/s13157-010-0111-1

Ojima, D. S, Lackett, J. M., 2002. Preparing for a Changing Climate: The Potential Consequences of Climate Variability and Change—Central Great Plains. Central Great Plains Steering Committee and Assessment Team, Colorado State University.

Patoine, A., Leavitt, P.R., 2006. Century-Long Synchrony of Fossil Algae in a Chain of Canadian

Prairie Lakes Published by : Ecological Society of America 87, 1710–1721.

Pham, S. V., Leavitt, P.R., McGowan, S., Wissel, B., Wassenaar, L.I., 2009. Spatial and temporal variability of prairie lake hydrology as revealed using stable isotopes of hydrogen and oxygen. Limnol. Oceanogr. 54, 101–118. https://doi.org/10.4319/lo.2009.54.1.0101

Rashford, B.S., Adams, R.M., Wu, J.J., Voldseth, R.A., Guntenspergen, G.R., Werner, B., Johnson, W.C., 2016. Impacts of climate change on land-use and wetland productivity in the Prairie Pothole Region of North America. Reg. Environ. Chang. 16. https://doi.org/10.1007/s10113-015-0768-3

Rozanski K., Araguas-Araguas, L., Gonfiantini, R., 1993. Isotopic patterns in modern global precipitation. American Geophysical Union, Geophysical Monograph 78, 1-35.

Rusak, J. a., Yan, N.D., Somers, K.M., McQueen, D.J., 1999. The Temporal Coherence of Zooplankton Population Abundances in Neighboring North-Temperate Lakes. Am. Nat. 153, 46–58. https://doi.org/10.1086/303147

Shaw, D. A., Vanderkamp, G., Conly, F. M., Pietroniro, A. and Martz, L., 2012, The Fill–Spill Hydrology of Prairie Wetland Complexes during Drought and Deluge. Hydrol. Process., 26: 3147–3156. doi:10.1002/hyp.8390

Shook, K., Pomeroy, J., 2012. Changes in the hydrological character of rainfall on the Canadian prairies. Hydrol. Process. 26. https://doi.org/10.1002/hyp.9383

Shook, K., Pomeroy, J., van der Kamp, G., 2015. The transformation of frequency distributions of

winter precipitation to spring streamflow probabilities in cold regions; case studies from the Canadian Prairies. J. Hydrol. 521, 395–409. https://doi.org/10.1016/j.jhydrol.2014.12.014

Sloan CE, 1972. Ground-water hydrology of prairie potholes in North Dakota. US Geol Surv Prof Pap 585-C:28

Solomon, S. (Ed.)., 2007. Climate change 2007-the physical science basis: Working group I contribution to the fourth assessment report of the IPCC (Vol. 4). Cambridge University Press.

Steen, V., Skagen, S.K., Noon, B.R., 2014. Vulnerability of breeding waterbirds to climate change in the Prairie Pothole Region, U.S.A. PLoS One 9. https://doi.org/10.1371/journal.pone.0096747

Steen, V.A., Skagen, S.K., Melcher, C.P., 2016. Implications of Climate Change for Wetland-Dependent Birds in the Prairie Pothole Region. Wetlands 36. https://doi.org/10.1007/s13157-016-0791-2

Stenseth, N. C., Ehrich, D., Rueness, E. K., Lingjærde, O. C., Chan, K., Boutin, S., Jakobsen, K. S. (2004). The effect of climatic forcing on population synchrony and genetic structuring of the canadian lynx. Proceedings of the National Academy of Sciences of the United States of America, 101(16), 6056-6061. doi:10.1073/pnas.0307123101

Stewart, R. E., & Kantrud, H. A., 1971. Classification of natural ponds and lakes in the glaciated

prairie region. Bureau of Sport Fisheries and Wildlife, U.S. Fish and Wildlife Service, Washington, D.C., USA. Resource Publication 92. 57 pp.

Systat Software, Inc., San Jose California USA.

Tondu, J.M.E., Turner, K.W., Wolfe, B.B., Hall, R.I., Edwards, T.W.D., McDonald, I., 2013. Using Water Isotope Tracers to Develop the Hydrological Component of a Long-Term Aquatic Ecosystem Monitoring Program for a Northern Lake-Rich Landscape. Arctic, Antarct. Alp. Res. 45, 594–614. https://doi.org/10.1657/1938-4246-45.4.594

Turner, K.W., Wolfe, B.B., Edwards, T.W.D., Lantz, T.C., Hall, R.I., Larocque, G., 2014. Controls on water balance of shallow thermokarst lakes and their relations with catchment characteristics: a multi-year, landscape-scale assessment based on water isotope tracers and remote sensing in Old Crow Flats, Yukon (Canada). Glob. Chang. Biol. 20, 1585–1603. https://doi.org/10.1111/gcb.12465

van der Kamp, G., Hayashi, M., & Gallen, D., 2003. Comparing the hydrology of grassed and cultivated catchments in the semi-arid Canadian prairies. Hydrological Processes, *17*(3), 559–575. doi:10.1002/hyp.1157

van der Kamp, G., Hayashi, M., 2008. Groundwater-wetland ecosystem interaction in the semiarid glaciated plains of North America. Hydrogeol. J. 17, 203–214. https://doi.org/10.1007/s10040-008-0367-1

van der Kamp, G., Hayashi, M., Bedard-Haughn, A., Pennock, D., 2016. Prairie Pothole Wetlands

– Suggestions for Practical and Objective Definitions and Terminology. Wetlands 36, 229–235. https://doi.org/10.1007/s13157-016-0809-9

van der Valk AG (ed), 1989. Northern Prairie wetlands. Iowa State University Press, Ames, p 400

Werner, B.A., Johnson, W.C., Guntenspergen, G.R., 2013. Evidence for 20th century climate warming and wetland drying in the North American Prairie Pothole Region. Ecol. Evol. 3. https://doi.org/10.1002/ece3.731

Williams, D. W., & Liebhold, A. M. (2000). Spatial synchrony of spruce budworm outbreaks in eastern north america. Ecology*, 81*(10), 2753-2766. doi:10.1890/0012-9658(2000)081[2753:SSOSBO]2.0.CO;2

Winter TC, LaBaugh JW, 2003. Hydrologic consideration in defining isolated wetlands. Wetlands 23:532–540

Woo, M.-K., Rowsell, R.D., 1993. Hydrology of a prairie slough. J. Hydrol. 146, 175–207. https://doi.org/10.1016/0022-1694(93)90275-E

Yi, Y., Brock, B.E., Falcone, M.D., Wolfe, B.B., Edwards, T.W.D., 2008. A coupled isotope tracer method to characterize input water to lakes. J. Hydrol. 350. https://doi.org/10.1016/j.jhydrol.2007.11.008

Zedler, J.B., Kercher, S., 2005. Wetland resources: Status, trends, ecosystem services, and restorability, Annual Review of Environment and Resources. https://doi.org/10.1146/annurev.energy.30.050504.144248

Zhang, H., Huang, G.H., Wang, D., Zhang, X., 2011. Uncertainty assessment of climate change impacts on the hydrology of small prairie wetlands. J. Hydrol. 396. https://doi.org/10.1016/j.jhydrol.2010.10.037

Zoltai, S.C., Vitt, D.H., 1995. Canadian wetlands: Environmental gradients and classification. Vegetatio 118, 131–137. https://doi.org/10.1007/BF00045195

5. Appendices

5.1 Appendix A. Number of wetlands sampled for water isotope composition and number of study wetlands which desiccated (in brackets) during each round of sampling in 2014 and 2015 (A1) as well as wetlands visited in both years (A2).

A1

Site Visit	Date Range	Number of Wetlands Sampled			
		Grassland	Parkland	Restored	Total
1	May 2 - May 15, 2014	24	24	N/A	48
	May 1 - May 15, 2015	24	24	24	72
2	May 15 - June 14, 2014	24	24	N/A	48
	May 15 - May 27, 2015	20 (4)	22 (2)	23 (1)	65 (7)
3	June 5 - June 25, 2014	22 (2)	23 (1)	N/A	45 (3)
	June 13 - June 20, 2015	6 (18)	13 (11)	20 (4)	39 (33)
4	June 21 - July 14, 2014	22 (2)	19 (5)	N/A	41 (7)
	June 23 - June 30, 2015	5 (19)	8 (16)	17 (7)	30 (42)
5	July 24 - Aug 24, 2014	16 (8)	13 (11)	N/A	29 (19)
	July 17 - Aug 7, 2015	1 (23)	10 (14)	14 (10)	25 (47)

A2

Site Visit	Date Range	Number of Wetlands Sampled (for sites visited both years)		
		Grassland	Parkland	Total
1	May 2 - May 15, 2014	12	12	24
	May 1 - May 9, 2015	12	12	24
2	May 16 - June 14, 2014	12	12	24
	May 15 - May 25, 2015	10 (2)	12	22 (2)
3	June 5 - June 25, 2014	12	12	24
	June 13 - June 17, 2015	5 (7)	6 (6)	11 (13)
4	June 21 - July 10, 2014	11 (1)	9 (3)	20 (4)
	June 27 - June 30, 2015	4 (8)	5 (7)	9 (15)
5	July 26 - Aug 24, 2014	8 (4)	5 (7)	13 (11)
	July 21 - Aug 5, 2015	1 (11)	6 (12)	7 (17)

5.2 Appendix B. Total precipitation, average temperature, and average relative humidity (RH) for the Alberta Grassland and Parkland study regions from November to August 2013-2014 and 2014-2015 (from Alberta AgroClimatic Information Service meteorological stations). Long-term average (1961-2015) precipitation and temperature values also shown.

Region	Month	Total Precipitation (mm)			Average Temperature (°C)			Average RH (%)	
		2013-2014	2014-2015	Long-term Average	2013-2014	2014-2015	Long-term Average	2013-2014	2014-2015
Grassland and Parkland	Nov	20.5	31.1	15.3	-7.2	-7.2	-4.4	84.6	83.5
	Dec	15.9	5.9	15.4	-14.1	-6.8	-10.8	81.0	84.4
	Jan	8.0	12.9	17.8	-8.1	-8.1	-12.5	78.6	80.2
	Feb	5.0	11.1	12.4	-16.2	-9.6	-9.4	76.1	81.3
	Mar	12.6	12.5	16.6	-7.8	0.6	-3.9	75.1	73.4
	Apr	20.0	12.2	22.9	3.5	5.5	4.4	67.3	57.3
	May	37.0	11.3	43.6	9.9	10.5	10.6	61.0	50.8
	Jun	76.1	39.8	74.9	13.7	16.2	14.8	68.7	62.9
	Jul	61.5	62.8	69.0	18.5	18.0	17.3	70.1	65.3
	Aug	58.8	74.2	51.0	16.9	16.7	16.5	73.1	67.3
	May-Aug	233.3	188.1	238.5	14.8	15.3	14.8	67.6	61.5
	Nov-Apr	82.0	85.7	100.5	-8.3	-4.3	-6.1	77.1	76.7
Grassland	Nov	14.7	33.5	13.3	-7.1	-7.1	-4.1	84.9	84.4
	Dec	10.8	7.3	13.7	-14.2	-7.0	-10.6	81.6	85.5
	Jan	4.0	9.0	14.6	-8.6	-8.3	-12.4	80.0	81.7
	Feb	2.3	5.9	10.3	-16.1	-9.5	-9.2	77.5	82.4
	Mar	10.4	8.3	14.7	-7.3	1.1	-3.4	77.0	73.1
	Apr	18.5	9.5	21.5	4.3	5.9	4.8	65.6	56.6
	May	37.4	7.3	40.0	10.4	10.7	10.9	59.6	49.8
	Jun	71.4	34.4	69.9	13.8	16.7	15.2	67.7	60.4
	Jul	49.2	43.0	52.8	19.2	18.7	18.0	66.0	60.9
	Aug	67.8	82.3	42.0	17.6	17.3	17.2	70.4	63.1
	May-Aug	225.7	166.9	204.7	15.3	15.9	15.3	65.1	58.5
	Nov-Apr	60.8	73.4	88.1	-8.2	-4.2	-5.8	77.8	77.3

Appendix B (continued)

Region	Month	Total Precipitation (mm)			Average Temperature (°C)			Average RH (%)	
		2013-2014	2014-2015	Long-term Average	2013-2014	2014-2015	Long-term Average	2013-2014	2014-2015
Parkland	Nov	26.3	28.8	17.3	-7.4	-7.3	-4.7	84.2	82.7
	Dec	21.0	4.6	17.2	-14.1	-6.6	-10.9	80.4	83.2
	Jan	11.9	16.7	21.1	-7.6	-7.8	-12.6	77.3	78.6
	Feb	7.6	16.2	14.6	-16.4	-9.8	-9.6	74.8	80.2
	Mar	14.7	16.7	18.5	-8.4	0.1	-4.5	73.3	73.6
	Apr	21.6	15.0	24.2	2.7	5.1	4.0	68.9	58.1
	May	36.6	15.4	47.2	9.4	10.4	10.4	62.3	51.9
	Jun	80.8	45.2	79.9	13.6	15.6	14.4	69.7	65.5
	Jul	73.8	82.5	85.3	17.8	17.4	16.7	74.3	69.8
	Aug	49.8	66.1	59.9	16.3	16.0	15.8	75.8	71.4
	May-Aug	241.0	209.3	272.2	14.3	14.8	14.3	70.1	64.4
	Nov-Apr	103.2	98.0	112.9	-8.5	-4.4	-6.4	76.5	76.1

5.3 Appendix C. Series of maps adapted from the Alberta AgroClimatic Information Service depicting snow pack accumulation in stubble fields relative to the long-term normal in late February, mid-March, and late March of 2014 (left) and 2015 (right). Study area is located within the black box. Note that the snow pack was low to very low, relative to the long-term normal, in a large portion of the study area in mid-March 2015.

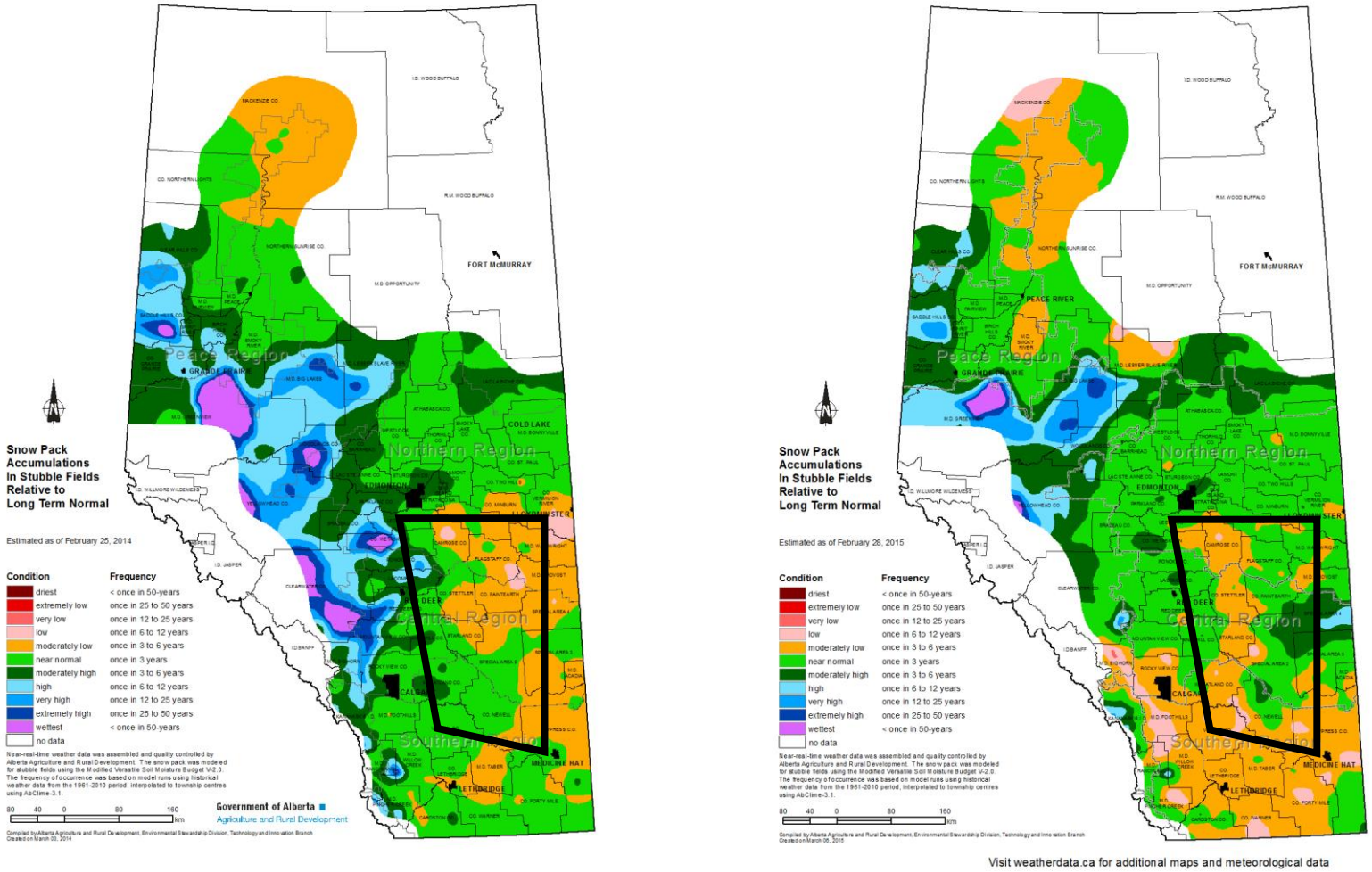

Visit weatherdata.ca for additional maps and meteorological data

Appendix C (continued)

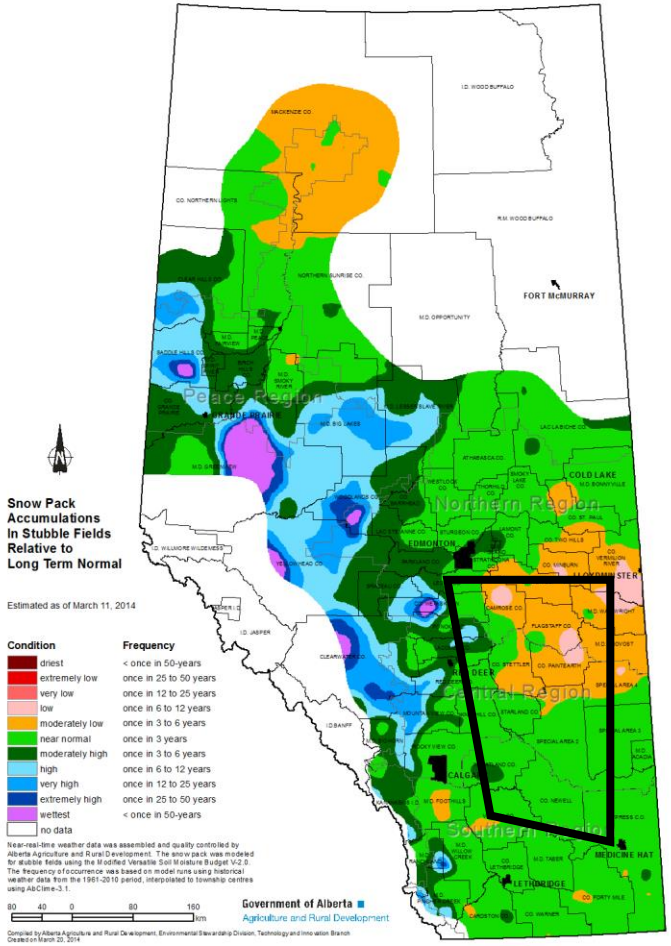

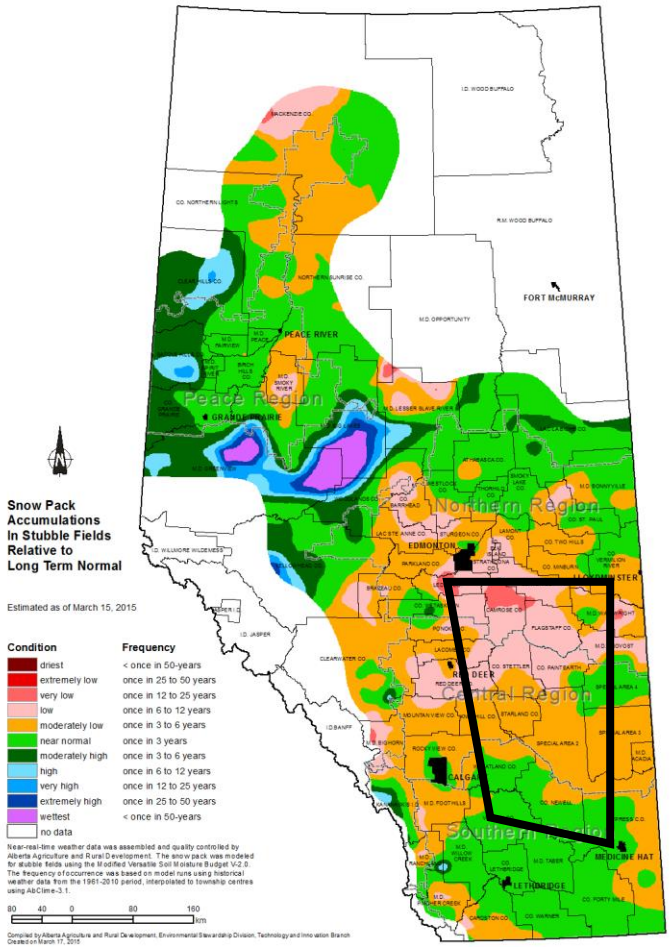

Visit weatherdata.ca for additional maps and meteorological data

Appendix C (continued)

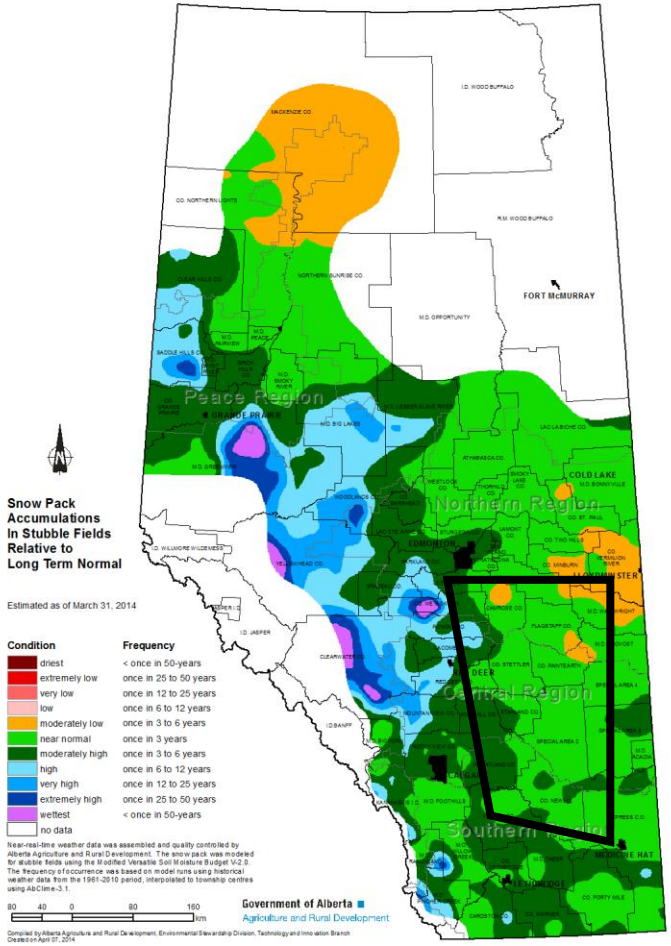

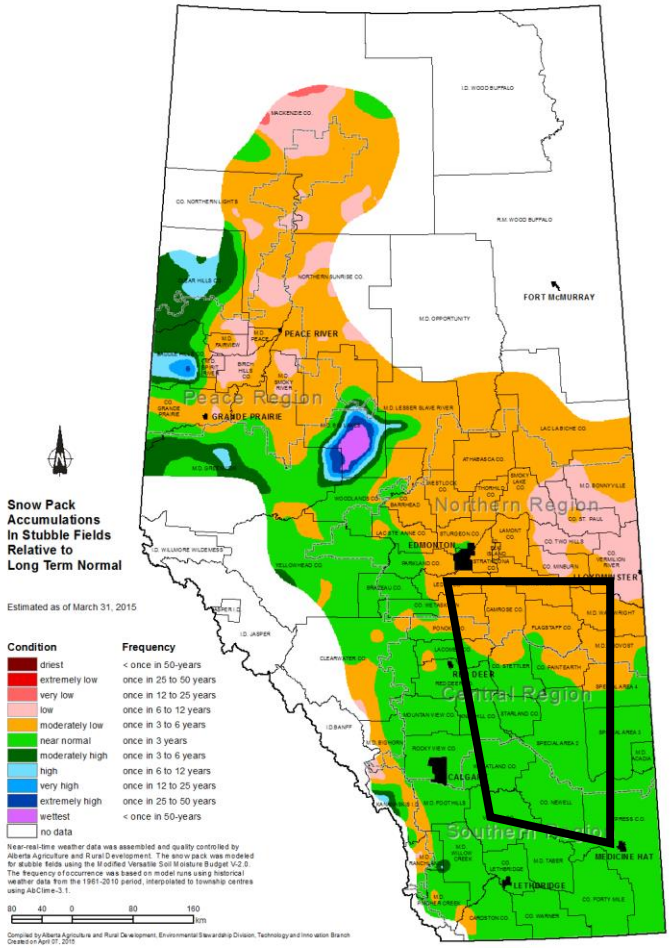

Visit weatherdata.ca for additional maps and meteorological data

5.4 Appendix D. Series of maps adapted from Alberta AgroClimatic Information Service depicting the pasture soil moisture departure from normal to a depth of 60 cm, monthly, from late February-July of 2014 (left) and 2015 (right). Study area located within the black box. Note that the soil moisture was 20-40mm above normal in the majority of the study region at the end of March 2015, indicating an earlier snowmelt.

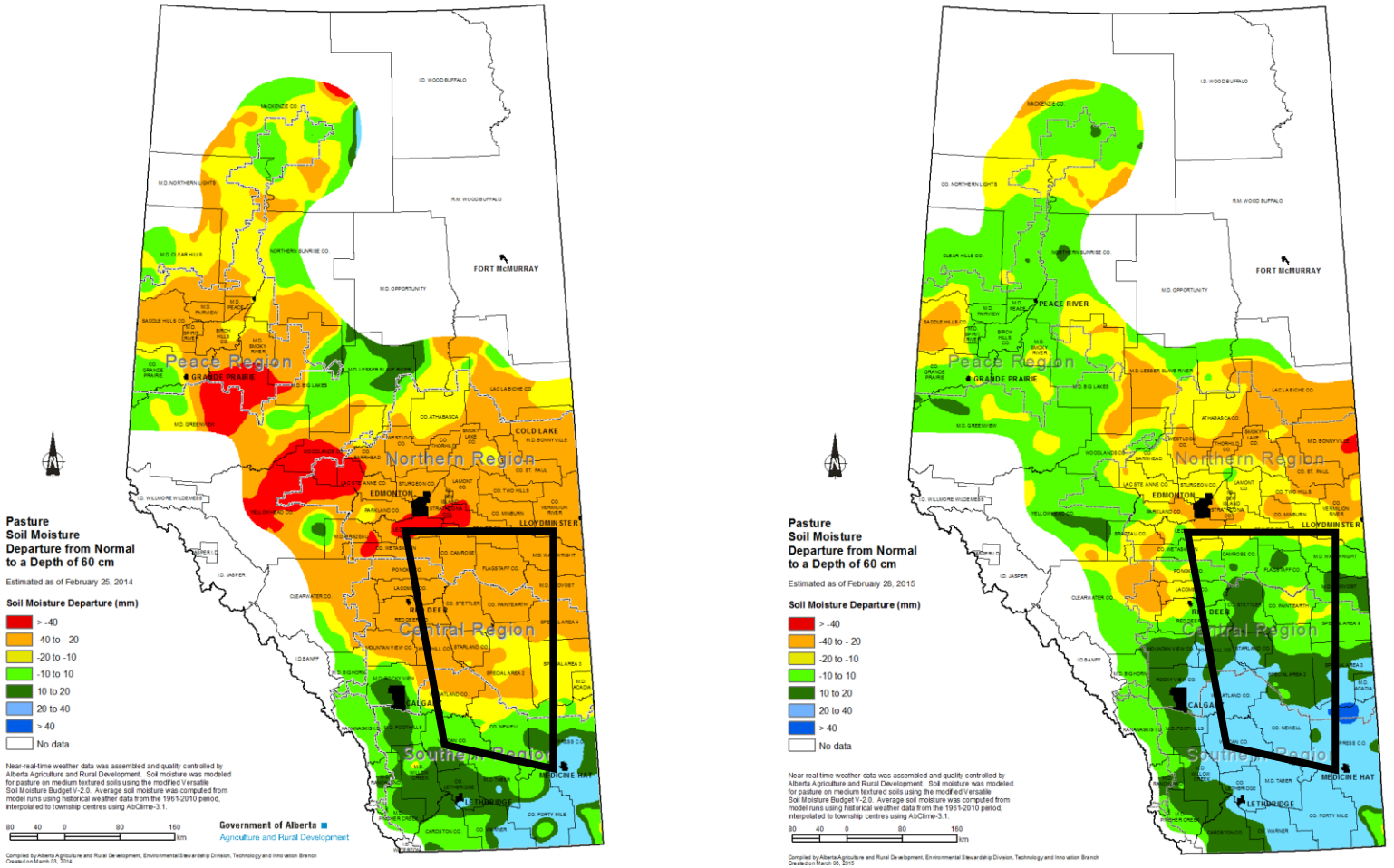

Appendix D (continued)

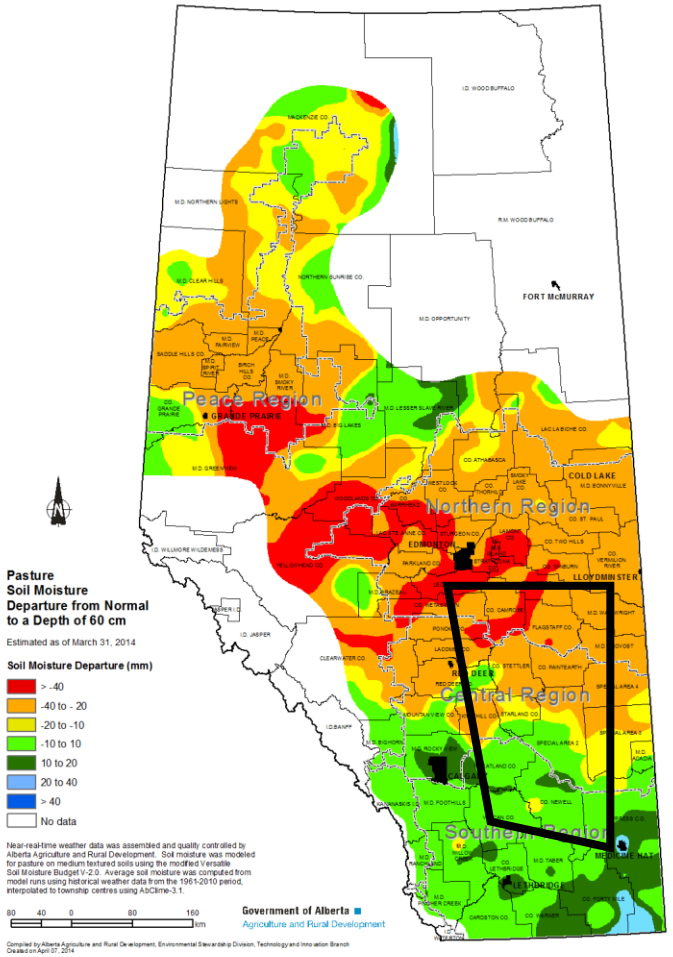

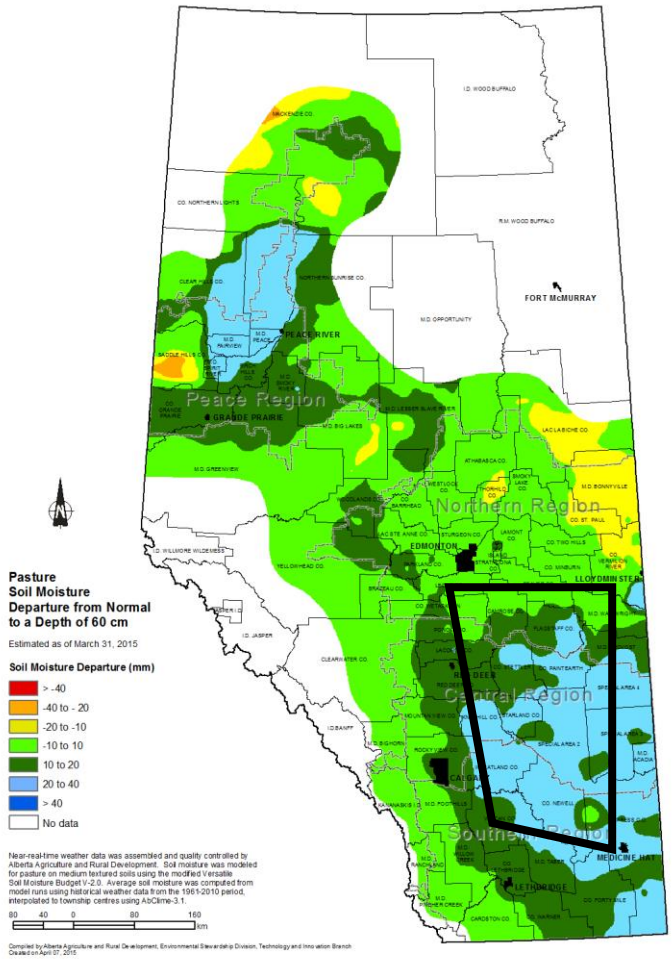

Appendix D (continued)

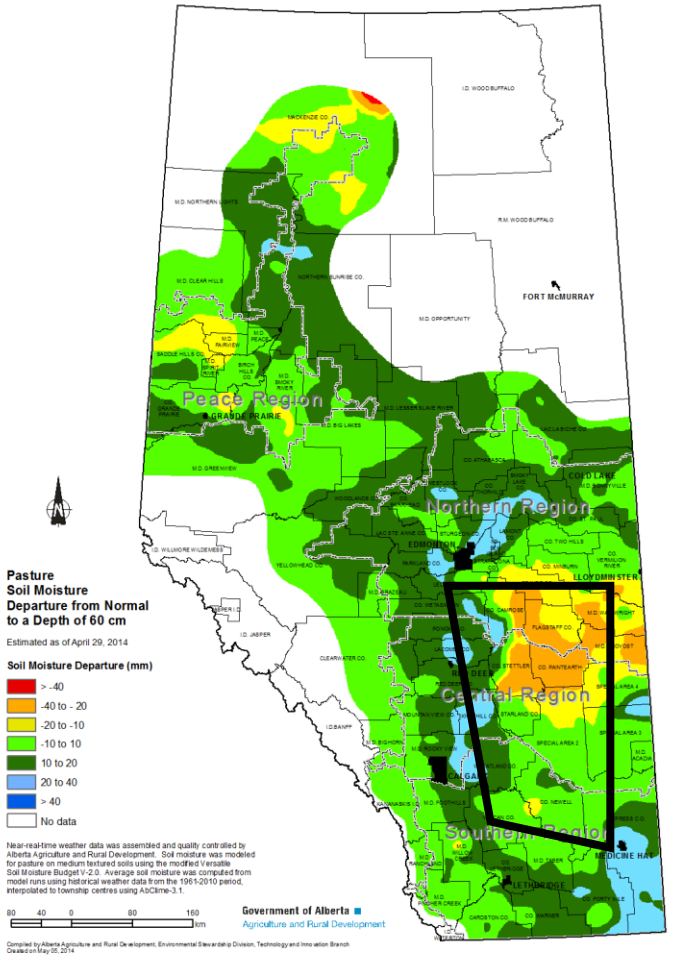

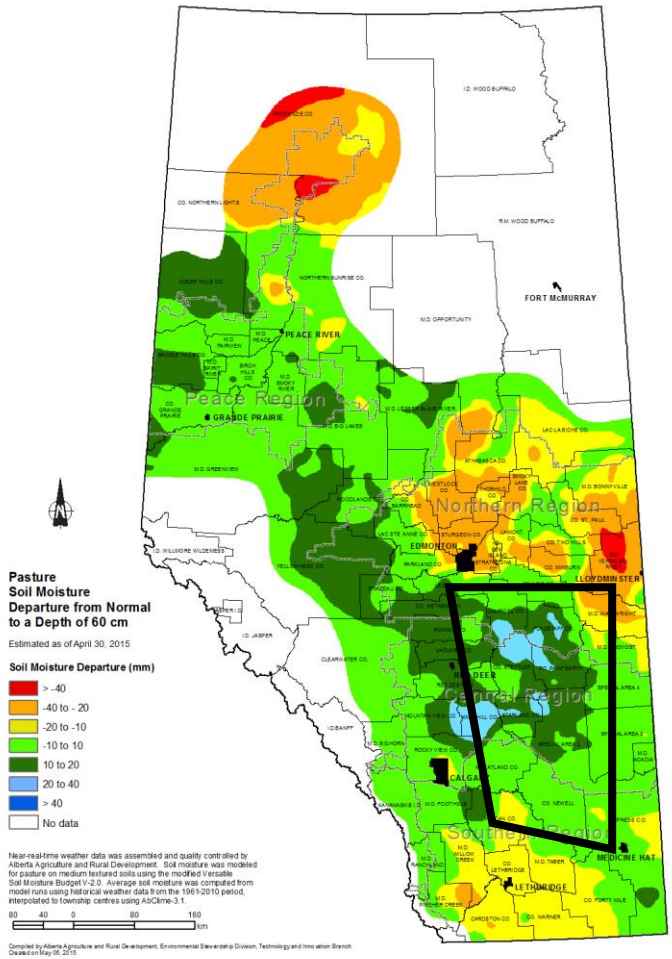

Appendix D (continued)

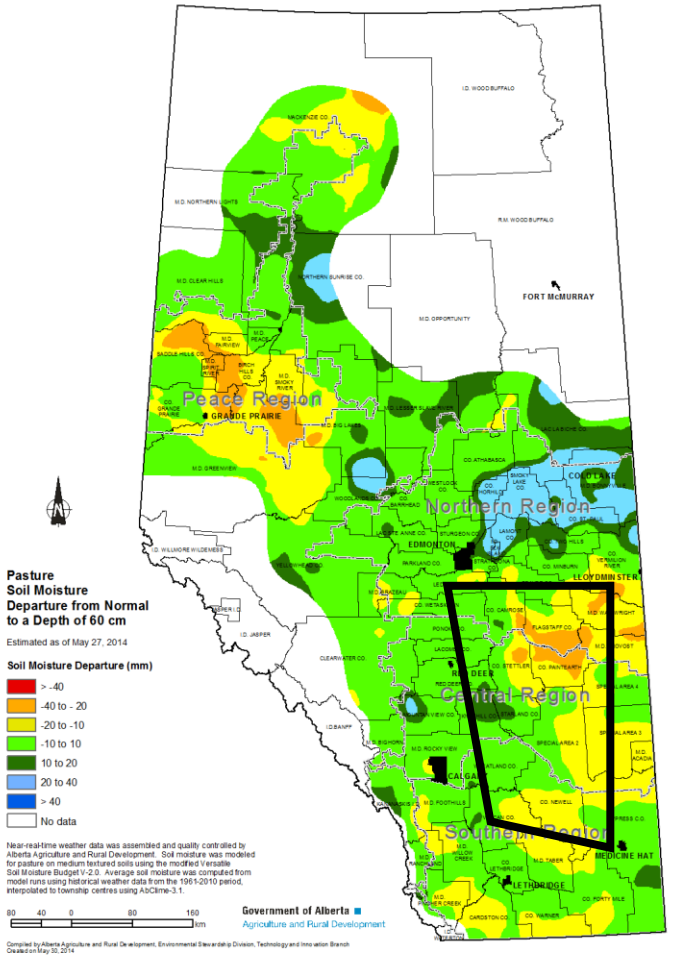

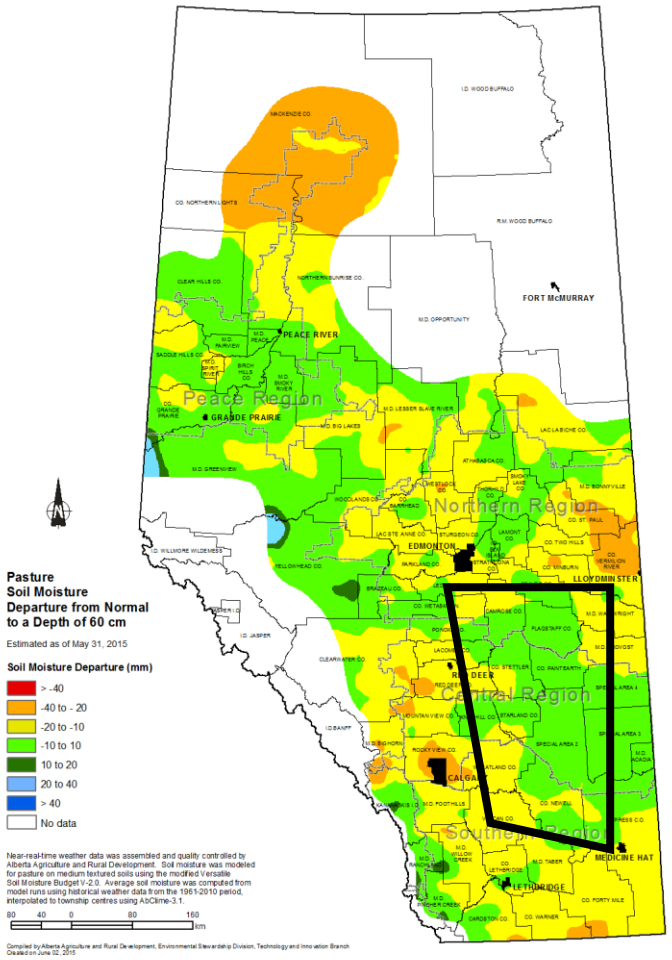

Appendix D (continued)

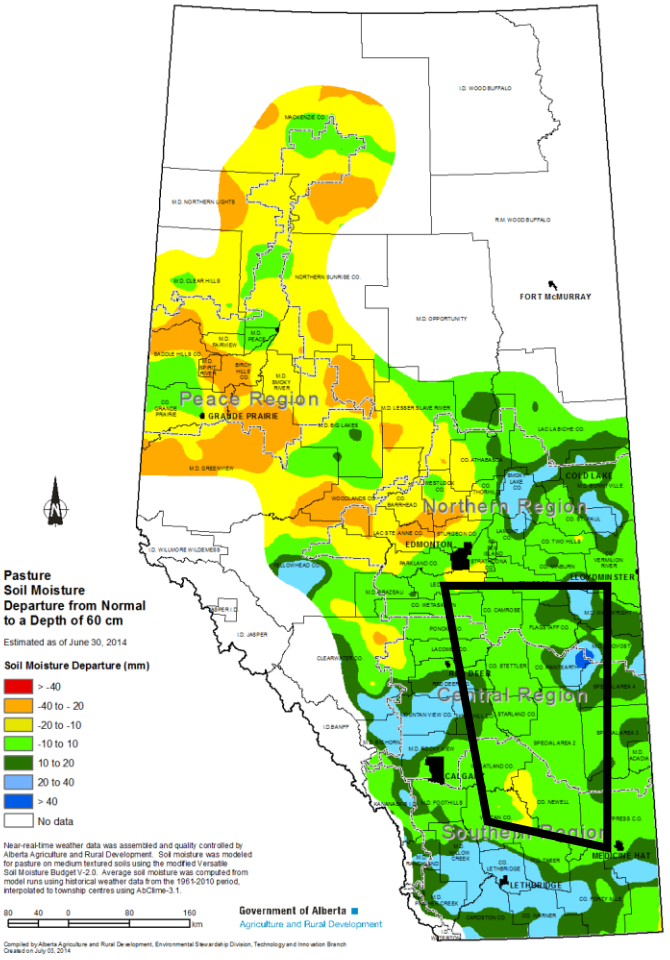

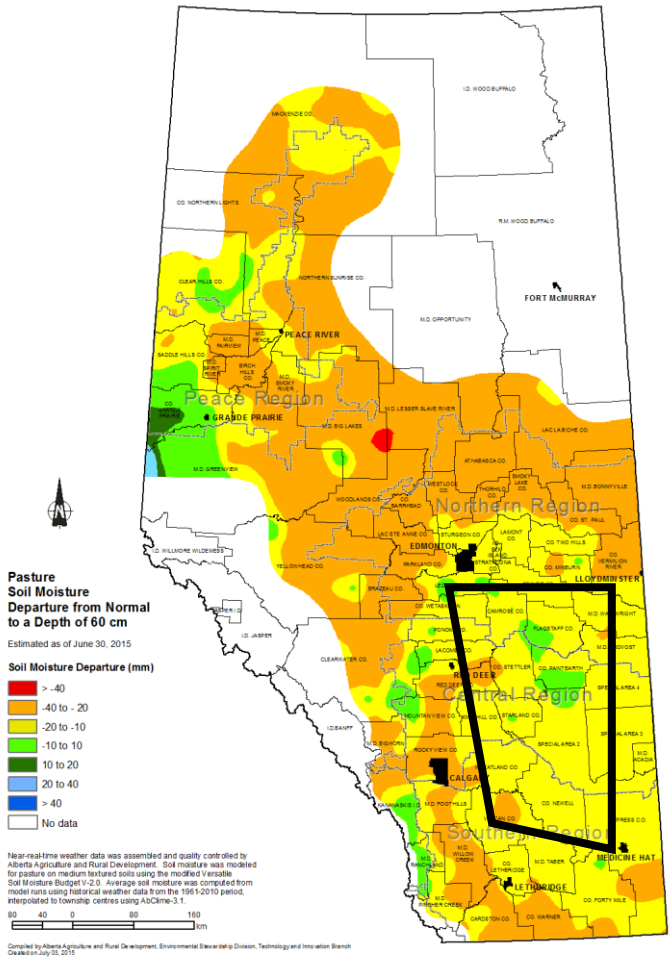

Appendix D (continued)

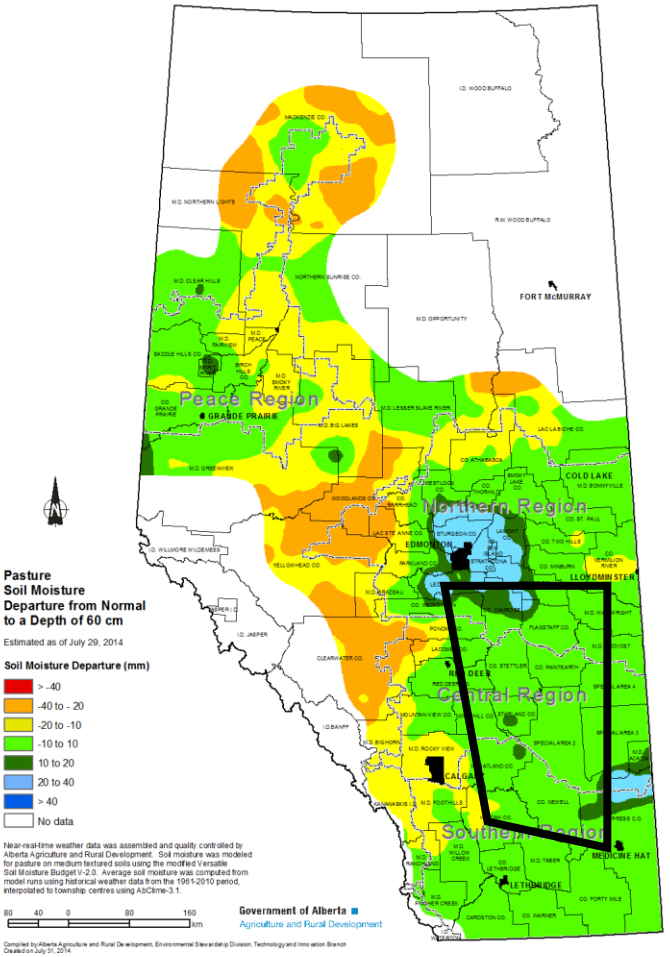

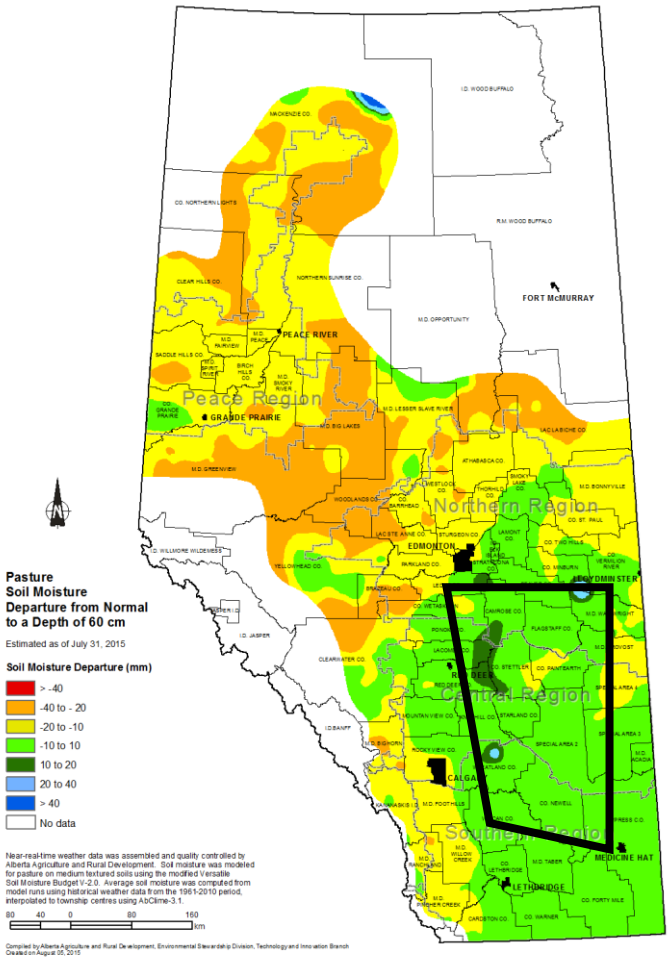

5.5 Appendix E. Water isotope compositions, δ_I, and E/I for all wetlands on all site visits. E/I values listed as >1.5 and δ_I values listed as N/A were not reported as the framework could not accurately estimate values for these wetlands, which were too far beyond steady-state conditions assumed by the model.

Region	Status	Site ID	Date	Visit	$\delta^{18}O$	$\delta^{2}H$	δ_I (^{18}O)	δ_I (^{2}H)	E/I
Grassland	Natural	152	06-May-14	1	-13.1	-128.2	-24.7	-190.6	0.45
Grassland	Natural	152	25-May-14	2	-8.9	-105.3	-25.7	-199.3	0.89
Grassland	Natural	152	24-Jun-14	3	-10.8	-97.9	-16.2	-121.7	0.25
Grassland	Natural	153	06-May-14	1	-18.8	-157.4	-23.7	-182.8	0.14
Grassland	Natural	153	31-May-14	2	-12.7	-129.2	-27.1	-210.2	0.59
Grassland	Natural	153	24-Jun-14	3	-8.0	-94.4	-21.3	-163.4	0.78
Grassland	Natural	153	09-Jul-14	4	-7.3	-93.7	-23.9	-183.9	1.03
Grassland	Natural	153	28-Jul-14	5	-10.3	-98.9	-17.3	-130.6	0.33
Grassland	Natural	158	13-May-14	1	-16.8	-147.5	-23.9	-184.4	0.23
Grassland	Natural	158	26-May-14	2	-12.7	-130.0	-27.3	-211.9	0.60
Grassland	Natural	158	12-Jun-14	3	-9.6	-114.2	-29.8	-232.6	1.03
Grassland	Natural	158	25-Jun-14	4	-9.7	-101.4	-19.7	-149.9	0.50
Grassland	Natural	165	08-May-14	1	-15.7	-139.3	-23.2	-178.6	0.25
Grassland	Natural	165	01-Jun-14	2	-9.9	-112.2	-27.7	-215.5	0.88
Grassland	Natural	165	23-Jun-14	3	-7.7	-92.5	-21.7	-166.1	0.84
Grassland	Natural	165	08-Jul-14	4	-6.1	-84.1	-22.6	-174.0	1.19
Grassland	Natural	173	08-May-14	1	-13.7	-128.3	-23.2	-178.7	0.35
Grassland	Natural	173	25-May-14	2	-9.3	-109.5	-28.8	-223.9	1.00
Grassland	Natural	173	23-Jun-14	3	-8.9	-87.7	-15.7	-117.3	0.36
Grassland	Natural	173	08-Jul-14	4	-8.3	-93.4	-20.0	-152.6	0.65
Grassland	Natural	173	31-Jul-14	5	-4.8	-77.0	-23.5	-180.9	>1.5
Grassland	Natural	202	09-May-14	1	-13.5	-130.3	-26.2	-202.6	0.47
Grassland	Natural	202	24-May-14	2	-8.0	-105.1	N/A	N/A	>1.5
Grassland	Natural	202	11-Jun-14	3	-6.2	-96.8	N/A	N/A	>1.5
Grassland	Natural	202	24-Jun-14	4	-9.3	-96.1	-19.3	-146.8	0.54
Grassland	Natural	203	13-May-14	1	-16.4	-143.3	-23.1	-177.5	0.22
Grassland	Natural	203	27-May-14	2	-12.8	-128.1	-25.3	-195.8	0.50
Grassland	Natural	203	11-Jun-14	3	-9.8	-113.4	-27.7	-214.8	0.89
Grassland	Natural	203	25-Jun-14	4	-8.4	-103.3	-26.1	-201.9	0.99
Grassland	Natural	203	03-Aug-14	5	1.9	-49.4	N/A	N/A	>1.5
Grassland	Natural	Kin1	05-May-14	1	-12.5	-121.6	-24.2	-186.5	0.47
Grassland	Natural	Kin1	24-May-14	2	-4.0	-82.9	N/A	N/A	>1.5
Grassland	Natural	124	04-May-14	1	-18.5	-153.8	-23.1	-178.1	0.13
Grassland	Natural	124	21-May-14	2	-15.6	-140.6	-24.5	-189.0	0.30
Grassland	Natural	124	07-Jun-14	3	-13.2	-127.6	-25.0	-193.1	0.47
Grassland	Natural	124	29-Jun-14	4	-10.0	-108.8	-25.6	-198.3	0.84
Grassland	Natural	124	16-Aug-14	5	-7.2	-86.4	-20.2	-153.9	0.99

Appendix E (continued)

Region	Status	Site ID	Date	Visit	$\delta^{18}O$	$\delta^{2}H$	δ_I (^{18}O)	δ_I (^{2}H)	E/I
Grassland	Natural	131	03-May-14	1	-18.2	-155.9	-24.8	-191.5	0.19
Grassland	Natural	131	20-May-14	2	-15.1	-138.0	-24.8	-191.7	0.34
Grassland	Natural	131	05-Jun-14	3	-11.4	-121.5	-29.4	-228.8	0.82
Grassland	Natural	131	21-Jun-14	4	-8.4	-101.9	-29.1	-226.8	1.28
Grassland	Natural	133	04-May-14	1	-17.1	-146.2	-23.0	-177.3	0.18
Grassland	Natural	133	17-May-14	2	-14.2	-132.9	-24.9	-192.3	0.40
Grassland	Natural	133	05-Jun-14	3	-9.6	-109.1	-29.0	-225.9	1.10
Grassland	Natural	133	21-Jun-14	4	-8.0	-93.9	-22.9	-175.9	1.02
Grassland	Natural	135	03-May-14	1	-22.1	-176.1	-24.4	-188.4	0.06
Grassland	Natural	135	04-Jun-14	2	-17.1	-149.3	-24.6	-190.3	0.24
Grassland	Natural	135	22-Jun-14	3	-14.2	-134.1	-25.4	-196.6	0.42
Grassland	Natural	135	28-Jun-14	4	-14.7	-134.3	-23.8	-183.3	0.33
Grassland	Natural	135	13-Aug-14	5	-11.6	-110.7	-20.0	-152.3	0.39
Grassland	Natural	142	04-May-14	1	-18.5	-155.9	-24.0	-185.4	0.16
Grassland	Natural	142	16-May-14	2	-15.4	-143.9	-27.3	-211.9	0.41
Grassland	Natural	142	07-Jun-14	3	-12.0	-122.4	-26.7	-206.7	0.66
Grassland	Natural	142	28-Jun-14	4	-9.8	-107.9	-25.9	-200.2	0.89
Grassland	Natural	142	11-Aug-14	5	-11.3	-89.6	-13.0	-95.6	0.08
Grassland	Natural	145	02-May-14	1	-18.1	-149.7	-22.3	-171.2	0.12
Grassland	Natural	145	20-May-14	2	-15.7	-135.9	-21.8	-167.5	0.21
Grassland	Natural	145	14-Jun-14	3	-12.7	-119.1	-21.5	-165.1	0.38
Grassland	Natural	145	30-Jun-14	4	-12.8	-111.2	-17.7	-133.6	0.21
Grassland	Natural	145	06-Aug-14	5	-7.6	-86.7	-18.1	-137.4	0.76
Grassland	Natural	149	15-May-14	1	-13.3	-121.0	-20.8	-158.8	0.30
Grassland	Natural	149	18-May-14	2	-12.7	-119.7	-21.7	-166.7	0.38
Grassland	Natural	149	14-Jun-14	3	-10.5	-106.6	-21.2	-162.7	0.56
Grassland	Natural	149	30-Jun-14	4	-9.4	-101.3	-21.8	-167.6	0.72
Grassland	Natural	149	05-Aug-14	5	-6.8	-86.9	-22.5	-173.2	1.28
Grassland	Natural	184	13-May-14	1	-17.1	-147.0	-23.5	-180.8	0.20
Grassland	Natural	184	04-Jun-14	2	-13.2	-127.6	-24.8	-191.7	0.47
Grassland	Natural	184	19-Jun-14	3	-11.2	-116.3	-25.2	-194.6	0.66
Grassland	Natural	184	29-Jun-14	4	-10.8	-109.3	-21.6	-165.4	0.53
Grassland	Natural	184	14-Aug-14	5	-5.7	-83.9	-27.8	-216.0	>1.5
Grassland	Natural	98	14-May-14	1	-13.3	-126.8	-24.7	-190.8	0.47
Grassland	Natural	98	22-May-14	2	-11.8	-118.1	-24.8	-191.8	0.61
Grassland	Natural	98	10-Jun-14	3	-7.7	-96.4	-30.9	-241.3	>1.5
Grassland	Natural	98	01-Jul-14	4	-5.9	-82.2	-25.5	-197.6	>1.5

Appendix E (continued)

Region	Status	Site ID	Date	Visit	$\delta^{18}O$	$\delta^{2}H$	δ_I (^{18}O)	δ_I (^{2}H)	E/I
Grassland	Natural	98	20-Aug-14	5	-11.0	-84.0	-11.9	-86.4	0.04
Grassland	Natural	101	10-May-14	1	-16.7	-145.7	-23.7	-182.7	0.23
Grassland	Natural	101	30-May-14	2	-12.2	-125.7	-26.9	-208.7	0.63
Grassland	Natural	101	15-Jun-14	3	-9.6	-109.3	-26.1	-202.1	0.86
Grassland	Natural	101	26-Jun-14	4	-8.7	-100.3	-23.0	-177.3	0.81
Grassland	Natural	109	10-May-14	1	-13.8	-132.5	-26.3	-203.9	0.47
Grassland	Natural	109	29-May-14	2	-9.7	-111.3	-30.5	-237.9	1.10
Grassland	Natural	109	16-Jun-14	3	-9.8	-104.1	-22.4	-171.8	0.65
Grassland	Natural	109	26-Jun-14	4	-6.8	-84.0	-20.0	-153.0	0.99
Grassland	Natural	109	17-Aug-14	5	-9.3	-74.2	-10.9	-78.8	0.09
Grassland	Natural	110	14-May-14	1	-13.6	-128.6	-23.5	-180.7	0.39
Grassland	Natural	110	02-Jun-14	2	-9.4	-109.9	-27.6	-214.1	0.99
Grassland	Natural	110	17-Jun-14	3	-8.6	-102.5	-25.4	-196.4	1.00
Grassland	Natural	110	01-Jul-14	4	-8.3	-95.7	-20.9	-159.9	0.76
Grassland	Natural	110	21-Aug-14	5	-3.8	-68.0	-18.3	-138.5	>1.5
Grassland	Natural	115	11-May-14	1	-15.9	-140.1	-23.2	-178.3	0.24
Grassland	Natural	115	02-Jun-14	2	-11.8	-119.7	-25.0	-193.5	0.60
Grassland	Natural	115	17-Jun-14	3	-10.4	-108.0	-22.6	-173.5	0.63
Grassland	Natural	115	09-Jul-14	4	-8.4	-96.0	-22.1	-169.8	0.87
Grassland	Natural	115	22-Aug-14	5	-8.6	-83.9	-14.3	-106.6	0.35
Grassland	Natural	117	10-May-14	1	-17.0	-147.9	-24.3	-187.6	0.23
Grassland	Natural	117	30-May-14	2	-11.6	-124.7	-31.4	-245.6	0.89
Grassland	Natural	117	16-Jun-14	3	-8.7	-105.8	-31.9	-249.3	1.38
Grassland	Natural	117	26-Jun-14	4	-7.1	-92.5	-28.0	-218.0	>1.5
Grassland	Natural	117	19-Aug-14	5	-13.4	-105.5	-15.0	-111.7	0.06
Grassland	Natural	186	14-May-14	1	-13.3	-128.2	-25.8	-199.4	0.51
Grassland	Natural	186	22-May-14	2	-12.3	-120.6	-24.4	-188.1	0.54
Grassland	Natural	186	08-Jun-14	3	-9.1	-104.5	-28.0	-218.0	1.18
Grassland	Natural	186	09-Jul-14	4	-7.3	-89.5	-23.4	-180.2	1.32
Grassland	Natural	186	22-Aug-14	5	-7.1	-79.7	-15.5	-115.6	0.70
Grassland	Natural	188	11-May-14	1	-13.3	-129.1	-25.5	-197.6	0.49
Grassland	Natural	188	02-Jun-14	2	-6.5	-96.0	N/A	N/A	>1.5
Grassland	Natural	188	27-Jun-14	4	-11.2	-97.4	-15.3	-114.6	0.20
Grassland	Natural	188	21-Aug-14	5	-8.8	-83.8	-14.1	-104.4	0.32
Parkland	Natural	67	05-May-14	1	-18.8	-159.8	-25.4	-196.7	0.19
Parkland	Natural	67	25-May-14	2	-10.3	-124.0	N/A	N/A	>1.5
Parkland	Natural	67	10-Jun-14	3	-7.0	-98.4	N/A	N/A	>1.5

Appendix E (continued)

Region	Status	Site ID	Date	Visit	$\delta^{18}O$	$\delta^{2}H$	δ_I (^{18}O)	δ_I (^{2}H)	E/I
Parkland	Natural	89	10-May-14	1	-16.1	-144.2	-25.7	-199.1	0.32
Parkland	Natural	89	27-May-14	2	-12.0	-128.4	N/A	N/A	1.24
Parkland	Natural	89	13-Jun-14	3	-12.0	-122.4	-28.5	-221.7	0.77
Parkland	Natural	89	28-Jun-14	4	-10.0	-110.3	-31.0	-241.6	1.25
Parkland	Natural	89	11-Aug-14	5	-7.3	-92.7	N/A	N/A	>1.5
Parkland	Natural	90	10-May-14	1	-20.3	-166.4	-24.4	-188.8	0.10
Parkland	Natural	90	27-May-14	2	-17.0	-153.3	-28.3	-220.1	0.36
Parkland	Natural	90	11-Jun-14	3	-15.2	-138.6	-25.5	-197.1	0.37
Parkland	Natural	90	29-Jun-14	4	-11.5	-118.5	-28.1	-218.5	0.83
Parkland	Natural	90	12-Aug-14	5	-6.2	-88.4	N/A	N/A	>1.5
Parkland	Natural	194	06-May-14	1	-12.2	-121.2	-26.1	-202.4	0.64
Parkland	Natural	194	04-Jun-14	2	-10.9	-110.0	-23.2	-178.5	0.66
Parkland	Natural	194	19-Jun-14	3	-9.2	-102.9	-27.1	-210.3	1.19
Parkland	Natural	194	30-Jun-14	4	-8.8	-100.7	-27.9	-216.6	1.35
Parkland	Natural	194	17-Aug-14	5	-6.3	-86.5	N/A	N/A	>1.5
Parkland	Natural	195	06-May-14	1	-17.0	-149.0	-25.3	-195.6	0.26
Parkland	Natural	195	23-May-14	2	-13.4	-124.5	-22.9	-176.0	0.39
Parkland	Natural	195	11-Jun-14	3	-8.3	-103.6	N/A	N/A	>1.5
Parkland	Natural	195	29-Jun-14	4	-8.5	-93.3	-20.3	-154.7	0.86
Parkland	Natural	Gad1	06-May-14	1	-19.4	-161.0	-24.0	-185.1	0.13
Parkland	Natural	Gad1	23-May-14	2	-15.1	-141.0	-26.4	-204.5	0.41
Parkland	Natural	Gad1	19-Jun-14	3	-12.9	-103.7	-15.0	-111.6	0.09
Parkland	Natural	Rum4	15-May-14	1	-16.5	-146.6	-24.9	-192.5	0.28
Parkland	Natural	Rum4	08-Jun-14	2	-12.3	-125.7	-27.5	-213.5	0.68
Parkland	Natural	Rum4	23-Jun-14	3	-10.8	-112.7	-24.2	-186.8	0.68
Parkland	Natural	Rum4	10-Jul-14	4	-9.2	-104.3	-25.3	-195.6	0.96
Parkland	Natural	Rum4	28-Jul-14	5	-8.7	-99.9	-23.5	-180.8	0.93
Parkland	Natural	Tol3	10-May-14	1	-12.2	-119.7	-25.0	-193.0	0.58
Parkland	Natural	Tol3	07-Jun-14	2	-8.9	-104.4	N/A	N/A	>1.5
Parkland	Natural	Tol3	23-Jun-14	3	-8.8	-95.8	-21.4	-164.3	0.87
Parkland	Natural	Tol3	14-Jul-14	4	-6.4	-87.6	N/A	N/A	>1.5
Parkland	Natural	Tol3	18-Aug-14	5	-6.8	-85.5	-24.5	-189.3	>1.5
Parkland	Natural	31	13-May-14	1	-16.8	-150.4	-26.9	-208.7	0.32
Parkland	Natural	31	20-May-14	2	-15.1	-140.3	-27.4	-213.1	0.45
Parkland	Natural	31	05-Jun-14	3	-12.8	-127.6	-29.0	-226.2	0.72
Parkland	Natural	31	21-Jun-14	4	-10.4	-112.0	-29.0	-226.0	1.09
Parkland	Natural	32	13-May-14	1	-17.8	-146.4	-22.1	-169.3	0.12

Appendix E (continued)

Region	Status	Site ID	Date	Visit	$\delta^{18}O$	$\delta^{2}H$	δ_I (^{18}O)	δ_I (^{2}H)	E/I
Parkland	Natural	32	21-May-14	2	-17.0	-142.0	-22.1	-169.3	0.15
Parkland	Natural	32	06-Jun-14	3	-16.6	-135.9	-20.3	-155.2	0.12
Parkland	Natural	32	21-Jun-14	4	-11.7	-109.2	-20.2	-154.4	0.44
Parkland	Natural	35	02-May-14	1	-18.4	-159.2	-26.3	-204.2	0.23
Parkland	Natural	35	19-May-14	2	-12.5	-133.7	N/A	N/A	>1.5
Parkland	Natural	56	03-May-14	1	-17.6	-151.7	-27.1	-210.1	0.26
Parkland	Natural	56	14-Jun-14	2	-8.8	-103.3	N/A	N/A	>1.5
Parkland	Natural	56	24-Jun-14	3	-8.6	-92.9	N/A	N/A	>1.5
Parkland	Natural	56	02-Jul-14	4	-7.8	-89.1	N/A	N/A	>1.5
Parkland	Natural	56	24-Aug-14	5	-4.0	-69.8	-11.2	-80.8	>1.5
Parkland	Natural	190	02-May-14	1	-20.0	-161.3	-23.1	-178.0	0.08
Parkland	Natural	190	18-May-14	2	-18.1	-151.9	-23.5	-180.9	0.16
Parkland	Natural	190	15-Jun-14	3	-14.2	-131.8	-24.6	-190.1	0.41
Parkland	Natural	190	26-Jun-14	4	-12.3	-121.8	-26.1	-202.3	0.66
Parkland	Natural	190	26-Jul-14	5	-11.9	-109.5	-18.8	-142.8	0.34
Parkland	Natural	Batl	09-May-14	1	-20.3	-165.2	-24.2	-186.4	0.10
Parkland	Natural	Batl	20-May-14	2	-19.0	-157.7	-24.0	-185.0	0.13
Parkland	Natural	Batl	05-Jun-14	3	-17.6	-146.3	-22.3	-171.7	0.14
Parkland	Natural	Batl	21-Jun-14	4	-15.6	-131.0	-20.2	-154.6	0.16
Parkland	Natural	JJcol	13-May-14	1	-17.9	-145.2	-21.2	-162.4	0.09
Parkland	Natural	JJcol	21-May-14	2	-16.5	-141.0	-23.2	-178.4	0.21
Parkland	Natural	JJcol	06-Jun-14	3	-15.0	-132.5	-23.5	-181.4	0.31
Parkland	Natural	JJcol	22-Jun-14	4	-12.9	-121.4	-25.1	-193.9	0.55
Parkland	Natural	JJcol	02-Aug-14	5	-11.2	-103.7	-18.6	-141.1	0.42
Parkland	Natural	Miq2	02-May-14	1	-16.5	-142.0	-23.0	-176.6	0.21
Parkland	Natural	Miq2	17-May-14	2	-14.2	-130.3	-23.8	-183.2	0.38
Parkland	Natural	Miq2	14-Jun-14	3	-11.5	-116.0	-25.8	-199.8	0.77
Parkland	Natural	Miq2	25-Jun-14	4	-11.0	-110.4	-23.2	-178.6	0.71
Parkland	Natural	Miq2	24-Jul-14	5	-9.6	-101.6	-22.6	-173.6	0.92
Parkland	Natural	10	05-May-14	1	-16.0	-141.7	-24.1	-186.2	0.27
Parkland	Natural	10	25-May-14	2	-13.3	-129.5	-27.2	-210.8	0.58
Parkland	Natural	10	09-Jun-14	3	-11.0	-118.4	-31.8	-248.8	1.10
Parkland	Natural	10	27-Jun-14	4	-8.8	-103.6	N/A	N/A	>1.5
Parkland	Natural	10	14-Aug-14	5	-5.1	-82.8	N/A	N/A	>1.5
Parkland	Natural	13	04-May-14	1	-17.9	-154.3	-25.3	-195.5	0.22
Parkland	Natural	13	29-May-14	2	-10.4	-119.4	N/A	N/A	>1.5
Parkland	Natural	13	17-Jun-14	3	-5.8	-91.6	N/A	N/A	>1.5

Appendix E (continued)

Region	Status	Site ID	Date	Visit	$\delta^{18}O$	$\delta^{2}H$	δ_I (^{18}O)	δ_I (^{2}H)	E/I
Parkland	Natural	18	04-May-14	1	-19.4	-161.6	-24.6	-190.3	0.14
Parkland	Natural	18	31-May-14	2	-13.3	-133.2	-31.2	-244.0	0.76
Parkland	Natural	18	17-Jun-14	3	-11.0	-120.6	N/A	N/A	1.32
Parkland	Natural	25	03-May-14	1	-21.6	-172.5	-24.2	-186.4	0.06
Parkland	Natural	25	30-May-14	2	-17.2	-148.8	-24.5	-189.1	0.22
Parkland	Natural	25	18-Jun-14	3	-13.7	-128.6	-24.8	-191.8	0.44
Parkland	Natural	25	01-Jul-14	4	-12.8	-118.6	-21.5	-164.5	0.37
Parkland	Natural	25	19-Aug-14	5	-10.9	-95.3	-15.0	-111.7	0.21
Parkland	Natural	30	14-May-14	1	-12.4	-126.0	-29.6	-230.7	0.77
Parkland	Natural	30	29-May-14	2	-9.1	-109.3	N/A	N/A	>1.5
Parkland	Natural	30	17-Jun-14	3	-5.5	-90.0	N/A	N/A	>1.5
Parkland	Natural	30	01-Jul-14	4	-11.6	-103.6	-16.8	-126.7	0.25
Parkland	Natural	182	14-May-14	1	-13.7	-136.3	-31.4	-245.2	0.72
Parkland	Natural	182	02-Jun-14	2	-8.5	-107.4	N/A	N/A	>1.5
Parkland	Natural	182	25-Jun-14	3	-9.7	-90.2	-14.8	-110.7	0.32
Parkland	Natural	182	01-Jul-14	4	-9.7	-95.3	-17.1	-128.9	0.46
Parkland	Natural	187	05-May-14	1	-10.4	-107.9	-27.5	-213.6	1.05
Parkland	Natural	187	01-Jun-14	2	-8.5	-100.7	N/A	N/A	>1.5
Parkland	Natural	187	10-Jun-14	3	-7.8	-96.3	N/A	N/A	>1.5
Parkland	Natural	187	28-Jun-14	4	-6.8	-89.5	N/A	N/A	>1.5
Parkland	Natural	187	16-Aug-14	5	-5.7	-76.6	N/A	N/A	>1.5
Parkland	Natural	200	05-May-14	1	-11.3	-113.5	-24.0	-185.5	0.66
Parkland	Natural	200	26-May-14	2	-9.5	-105.2	-27.2	-210.7	1.13
Parkland	Natural	200	09-Jun-14	3	-8.4	-100.1	-31.6	-247.3	>1.5
Parkland	Natural	200	27-Jun-14	4	-7.5	-92.2	-27.5	-213.5	>1.5
Parkland	Natural	200	13-Aug-14	5	-5.2	-80.8	N/A	N/A	>1.5
Grassland	Natural	152	01-May-15	1	-5.6	-86.1	-20.5	-156.5	0.88
Grassland	Natural	153	01-May-15	1	-7.6	-98.2	-21.6	-165.7	0.74
Grassland	Natural	153	12-May-15	2	-4.5	-82.9	-22.0	-168.8	1.12
Grassland	Natural	173	01-May-15	1	-9.6	-101.7	-19.4	-147.4	0.48
Grassland	Natural	173	23-May-15	2	-3.4	-71.3	-20.0	-152.2	1.30
Grassland	Natural	173	13-Jun-15	3	-1.2	-59.8	-20.2	-154.3	>1.5
Grassland	Natural	173	28-Jun-15	4	5.1	-38.1	21.5	185.0	>1.5
Grassland	Natural	202	02-May-15	1	-7.9	-96.3	-21.8	-167.5	0.79
Grassland	Natural	202	12-May-15	2	-3.0	-72.0	-25.7	-198.7	>1.5
Grassland	Natural	131	08-May-15	1	-7.4	-97.7	-25.9	-200.9	1.11
Grassland	Natural	142	08-May-15	1	-12.4	-116.3	-20.2	-154.3	0.32

Appendix E (continued)

Region	Status	Site ID	Date	Visit	$\delta^{18}O$	$\delta^{2}H$	δ_I (^{18}O)	δ_I (^{2}H)	E/I
Grassland	Natural	142	20-May-15	2	-10.9	-107.1	-19.4	-147.8	0.39
Grassland	Natural	145	08-May-15	1	-14.0	-114.3	-16.8	-126.2	0.10
Grassland	Natural	145	20-May-15	2	-12.5	-106.8	-16.6	-124.6	0.17
Grassland	Natural	145	14-Jun-15	3	-9.1	-92.5	-17.0	-128.0	0.40
Grassland	Natural	145	30-Jun-15	4	-7.1	-83.0	-17.1	-129.4	0.61
Grassland	Natural	184	08-May-15	1	-10.4	-111.1	-22.5	-172.7	0.55
Grassland	Natural	184	20-May-15	2	-6.7	-91.2	-23.0	-177.4	0.99
Grassland	Natural	308	07-May-15	1	-9.8	-104.5	-21.1	-161.7	0.54
Grassland	Natural	308	20-May-15	2	-5.1	-81.2	-23.4	-180.6	1.32
Grassland	Natural	312	08-May-15	1	-11.2	-111.7	-21.1	-161.3	0.43
Grassland	Natural	312	20-May-15	2	-7.9	-96.5	-22.6	-174.0	0.83
Grassland	Natural	345	08-May-15	1	-7.5	-94.8	-22.8	-175.2	0.89
Grassland	Natural	345	19-May-15	2	-3.8	-74.7	-23.6	-181.7	>1.5
Grassland	Natural	346	06-May-15	1	-11.6	-115.1	-21.5	-164.9	0.42
Grassland	Natural	346	19-May-15	2	-7.7	-96.0	-22.8	-175.7	0.88
Grassland	Natural	366	06-May-15	1	-6.4	-86.1	-20.8	-158.8	0.94
Grassland	Natural	379	05-May-15	1	-7.6	-93.6	-23.0	-177.1	0.96
Grassland	Natural	379	16-May-15	2	-3.4	-69.4	-24.4	-188.6	>1.5
Grassland	Natural	101	03-May-15	1	-11.9	-120.2	-22.1	-169.9	0.44
Grassland	Natural	101	22-May-15	2	-5.8	-91.8	-24.6	-190.2	1.16
Grassland	Natural	101	14-Jun-15	3	-3.3	-76.5	-23.6	-181.7	>1.5
Grassland	Natural	109	02-May-15	1	-9.0	-103.1	-21.7	-166.5	0.69
Grassland	Natural	109	14-May-15	2	-3.4	-76.9	-27.9	-216.5	>1.5
Grassland	Natural	110	04-May-15	1	-11.3	-108.8	-18.5	-140.7	0.33
Grassland	Natural	110	21-May-15	2	-7.2	-90.1	-19.0	-144.2	0.70
Grassland	Natural	110	15-Jun-15	3	-3.8	-72.6	-18.5	-140.5	1.15
Grassland	Natural	110	30-Jun-15	4	-2.0	-63.3	-18.6	-141.2	>1.5
Grassland	Natural	110	30-Jul-15	5	-1.7	-58.3	-16.0	-119.8	1.35
Grassland	Natural	115	04-May-15	1	-11.7	-114.2	-20.3	-155.2	0.38
Grassland	Natural	115	21-May-15	2	-8.0	-93.7	-19.4	-147.6	0.65
Grassland	Natural	115	15-Jun-15	3	-2.7	-68.5	-21.9	-168.4	>1.5
Grassland	Natural	115	30-Jun-15	4	-1.9	-62.0	-19.3	-147.2	>1.5
Grassland	Natural	336	02-May-15	1	-9.7	-107.8	-21.2	-162.2	0.57
Grassland	Natural	336	14-May-15	2	-4.8	-84.8	-22.7	-174.5	1.26
Grassland	Natural	338	03-May-15	1	-10.0	-104.3	-19.6	-149.7	0.49
Grassland	Natural	338	19-May-15	2	-6.7	-85.0	-18.1	-137.6	0.77
Grassland	Natural	360	04-May-15	1	-8.6	-101.6	-22.6	-173.4	0.80

Appendix E (continued)

Region	Status	Site ID	Date	Visit	$\delta^{18}O$	$\delta^{2}H$	δ_I (^{18}O)	δ_I (^{2}H)	E/I
Grassland	Natural	360	21-May-15	2	-2.3	-68.4	-25.9	-200.9	>1.5
Grassland	Natural	375	02-May-15	1	-8.2	-101.7	-23.8	-183.5	0.92
Grassland	Natural	375	22-May-15	2	1.7	-54.6	N/A	N/A	>1.5
Grassland	Natural	384	03-May-15	1	-6.7	-89.3	-20.6	-157.1	0.91
Grassland	Natural	388	03-May-15	1	-12.2	-117.1	-20.0	-153.0	0.34
Grassland	Natural	388	22-May-15	2	-6.9	-93.2	-20.9	-160.1	0.84
Grassland	Natural	388	14-Jun-15	3	-3.4	-75.2	-21.0	-160.9	1.41
Grassland	Natural	388	29-Jun-15	4	-1.0	-62.2	-20.8	-159.3	>1.5
Parkland	Natural	67	04-May-15	1	-14.7	-131.4	-21.9	-167.6	0.27
Parkland	Natural	67	20-May-15	2	-10.4	-109.0	-22.2	-170.1	0.60
Parkland	Natural	90	04-May-15	1	-16.2	-141.9	-22.9	-176.1	0.23
Parkland	Natural	90	20-May-15	2	-13.6	-127.6	-22.8	-175.7	0.37
Parkland	Natural	90	16-Jun-15	3	-8.2	-100.6	-25.7	-199.0	1.09
Parkland	Natural	90	27-Jun-15	4	-6.7	-92.4	-27.5	-213.9	1.56
Parkland	Natural	90	24-Jul-15	5	-9.9	-97.4	-17.3	-130.8	0.39
Parkland	Natural	195	03-May-15	1	-12.1	-117.6	-22.0	-168.9	0.44
Parkland	Natural	195	20-May-15	2	-6.3	-93.4	N/A	N/A	>1.5
Parkland	Natural	195	16-Jun-15	3	-6.7	-80.1	-16.6	-125.0	0.72
Parkland	Natural	195	27-Jun-15	4	-5.3	-80.3	-22.7	-174.4	>1.5
Parkland	Natural	195	27-Jul-15	5	-13.0	-110.1	-16.8	-126.8	0.16
Parkland	Natural	301	07-May-15	1	-8.0	-96.9	-21.6	-165.3	0.79
Parkland	Natural	301	19-May-15	2	-2.9	-71.7	-24.9	-192.3	>1.5
Parkland	Natural	377	04-May-15	1	-13.4	-129.0	-25.6	-197.9	0.50
Parkland	Natural	377	20-May-15	2	-8.7	-102.9	-29.4	-228.7	1.35
Parkland	Natural	395	07-May-15	1	-13.9	-132.2	-23.4	-180.0	0.38
Parkland	Natural	395	19-May-15	2	-11.6	-118.8	-22.8	-175.3	0.51
Parkland	Natural	395	17-Jun-15	3	-4.8	-80.2	-21.7	-166.6	1.39
Parkland	Natural	Rum4	09-May-15	1	-14.0	-126.9	-21.1	-161.7	0.27
Parkland	Natural	Rum4	19-May-15	2	-11.4	-116.7	-22.4	-172.5	0.49
Parkland	Natural	Rum4	17-Jun-15	3	-7.7	-95.1	-21.4	-164.0	0.79
Parkland	Natural	Rum4	27-Jun-15	4	-7.2	-96.3	-24.6	-190.3	1.06
Parkland	Natural	Rum4	21-Jul-15	5	-11.7	-104.5	-16.8	-126.7	0.22
Parkland	Natural	31	03-May-15	1	-15.7	-127.7	-18.7	-142.0	0.10
Parkland	Natural	31	14-May-15	2	-12.4	-113.4	-19.5	-148.7	0.30
Parkland	Natural	32	03-May-15	1	-16.2	-135.7	-21.0	-160.5	0.15
Parkland	Natural	32	21-May-15	2	-12.9	-118.6	-21.4	-164.1	0.34
Parkland	Natural	56	06-May-15	1	-12.8	-122.1	-24.8	-191.6	0.50

Appendix E (continued)

Region	Status	Site ID	Date	Visit	$\delta^{18}O$	$\delta^{2}H$	δ_I (^{18}O)	δ_I (^{2}H)	E/I
Parkland	Natural	56	23-May-15	2	-8.3	-99.9	N/A	N/A	>1.5
Parkland	Natural	190	02-May-15	1	-15.0	-131.9	-21.6	-165.5	0.23
Parkland	Natural	190	21-May-15	2	-11.7	-114.9	-22.1	-169.4	0.47
Parkland	Natural	190	14-Jun-15	3	-8.0	-99.1	-28.1	-218.2	1.32
Parkland	Natural	190	27-Jun-15	4	-4.7	-87.1	N/A	N/A	>1.5
Parkland	Natural	190	01-Aug-15	5	-6.8	-91.3	-28.0	-217.5	>1.5
Parkland	Natural	317	02-May-15	1	-15.0	-135.9	-23.0	-176.9	0.29
Parkland	Natural	317	22-May-15	2	-9.2	-108.1	-26.2	-203.3	0.94
Parkland	Natural	333	08-May-15	1	-14.9	-136.0	-23.3	-179.8	0.31
Parkland	Natural	333	23-May-15	2	-10.5	-112.8	-24.1	-185.6	0.66
Parkland	Natural	333	14-Jun-15	3	-9.7	-106.6	-22.9	-176.0	0.68
Parkland	Natural	333	30-Jul-15	5	-9.6	-104.3	-21.8	-166.9	0.63
Parkland	Natural	351	02-May-15	1	-12.8	-117.4	-19.9	-151.6	0.29
Parkland	Natural	351	15-May-15	2	-8.7	-96.4	-19.8	-151.0	0.62
Parkland	Natural	365	02-May-15	1	-17.6	-147.0	-22.2	-170.6	0.14
Parkland	Natural	365	21-May-15	2	-14.1	-129.5	-22.6	-174.0	0.33
Parkland	Natural	365	14-Jun-15	3	-11.1	-111.4	-21.8	-167.1	0.53
Parkland	Natural	396	01-May-15	1	-18.7	-149.3	-20.9	-159.9	0.07
Parkland	Natural	396	14-May-15	2	-17.4	-143.0	-21.0	-160.7	0.12
Parkland	Natural	398	03-May-15	1	-17.6	-144.3	-21.0	-160.8	0.11
Parkland	Natural	398	22-May-15	2	-15.2	-134.4	-21.8	-167.3	0.24
Parkland	Natural	398	13-Jun-15	3	-11.3	-112.0	-20.8	-159.2	0.44
Parkland	Natural	398	27-Jun-15	4	-10.8	-110.2	-21.5	-164.4	0.52
Parkland	Natural	398	17-Jul-15	5	-16.3	-129.3	-18.1	-137.2	0.06
Parkland	Natural	10	04-May-15	1	-12.6	-120.2	-21.5	-164.9	0.40
Parkland	Natural	10	20-May-15	2	-10.6	-109.5	-21.4	-164.2	0.56
Parkland	Natural	10	16-Jun-15	3	-6.5	-89.3	-24.0	-184.8	1.39
Parkland	Natural	10	27-Jun-15	4	-4.4	-82.4	N/A	N/A	>1.5
Parkland	Natural	10	25-Jul-15	5	-7.4	-88.0	-18.7	-141.9	0.81
Parkland	Natural	13	05-May-15	1	-9.6	-102.1	-20.2	-154.6	0.60
Parkland	Natural	13	18-May-15	2	-4.8	-75.2	-19.2	-146.4	1.49
Parkland	Natural	13	05-Aug-15	5	-9.8	-94.0	-15.9	-119.5	0.34
Parkland	Natural	18	06-May-15	1	-13.2	-125.6	-23.0	-177.1	0.42
Parkland	Natural	18	25-May-15	2	-10.2	-112.8	-26.2	-203.0	0.87
Parkland	Natural	18	15-Jun-15	3	-7.1	-91.6	-23.1	-177.6	1.21
Parkland	Natural	182	06-May-15	1	-9.5	-103.3	-21.2	-162.3	0.67
Parkland	Natural	182	17-May-15	2	-4.6	-75.0	-19.7	-149.9	>1.5

Appendix E (continued)

Region	Status	Site ID	Date	Visit	$\delta^{18}O$	$\delta^{2}H$	δ_I (^{18}O)	δ_I (^{2}H)	E/I
Parkland	Natural	321	05-May-15	1	-12.3	-118.2	-21.3	-163.0	0.41
Parkland	Natural	321	26-May-15	2	-4.2	-81.1	N/A	N/A	>1.5
Parkland	Natural	321	15-Jun-15	3	-4.8	-76.2	-19.3	-146.8	1.40
Parkland	Natural	344	09-May-15	1	-13.1	-120.0	-19.8	-151.2	0.29
Parkland	Natural	344	19-May-15	2	-11.8	-112.8	-19.5	-148.3	0.35
Parkland	Natural	344	17-Jun-15	3	-8.0	-96.3	-20.6	-157.8	0.77
Parkland	Natural	344	27-Jun-15	4	-7.7	-93.4	-19.8	-151.1	0.76
Parkland	Natural	344	22-Jul-15	5	-7.7	-88.9	-17.6	-132.9	0.62
Parkland	Natural	368	05-May-15	1	-14.8	-130.5	-21.3	-162.9	0.25
Parkland	Natural	368	26-May-15	2	-11.7	-118.3	-23.8	-183.4	0.59
Parkland	Natural	368	15-Jun-15	3	-10.7	-109.7	-21.6	-165.5	0.58
Parkland	Natural	368	27-Jun-15	4	-11.0	-108.2	-20.2	-154.0	0.46
Parkland	Natural	368	05-Aug-15	5	-9.5	-92.1	-16.0	-120.0	0.38
Parkland	Restored	Baron-01	05-May-15	1	-10.5	-112.3	-24.0	-185.1	0.69
Parkland	Restored	Baron-01	20-May-15	2	-6.9	-93.9	-27.3	-211.8	>1.5
Parkland	Restored	Beltz-03	06-May-15	1	-14.8	-131.7	-21.8	-167.0	0.26
Parkland	Restored	Beltz-03	26-May-15	2	-11.8	-116.4	-22.0	-169.1	0.47
Parkland	Restored	Beltz-03	18-Jun-15	3	-9.4	-106.4	-24.2	-186.7	0.84
Parkland	Restored	Beltz-03	24-Jun-15	4	-8.7	-104.5	-26.8	-207.8	1.11
Parkland	Restored	Beltz-03	23-Jul-15	5	-7.5	-93.9	-23.1	-177.5	1.08
Parkland	Restored	Bergq-07	01-May-15	1	-14.6	-130.3	-21.2	-162.6	0.25
Parkland	Restored	Bergq-07	23-May-15	2	-10.8	-110.6	-21.0	-160.5	0.52
Parkland	Restored	Bergq-07	14-Jun-15	3	-7.2	-92.9	-22.0	-169.0	1.06
Parkland	Restored	Bergq-07	27-Jun-15	4	-5.2	-84.1	-25.5	-197.7	>1.5
Parkland	Restored	Bergq-07	07-Aug-15	5	-5.5	-80.5	-19.7	-150.0	1.28
Parkland	Restored	Busen-01	01-May-15	1	-16.2	-139.7	-21.8	-167.0	0.20
Parkland	Restored	Busen-01	24-May-15	2	-10.3	-114.2	-25.3	-195.8	0.80
Parkland	Restored	Caine-01	04-May-15	1	-12.3	-121.0	-22.9	-175.9	0.48
Parkland	Restored	Caine-01	21-May-15	2	-8.4	-102.4	-25.7	-198.6	1.13
Parkland	Restored	Colli-02	07-May-15	1	-15.3	-133.9	-21.4	-164.3	0.23
Parkland	Restored	Colli-02	25-May-15	2	-11.4	-112.5	-20.8	-158.8	0.47
Parkland	Restored	Colli-02	17-Jun-15	3	-6.6	-88.3	-22.2	-170.4	1.29
Parkland	Restored	Colli-02	23-Jun-15	4	-4.5	-85.9	N/A	N/A	>1.5
Parkland	Restored	Forbs-10	02-May-15	1	-13.5	-130.5	-24.0	-185.3	0.44
Parkland	Restored	Forbs-10	23-May-15	2	-8.6	-104.2	-25.0	-193.4	1.02
Parkland	Restored	Forbs-10	13-Jun-15	3	-4.0	-78.6	-28.7	-223.7	>1.5
Parkland	Restored	Gilbe-02	05-May-15	1	-15.9	-133.2	-20.0	-152.5	0.15

Appendix E (continued)

Region	Status	Site ID	Date	Visit	$\delta^{18}O$	$\delta^{2}H$	δ_I (^{18}O)	δ_I (^{2}H)	E/I
Parkland	Restored	Gilbe-02	20-May-15	2	-13.9	-124.3	-20.2	-154.2	0.26
Parkland	Restored	Gilbe-02	17-Jun-15	3	-10.9	-108.7	-20.0	-152.5	0.48
Parkland	Restored	Gilbe-02	25-Jun-15	4	-9.8	-106.0	-21.8	-167.5	0.70
Parkland	Restored	Gilbe-02	21-Jul-15	5	-8.8	-97.1	-19.5	-148.2	0.68
Parkland	Restored	Grand-06	05-May-15	1	-13.6	-123.5	-20.4	-155.9	0.29
Parkland	Restored	Grand-06	26-May-15	2	-10.5	-109.9	-21.7	-166.6	0.61
Parkland	Restored	Grand-06	20-Jun-15	3	-8.6	-99.3	-21.5	-164.6	0.84
Parkland	Restored	Grand-06	24-Jun-15	4	-7.7	-97.1	-24.1	-186.0	1.20
Parkland	Restored	Grand-06	25-Jul-15	5	-7.0	-89.7	-21.6	-165.2	1.14
Parkland	Restored	Green-03	04-May-15	1	-13.9	-127.3	-21.7	-166.5	0.32
Parkland	Restored	Green-03	21-May-15	2	-10.4	-110.5	-22.6	-173.9	0.65
Parkland	Restored	Green-03	20-Jun-15	3	-5.3	-86.1	-31.2	-244.0	>1.5
Parkland	Restored	Green-03	25-Jun-15	4	-4.1	-81.8	N/A	N/A	>1.5
Parkland	Restored	Green-03	24-Jul-15	5	-9.0	-97.4	-18.8	-143.0	0.62
Parkland	Restored	Heber-03	05-May-15	1	-10.0	-108.8	-22.7	-174.7	0.73
Parkland	Restored	Heber-03	26-May-15	2	-4.8	-82.3	-29.2	-227.0	>1.5
Parkland	Restored	Heber-03	16-Jun-15	3	-3.0	-72.8	N/A	N/A	>1.5
Parkland	Restored	Heber-03	24-Jun-15	4	-2.3	-69.3	N/A	N/A	>1.5
Parkland	Restored	Heber-03	29-Jul-15	5	-4.1	-74.1	-22.4	-172.4	>1.5
Parkland	Restored	Hille-03	04-May-15	1	-11.9	-111.9	-19.3	-146.7	0.35
Parkland	Restored	Hille-03	20-May-15	2	-9.9	-103.8	-20.2	-153.8	0.56
Parkland	Restored	Hille-03	missing	3	-7.5	-90.2	-19.6	-149.5	0.87
Parkland	Restored	Hille-03	25-Jun-15	4	-6.5	-88.4	-22.8	-175.0	1.31
Parkland	Restored	Hille-03	20-Jul-15	5	-6.2	-83.9	-20.3	-154.7	1.17
Parkland	Restored	Holt-04	03-May-15	1	-16.1	-139.5	-22.6	-173.7	0.22
Parkland	Restored	Holt-04	27-May-15	2	-11.7	-118.1	-24.6	-190.4	0.62
Parkland	Restored	Holt-04	16-Jun-15	3	-8.9	-102.1	-25.9	-200.6	1.12
Parkland	Restored	Holt-04	26-Jun-15	4	-7.9	-97.8	-28.4	-220.5	>1.5
Parkland	Restored	Holt-04	27-Jul-15	5	-9.0	-98.1	-20.9	-160.2	0.77
Parkland	Restored	Hwy53-02	04-May-15	1	-10.1	-105.7	-22.2	-170.2	0.67
Parkland	Restored	Hwy53-02	21-May-15	2	-8.6	-97.6	-22.7	-174.4	0.94
Parkland	Restored	Hwy53-02	18-Jun-15	3	-7.0	-87.4	-21.7	-166.8	1.25
Parkland	Restored	Hwy53-02	25-Jun-15	4	-6.4	-86.9	-26.3	-203.9	>1.5
Parkland	Restored	Hwy53-02	04-Aug-15	5	-5.6	-81.8	-27.0	-209.6	>1.5
Parkland	Restored	Kerbe-02	06-May-15	1	-12.3	-116.5	-19.9	-151.7	0.33
Parkland	Restored	Kerbe-02	25-May-15	2	-10.6	-107.6	-19.8	-150.6	0.46
Parkland	Restored	Kerbe-02	16-Jun-15	3	-8.9	-98.8	-19.6	-149.2	0.61

Appendix E (continued)

Region	Status	Site ID	Date	Visit	$\delta^{18}O$	$\delta^{2}H$	δ_I (^{18}O)	δ_I (^{2}H)	E/I
Parkland	Restored	Kerbe-02	24-Jun-15	4	-7.2	-95.7	-23.0	-177.3	1.03
Parkland	Restored	Kerbe-02	23-Jul-15	5	-7.3	-91.2	-19.7	-150.1	0.82
Parkland	Restored	Kinvi-03	06-May-15	1	-9.4	-101.3	-20.4	-155.6	0.64
Parkland	Restored	Kinvi-03	25-May-15	2	-7.4	-93.0	-22.5	-172.6	1.10
Parkland	Restored	Kinvi-03	17-Jun-15	3	-5.7	-84.3	-24.6	-190.1	>1.5
Parkland	Restored	Kinvi-03	23-Jun-15	4	-5.4	-84.6	-28.5	-221.8	>1.5
Parkland	Restored	Kinvi-03	28-Jul-15	5	-5.1	-80.7	-24.4	-188.2	>1.5
Parkland	Restored	Kinvi-06	06-May-15	1	-10.5	-108.4	-21.4	-164.1	0.58
Parkland	Restored	Kinvi-06	25-May-15	2	-8.4	-97.5	-21.6	-165.4	0.86
Parkland	Restored	Kinvi-06	17-Jun-15	3	-6.4	-88.1	-23.7	-183.0	1.46
Parkland	Restored	Kinvi-06	23-Jun-15	4	-7.6	-92.3	-21.0	-160.7	0.95
Parkland	Restored	Kinvi-06	28-Jul-15	5	-7.2	-91.0	-21.9	-168.1	1.10
Parkland	Restored	Labyr-02	01-May-15	1	-11.4	-109.3	-19.1	-145.0	0.37
Parkland	Restored	Labyr-56	03-May-15	1	-18.0	-148.5	-21.7	-166.2	0.12
Parkland	Restored	Labyr-56	23-May-15	2	-14.4	-128.3	-20.8	-159.3	0.25
Parkland	Restored	Labyr-56	16-Jun-15	3	-8.3	-101.4	-24.3	-187.7	1.01
Parkland	Restored	Labyr-56	27-Jun-15	4	-3.9	-85.4	N/A	N/A	>1.5
Parkland	Restored	Mika-10	03-May-15	1	-14.2	-129.2	-21.9	-168.3	0.31
Parkland	Restored	Mika-10	27-May-15	2	-8.9	-105.5	-26.0	-201.7	1.05
Parkland	Restored	Mika-10	17-Jun-15	3	-6.5	-91.3	-26.2	-202.9	>1.5
Parkland	Restored	Mika-10	24-Jun-15	4	-5.5	-88.0	N/A	N/A	>1.5
Parkland	Restored	Mika-10	19-Jul-15	5	-10.5	-102.3	-18.0	-136.2	0.39
Parkland	Restored	Ozmen-05	02-May-15	1	-16.7	-144.4	-23.9	-184.1	0.23
Parkland	Restored	Ozmen-05	24-May-15	2	-12.6	-124.1	-27.0	-209.6	0.65
Parkland	Restored	Ozmen-05	15-Jun-15	3	-9.8	-109.0	N/A	N/A	1.41
Parkland	Restored	Ozmen-05	26-Jun-15	4	-9.2	-106.0	N/A	N/A	>1.5
Parkland	Restored	Parlb-01	03-May-15	1	-18.3	-146.8	-20.7	-158.1	0.08
Parkland	Restored	Parlb-01	27-May-15	2	-14.5	-128.1	-20.6	-157.6	0.24
Parkland	Restored	Parlb-01	20-Jun-15	3	-13.6	-118.5	-18.5	-140.1	0.20
Parkland	Restored	Parlb-01	26-Jun-15	4	-13.4	-118.0	-18.7	-142.3	0.22
Parkland	Restored	Parlb-01	22-Jul-15	5	-12.9	-112.6	-17.6	-133.2	0.20
Parkland	Restored	Pearl-06	02-May-15	1	-14.4	-130.4	-23.3	-179.4	0.34
Parkland	Restored	Pearl-06	24-May-15	2	-7.1	-96.0	N/A	N/A	>1.5
Parkland	Restored	Pearl-06	14-Jun-15	3	-11.6	-111.6	-21.5	-165.2	0.50
Parkland	Restored	Retta-09	01-May-15	1	-16.7	-140.9	-21.3	-163.4	0.16
Parkland	Restored	Retta-09	23-May-15	2	-10.4	-111.3	-22.9	-176.1	0.65
Parkland	Restored	Retta-09	13-Jun-15	3	-7.2	-86.4	-17.8	-134.5	0.75

5.6 Appendix F.

Isotope compositions of precipitation samples taken during the 2014 and 2015 sampling season. Although many of the samples of rain and snow collected during my study plotted on the Global Meteoric Water Line (GMWL), I was able to collect too few samples of precipitation to comfortably use them in my calculations for this research. Further, many plotted below the GMWL, indicating that they had experienced some evaporation during collection, despite my best efforts to minimize evaporative enrichment during sampling. This was particularly evident in rain samples from 2014. Regardless, the general pattern of samples conforms to expectation with snow plotting lower along the GMWL than rain, on average.

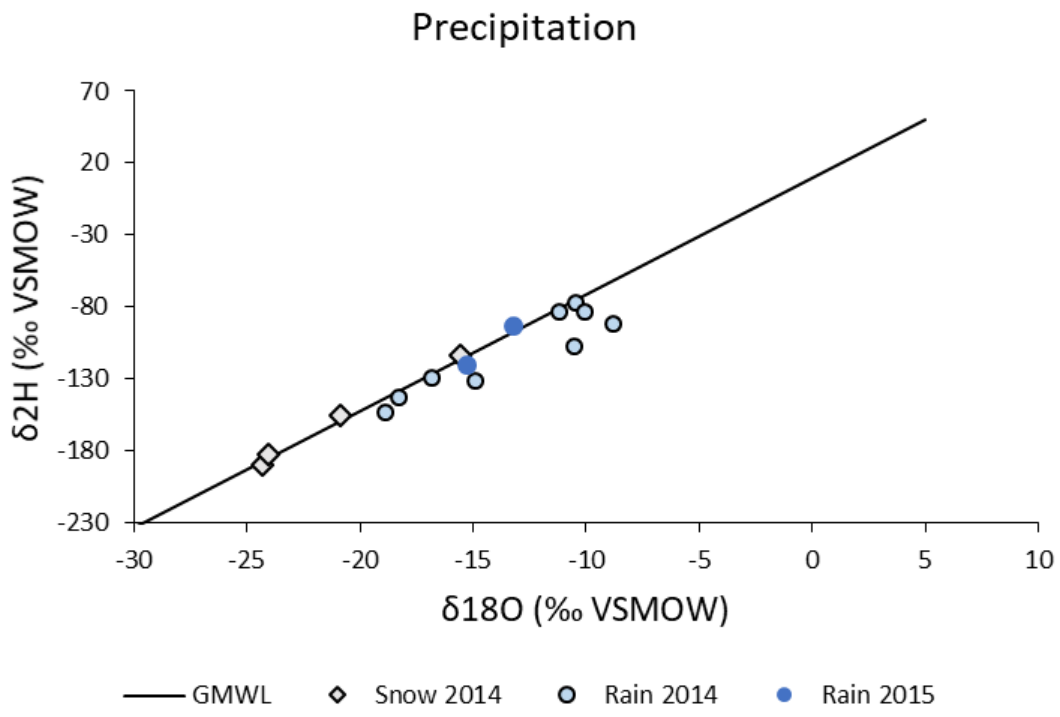

5.7 Appendix G.

WEL slopes for the 96 study wetlands, comparing 24 sites across two years (2014 and 2015), 24 sites in the Grassland to 24 sites in the Parkland in two separate years, and 24 natural sites to 24 restored sites in the Parkland in 2015. Enlarged symbols represent the average slope values. Conforming to expectations, the slopes of the WELs display differences among regions and between years. Generally, drier conditions with lower relative humidity and higher potential evapotranspiration rates yield gentler slopes. A gentler slope indicates that the ratio of enrichment of the hydrogen isotope to the enrichment of the oxygen isotope is closer to one.

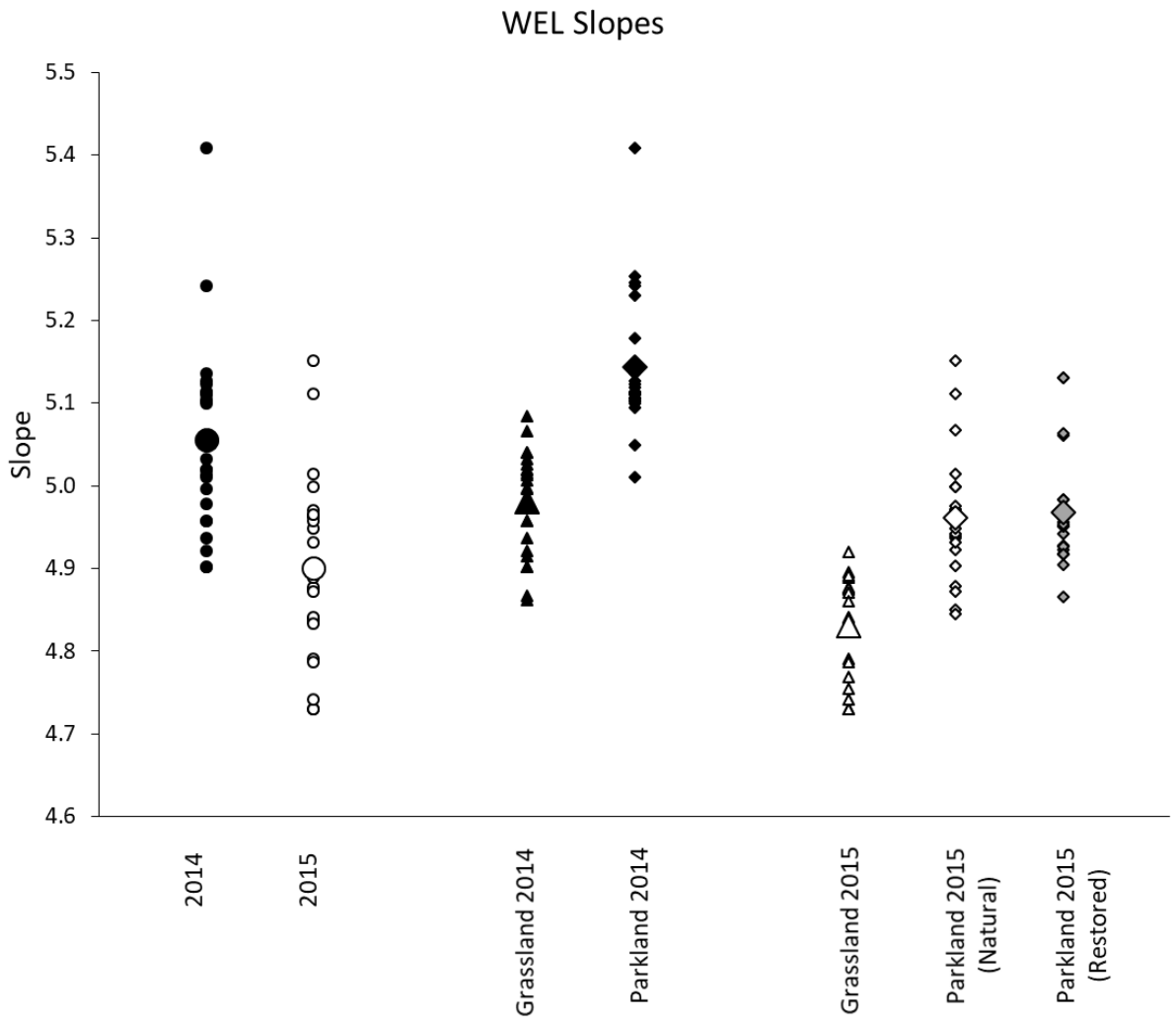

5.8 Appendix H. Parameters used to construct the isotopic framework, from all meteorological stations in 2014 and 2015.

Parameter	Brooks		Cabin Lake		Craigmyle	Drumheller East		Finnegan	Hand Hills		Lathom
	2014	2015	2014	2015	2015	2014	2015	2015	2014	2015	2014
h (%)	66.9	60.0	63.7	55.4	63.5	65.6	59.3	60.2	66.3	60.8	62.0
T (K)	289.3	289.8	289.0	289.8	288.2	289.2	289.3	289.1	287.8	288.1	289.3
α^* (^{18}O)	1.0101	1.0101	1.0102	1.0101	1.0102	1.0101	1.0101	1.0101	1.0103	1.0102	1.0101
α^* (^{2}H)	1.0889	1.0884	1.0893	1.0883	1.0903	1.0891	1.0889	1.0892	1.0909	1.0905	1.0890
ε^* (^{18}O) ‰	10.1	10.1	10.2	10.1	10.2	10.1	10.1	10.1	10.3	10.2	10.1
ε^* (^{2}H) ‰	88.9	88.4	89.3	88.3	90.3	89.1	88.9	89.2	90.9	90.5	89.0
ε_K (^{18}O) ‰	4.7	5.7	5.2	6.3	5.2	4.9	5.8	5.7	4.8	5.6	5.4
ε_K (^{2}H) ‰	4.1	5.0	4.5	5.6	4.6	4.3	5.1	5.0	4.2	4.9	4.8
δ_{As} (^{18}O) ‰	-21.8	-21.9	-22.2	-22.0	-22.1	-22.5	-21.7	-21.8	-22.7	-22.1	-22.0
δ_{As} (^{2}H) ‰	-164.8	-165.0	-167.8	-165.9	-167.4	-169.7	-163.9	-165.0	-171.8	-167.3	-166.2
δ_P (^{18}O) ‰	-16.6	-16.8	-17.2	-16.8	-16.8	-17.4	-16.5	-16.6	-17.6	-16.8	-16.8
δ_P (^{2}H) ‰	-125.8	-127.5	-130.4	-127.5	-127.5	-131.9	-125.3	-125.8	-133.3	-127.2	-127.2
δ^* (^{18}O) ‰	0.3	4.4	1.7	7.7	2.1	0.3	5.1	4.4	-0.2	3.9	3.0
δ^* (^{2}H) ‰	-41.8	-24.8	-36.9	-11.3	-34.5	-44.3	-20.5	-24.1	-45.9	-26.6	-30.9
δ_{SSL} (^{18}O) ‰	-5.5	-4.3	-5.3	-3.5	-5.0	-6.0	-3.9	-4.2	-6.2	-4.4	-4.7
δ_{SSL} (^{2}H) ‰	-72.5	-70.1	-74.4	-68.3	-72.0	-77.5	-67.5	-68.7	-78.4	-70.2	-71.3
WEL Slope	4.98	4.84	4.94	4.74	4.92	4.96	4.84	4.84	5.03	4.88	4.87

Appendix H (continued)

Parameter	Pollockville		Rolling Hills		Sheerness		Spondin		Tide Lake		Youngstown	
	2014	2015	2014	2015	2014	2015	2014	2015	2014	2015	2014	2015
h (%)	66.1	59.5	63.6	57.0	63.5	56.0	67.9	60.2	62.5	52.9	65.9	59.3
T (K)	288.8	289.2	289.3	289.8	288.4	289.1	287.9	288.3	289.4	290.2	288.4	289.0
α^* (^{18}O)	1.0102	1.0101	1.0101	1.0101	1.0102	1.0101	1.0103	1.0102	1.0101	1.0100	1.0102	1.0102
α^* (^{2}H)	1.0897	1.0891	1.0890	1.0884	1.0900	1.0892	1.0908	1.0903	1.0889	1.0879	1.0901	1.0894
ε^* (^{18}O) ‰	10.2	10.1	10.1	10.1	10.2	10.1	10.3	10.2	10.1	10.0	10.2	10.2
ε^* (^{2}H) ‰	89.7	89.1	89.0	88.4	90.0	89.2	90.8	90.3	88.9	87.9	90.1	89.4
ε_K (^{18}O) ‰	4.8	5.7	5.2	6.1	5.2	6.3	4.6	5.7	5.3	6.7	4.8	5.8
ε_K (^{2}H) ‰	4.2	5.1	4.6	5.4	4.6	5.5	4.0	5.0	4.7	5.9	4.3	5.1
δ_{As} (^{18}O) ‰	-22.2	-22.6	-21.8	-21.9	-22.6	-22.4	-23.0	-22.7	-21.8	-21.7	-22.6	-22.4
δ_{As} (^{2}H) ‰	-167.6	-170.4	-164.6	-165.0	-170.9	-169.1	-173.5	-172.2	-164.7	-164.0	-171.0	-169.3
δ_P (^{18}O) ‰	-17.1	-17.6	-16.6	-16.8	-17.7	-17.3	-18.0	-17.7	-16.7	-16.7	-17.7	-17.3
δ_P (^{2}H) ‰	-129.3	-133.3	-125.9	-127.5	-133.8	-131.3	-136.3	-134.2	-126.6	-126.6	-134.0	-131.3
δ^* (^{18}O) ‰	0.4	4.0	2.2	6.6	1.5	7.0	-1.3	3.6	2.8	10.0	0.1	4.5
δ^* (^{2}H) ‰	-42.2	-28.7	-33.4	-15.4	-39.0	-15.4	-51.6	-30.8	-30.9	-0.2	-45.0	-26.1
δ_{SSL} (^{18}O) ‰	-5.7	-5.0	-4.8	-3.7	-5.7	-4.0	-6.8	-5.1	-4.7	-2.9	-6.1	-4.6
δ_{SSL} (^{2}H) ‰	-74.8	-75.4	-70.6	-68.6	-77.2	-71.7	-81.7	-76.3	-70.5	-65.7	-78.5	-73.4
WEL Slope	5.00	4.84	4.91	4.79	4.96	4.78	5.08	4.86	4.90	4.73	5.02	4.83

Appendix H (continued)

Parameter	Alliance		Battle River Headwaters	Big Valley		Breton	Camrose City Airport		Delburne	
	2014	2015	2014	2014	2015	2015	2014	2015	2014	2015
h (%)	69.2	62.6	71.8	65.7	59.5	63.8	76.9	70.4	69.4	63.9
T (K)	288.0	288.3	286.4	288.0	288.3	287.5	287.9	288.3	287.7	287.9
α^* (^{18}O)	1.0102	1.0102	1.0104	1.0103	1.0102	1.0103	1.0103	1.0102	1.0103	1.0103
α^* (^{2}H)	1.0906	1.0902	1.0927	1.0906	1.0902	1.0912	1.0908	1.0903	1.0910	1.0907
ε^* (^{18}O) ‰	10.2	10.2	10.4	10.3	10.2	10.3	10.3	10.2	10.3	10.3
ε^* (^{2}H) ‰	90.6	90.2	92.7	90.6	90.2	91.2	90.8	90.3	91.0	90.7
ε_K (^{18}O) ‰	4.4	5.3	4.0	4.9	5.7	5.1	3.3	4.2	4.3	5.1
ε_K (^{2}H) ‰	3.8	4.7	3.5	4.3	5.1	4.5	2.9	3.7	3.8	4.5
δ_{As} (^{18}O) ‰	-23.1	-23.1	-23.9	-23.0	-22.6	-23.0	-23.5	-22.6	-23.2	-23.5
δ_{As} (^{2}H) ‰	-174.7	-174.7	-180.2	-173.4	-170.6	-173.9	-177.2	-171.1	-175.3	-177.2
δ_P (^{18}O) ‰	-18.1	-18.1	-18.7	-17.9	-17.4	-17.9	-18.5	-17.7	-18.1	-18.5
δ_P (^{2}H) ‰	-137.8	-136.9	-141.8	-135.6	-131.9	-136.1	-140.3	-133.8	-136.9	-140.3
δ^* (^{18}O) ‰	-2.2	1.6	-4.0	-0.1	4.2	1.1	-6.1	-2.3	-2.3	0.4
δ^* (^{2}H) ‰	-56.2	-40.6	-65.2	-46.7	-27.1	-41.5	-73.4	-54.9	-56.8	-46.2
δ_{SSL} (^{18}O) ‰	-7.2	-6.0	-8.3	-6.4	-4.8	-6.0	-9.0	-7.0	-7.3	-6.6
δ_{SSL} (^{2}H) ‰	-84.0	-80.4	-89.1	-80.3	-73.9	-79.3	-90.5	-80.7	-83.9	-83.8
WEL Slope	5.11	4.90	5.23	5.01	4.85	4.97	5.41	5.15	5.09	4.97

Appendix H (continued)

Parameter	Ferintosh		Fleet	Forestburg		Kessler	Lacombe		New Sarepta		Prentiss	
	2014	2015	2014	2014	2015	2015	2014	2015	2014	2015	2014	2015
h (%)	72.3	67.0	69.7	68.7	64.1	65.1	73.4	69.3	70.7	62.2	67.0	61.9
T (K)	287.4	287.6	287.7	287.9	288.1	288.2	287.5	287.7	287.6	288.1	287.1	287.5
α^* (^{18}O)	1.0103	1.0103	1.0103	1.0103	1.0102	1.0102	1.0103	1.0103	1.0103	1.0102	1.0103	1.0103
α^* (^{2}H)	1.0914	1.0911	1.0910	1.0907	1.0904	1.0903	1.0912	1.0910	1.0911	1.0905	1.0917	1.0913
ε^* (^{18}O) ‰	10.3	10.3	10.3	10.3	10.2	10.2	10.3	10.3	10.3	10.2	10.3	10.3
ε^* (^{2}H) ‰	91.4	91.1	91.0	90.7	90.4	90.3	91.2	91.0	91.1	90.5	91.7	91.3
ε_K (^{18}O) ‰	3.9	4.7	4.3	4.4	5.1	4.9	3.8	4.4	4.2	5.4	4.7	5.4
ε_K (^{2}H) ‰	3.5	4.1	3.8	3.9	4.5	4.4	3.3	3.8	3.7	4.7	4.1	4.8
δ_{As} (^{18}O) ‰	-23.4	-23.0	-23.1	-23.2	-23.2	-23.0	-23.4	-22.3	-23.8	-22.4	-23.5	-23.3
δ_{As} (^{2}H) ‰	-176.5	-173.8	-174.8	-175.6	-175.1	-173.2	-177.1	-168.6	-179.5	-169.6	-177.4	-176.2
δ_P (^{18}O) ‰	-18.4	-18.0	-18.2	-18.3	-18.2	-17.9	-18.3	-17.1	-18.8	-17.4	-18.4	-18.3
δ_P (^{2}H) ‰	-139.3	-136.3	-137.8	-138.6	-137.8	-135.6	-138.9	-129.3	-143.2	-131.5	-139.3	-138.5
δ^* (^{18}O) ‰	-3.9	-0.8	-2.4	-2.1	0.5	0.2	-4.5	-1.4	-3.6	2.6	-1.2	2.0
δ^* (^{2}H) ‰	-63.6	-49.5	-56.9	-55.9	-44.9	-45.4	-66.6	-49.0	-64.1	-33.4	-52.8	-38.9
δ_{SSL} (^{18}O) ‰	-8.0	-6.6	-7.3	-7.2	-6.3	-6.3	-8.3	-6.3	-8.1	-5.1	-7.0	-5.9
δ_{SSL} (^{2}H) ‰	-86.7	-81.1	-83.9	-84.5	-81.7	-80.1	-87.8	-76.2	-89.7	-74.3	-84.4	-80.8
WEL Slope	5.25	5.07	5.14	5.10	4.97	4.99	5.24	5.11	5.18	4.92	5.05	4.93

Appendix H (continued)

Parameter	Rosalind		Stettler		Thorsby	Wetaskiwin	
	2014	2015	2014	2015	2015	2014	2015
h (%)	68.6	62.7	69.2	63.6	62.2	70.0	65.3
T (K)	287.9	288.1	287.7	287.9	287.8	287.7	287.8
α^* (^{18}O)	1.0103	1.0102	1.0103	1.0103	1.0103	1.0103	1.0103
α^* (^{2}H)	1.0907	1.0904	1.0910	1.0908	1.0908	1.0910	1.0908
ε^* (^{18}O) ‰	10.3	10.2	10.3	10.3	10.3	10.3	10.3
ε^* (^{2}H) ‰	90.7	90.4	91.0	90.8	90.8	91.0	90.8
ε_K (^{18}O) ‰	4.5	5.3	4.4	5.2	5.4	4.3	4.9
ε_K (^{2}H) ‰	3.9	4.7	3.8	4.5	4.7	3.8	4.3
δ_{As} (^{18}O) ‰	-23.3	-23.2	-23.3	-22.9	-22.7	-23.4	-22.3
δ_{As} (^{2}H) ‰	-176.0	-175.1	-176.2	-172.8	-171.5	-177.1	-168.5
δ_P (^{18}O) ‰	-18.4	-18.2	-18.3	-17.8	-17.6	-18.4	-17.1
δ_P (^{2}H) ‰	-139.3	-137.8	-138.6	-134.9	-133.8	-139.6	-129.3
δ^* (^{18}O) ‰	-2.1	1.4	-2.4	1.3	2.4	-2.9	0.9
δ^* (^{2}H) ‰	-56.1	-41.1	-57.4	-40.4	-35.1	-60.1	-39.7
δ_{SSL} (^{18}O) ‰	-7.3	-6.1	-7.4	-5.9	-5.4	-7.6	-5.5
δ_{SSL} (^{2}H) ‰	-85.0	-80.9	-85.0	-78.4	-76.3	-86.4	-74.0
WEL Slope	5.11	4.93	5.10	4.96	4.94	5.13	5.00

5.9 Appendix I. Bootstrap confidence interval (CI) estimations for $\delta^{18}O$, $\delta^{2}H$, and E/I ratios for all comparisons. Bootstrapping involved the random resampling of 70% of the full sample without replacement. Non-overlapping 90% CI values indicate significantly different mean values.

Comparison	Variable		N (70%)	Estimate of Mean				90% CI for Mean	
				Bootstrap Estimate	Estimate from Original Data	Bias	Standard Error	Lower	Upper
2014 vs 2015	$\delta^{18}O$	2014	193	0.86640	0.86639	0.00000	0.01023	0.84804	0.88199
		2015	56	0.85818	0.85929	-0.00111	0.06842	0.68861	0.94333
	$\delta^{2}H$	2014	193	0.94769	0.94789	-0.00020	0.00451	0.94004	0.95464
		2015	56	0.89562	0.89510	0.00052	0.05729	0.74292	0.96453
	E/I	2014	193	0.40874	0.40899	-0.00025	0.04850	0.32776	0.48622
		2015	56	0.72604	0.73059	-0.00455	0.11213	0.50406	0.88777
2014 Grassland vs Parkland	$\delta^{18}O$	Grassland	177	0.79626	0.79624	0.00002	0.01619	0.76858	0.82177
		Parkland	177	0.87872	0.87936	-0.00064	0.01485	0.85292	0.90153
	$\delta^{2}H$	Grassland	177	0.93837	0.93837	-0.00001	0.00498	0.92987	0.94623
		Parkland	177	0.94065	0.94094	-0.00029	0.00634	0.93046	0.95113
	E/I	Grassland	177	0.40000	0.39855	0.00145	0.04270	0.32036	0.46214
		Parkland	177	0.47479	0.47468	0.00010	0.05891	0.36468	0.55803
2015 Grassland vs Parkland (Natural and Restored)	$\delta^{18}O$	Grassland	18	0.97153	0.96956	0.00197	0.02374	0.95700	1.00000
		Parkland	64	0.78357	0.78032	0.00325	0.06477	0.65400	0.86954
		Restored	133	0.88724	0.88601	0.00123	0.01767	0.85206	0.91044
	$\delta^{2}H$	Grassland	18	0.98266	0.98292	-0.00026	0.01105	0.98200	0.99900
		Parkland	64	0.83630	0.83347	0.00283	0.05365	0.73019	0.90721
		Restored	133	0.92147	0.92054	0.00093	0.01328	0.89428	0.93890
	E/I	Grassland	18	0.97143	0.96936	0.00207	0.03197	0.89900	1.00000
		Parkland	64	0.60749	0.60543	0.00206	0.08810	0.44257	0.73891
		Restored	133	0.80499	0.80394	0.00106	0.02536	0.76121	0.84548